

**Dissecting the GA regulation
of cell expansion in the root
of *Arabidopsis thaliana***

Ester Cancho Sánchez, BSc, MSc.

Thesis submitted to the University of Nottingham
for the degree of Doctor of Philosophy.

SEPTEMBER 2012

ABSTRACT

Gibberellins (GAs) represent an important class of hormonal signal that regulate growth and developmental processes during the plant life cycle. GA promotes growth through the targeted degradation of the nuclear localized DELLA repressor proteins via the ubiquitin proteasome pathway. Whilst DELLAs do not appear to bind directly to DNA, recent evidence suggests that they interact with several different classes of transcription factors to control the expression of downstream genes in a GA-dependent manner.

In order to pinpoint the genes targeted by GA to promote root growth, several genetic approaches have been pursued in this thesis. These approaches took advantage of the previous observation that targeting expression of a steroid regulated non-degradable form of DELLA in endodermal cells (using the *SCR:gai-GR* transgene) blocked root elongation (Ubeda-Tomás et al., 2008, 2009). The *SCR:gai-GR* line was initially mutagenized to select mutants that no longer exhibit steroid-inducible root growth inhibition. Several mutant lines have been selected, characterised and subjected to next-generation sequencing to reveal whether they disrupt novel downstream components of the GA signalling pathway.

The *SCR:gai-GR* line has also been used in transcriptomic studies and a number of novel downstream targets identified for functional characterisation. Finally, several GA-regulated genes encoding cell wall modifying enzymes belonging to the xyloglucan endotransglucosylase/hydrolase (XTH) family have been functionally characterised. Multiple XTH mutant combinations exhibit root elongation defects and altered cell expansion dynamics, hence providing new insight into how GAs may regulate cell wall remodelling enzymes to promote root cell expansion.

ACKNOWLEDGMENTS

First of all, I would like to thank my supervisor Prof. Malcolm Bennett for giving me the opportunity to complete this PhD. I feel grateful to have been mentored for someone with such an incredible a passion for sciences. Also, I would like to express my gratitude to Dr. Susana Ubeda-Tomás, for her kind guidance and advice during this research.

My special thanks go to Dr. Ranjan Swarup, first for giving me the opportunity to work with him during my masters and then for his invaluable help during the length of my PhD. His enthusiasm, energy, endless knowledge and his memory! have never stopped amazing me. I am also grateful to Prof. Tobias Baskin, for generously taking me in his lab and helping me with my experiments.

My gratitude extends to all the past and present members of Malcolm Bennett's lab group and CPIB for their continuous help and for making life in the lab an enjoyable one! I am also thankful to all technicians and office staff for their sympathy and help.

A big thank you to all my friends in Nottingham to make my time here a very good one and indirectly supporting me towards the completion of this thesis. I am especially thankful to Jose and Clem for being there whenever I need it and to whom I'll miss.

I cannot thank enough to Fran for all his help during my PhD, even when he is being yelling at me because he is already explained me thousand times how a software program works! I really couldn't have done without you.

Finally, I must thank to all my family. To my parents whom always have worked incredibly hard to give us the best and for their unconditional support whatever I've decided to do. I wouldn't be here without the support of all my sisters, especially from Montse and Anna whom I am totally thankful for always encouraging me.

Moltes gràcies a tots!

TABLE OF CONTENTS

ABSTRACT	I
ACKNOWLEDGEMENTS	II
TABLE OF CONTENTS	III
ABBREVIATIONS	X
CHAPTER 1: GENERAL INTRODUCTION	1
1.1 <i>Arabidopsis thaliana</i>	1
1.2 Plant hormones	3
1.3 Gibberellins	5
1.3.1 General description	5
1.3.2 Gibberellins biosynthesis and deactivation	7
1.3.3 GA signalling	9
1.3.3.1 GA binding to the GID1 receptor	9
1.3.3.2 DELLA proteins are growth repressors	10
1.3.3.3 DELLA degradation through the 26 proteasome	12
1.3.3.4 GA homeostasis	13
1.3.3.5 DELLA downstream targets	15
1.4 Root development in <i>A. thaliana</i>	17
1.4.1 Study of root development in <i>Arabidopsis thaliana</i>	17
1.4.2 <i>Arabidopsis</i> root structure	18
1.5 GA regulation of cell expansion	20
1.5.1 Root cell expansion	20
1.5.2 Hormonal control of root cell expansion	22
1.5.3 GA control of tissue-specific root cell expansion and division	24
1.5.4 The plant cell wall	26
	III

1.5.5	Root cell wall modifying enzymes	27
1.5.6	GA regulation of cell wall remodelling enzymes	30
1.6	Objectives of this thesis	32
 CHAPTER 2: GENERAL MATERIALS AND METHODS		34
2.1	Plant material and physiological assays	34
2.1.1	Seed stock	34
2.1.2	Seed sterilization	34
2.1.3	Growth media	35
2.1.4	Stratification	35
2.1.5	Seed collection and cross pollination	35
2.2	Physiological assays	36
2.2.1	Root growth assays and image analysis	36
2.2.2	Confocal microscopy for root analysis	37
2.3	Nucleic acid isolation	37
2.3.1	Genomic DNA extraction	37
2.3.2	RNA extraction	38
2.3.3	cDNA synthesis	39
2.3.4	Polymerase Chain Reaction (PCR)	39
2.3.5	Agarose gel electrophoresis	40
2.3.6	DNA purification from gel	41
2.4	Cloning	41
2.4.1	Restriction enzyme digestion	41
2.4.2	Ligation Reaction	42
2.4.3	Preparation of <i>E. coli</i> DH5 α chemically competent cells	42
2.4.4	Transformation of <i>E. coli</i> DH5 α competent cells	43
2.4.5	Transformation of <i>Agrobacterium</i> competent cells	43

2.4.6	Colony PCR	44
2.4.7	Plasmid DNA extraction	44
2.4.8	<i>Arabidopsis</i> floral dip transformation	45
 CHAPTER 3: FORWARD GENETIC SCREEN TO IDENTIFY NOVEL GA MUTANTS TO STUDY ROOT CELL EXPANSION (STUDY OF THE FAST NEUTRON <i>SCR::gai-GR-YFP</i> POPULATIONS)		46
3.1	Introduction.	46
3.2	Materials and Methods.	49
3.2.1	Plant material	49
3.2.2	Fast neutron mutagenesis	49
3.2.3	Root growth assay for selection of putative mutants	50
3.2.3.1	Screening of the mutagenized <i>SCR::gai-GR-YFP</i> M2 population	50
3.2.4	Confirmation of the <i>SCR::gai-GR-YFP</i> transgene integrity	50
3.2.4.1	Confirmation of the transgene presence by PCR	50
3.2.4.2	Confirmation of the transgene expression by RT-PCR	51
3.2.4.3	Sequencing of the <i>gai</i> negative mutation	52
3.2.5	Phenotypic characterization of putative FN mutants	52
3.2.5.1	Root length and growth rate assay	52
3.2.5.2	Root meristem and root cell analyses of putative mutants	53
3.2.6	Next generation sequencing of putative mutants	53
3.3	Results.	54
3.3.1	Root growth assay for selection of putative mutants	54
3.3.1.1	Screening of the mutagenized <i>SCR::gai-GR-YFP</i> M2 population	54
3.3.1.2	Validation of the mutant phenotype	55
3.3.2	Confirmation of the <i>SCR::gai-GR-YFP</i> transgene integrity	57

3.3.2.1	Confirmation for the presence of the transgene	57
3.3.2.2	Confirmation of the <i>SCR::gai-GR-YFP</i> transgene expression	58
3.3.2.3	Sequencing of the <i>gai</i> negative mutation	60
3.3.3	All the putative FN mutants are recessive mutations	60
3.3.4	Phenotypic analysis	61
3.3.4.1	Growth rate analysis	61
3.3.4.2	Cell production rate analysis	62
3.3.5	Next generation sequencing of putative mutants	63
3.4	Discussion.	65
 CHAPTER 4: REVERSE GENETIC SCREEN TO STUDY GA REGULATED ROOT CELL EXPANSION		69
4.1	Introduction.	69
4.1.1	Transcriptomics	69
4.1.2	The Affymetrix gene chip system	70
4.1.3	Transcriptomic experiments for root studies	72
4.1.4	Transcriptomic approach to dissect GA regulated root cell expansion	73
4.2	Materials and Methods.	74
4.2.1	Plant material and sample preparation	74
4.2.2	Affymetrix hybridization	75
4.2.3	DEX- <i>SCR::gai-GR-YFP</i> TXM data analysis	76
4.2.3.1	Procedure for analysis of transcriptomics data	76
4.2.3.2	Quality assessment	77
4.2.3.2.1	Analysis of the arrays integrity	77
4.2.3.2.2	Analysis of the variability of the samples	78

4.2.3.2.3	Analysis of the variability of probe intensities between arrays	80
4.2.3.2.4	RNA degradation	81
4.2.3.3	Pre-processing of the microarray data	84
4.2.3.4	Quality control plots on pre-processed data	86
4.2.3.5	Statistical analysis of <i>gai</i> -DEX microarray data	87
4.2.4	Selection of genes of interest	89
4.2.5	Gene ontology analysis	90
4.2.6	Functional analysis of selected GA regulated genes	91
4.2.6.1	Identification of T-DNA insertion lines	91
4.2.6.2	Root growth assay	91
4.2.6.3	Promoter analysis of <i>gai</i> -DEX regulated genes	92
4.3	Results.	92
4.3.1	Experimental design of the <i>SCR::gai-GR</i> transcriptomics experiment	92
4.3.2	Exploratory analysis & visualisation of result of genes	93
4.3.2.1	Identification of <i>SCR::gai-GR</i> regulated genes	93
4.3.2.2	Hierarchical clustering revealed associations between functional classes of genes in the GA dataset	96
4.3.3	Selection of candidate genes downstream of GA signal transduction pathway	99
4.3.3.1	Pipeline to select candidate DELLA responsive genes	99
4.3.3.2	Gene ontology analysis of candidate genes	102
4.3.4	Functional analysis of selected GA regulated genes	107
4.3.4.1	Analysis of differentially regulated genes that may be directly involved in the GA regulation of root cell expansion	107
4.3.4.2	Genes upregulated in the <i>gai</i> -DEX transcriptomics assay show defects in root length	110

4.3.4.3	Promoter studies of genes where T-DNA mutation caused a root growth defect	113
4.4	Discussion.	116
4.4.1	DEX- <i>SCR</i> :: <i>gai-GR-YFP</i> TXM data analysis	117
4.4.2	Selection of candidate genes	118
4.4.3	Functional characterisation of candidate genes	119
 CHAPTER 5: ANALYSIS OF MEMBERS OF THE XYLOGLUCAN ENDOTRANSGLYCOSYLASE FAMILY IN THEIR ROLE IN GA REGULATED CELL EXPANSION		 124
5.1	Introduction.	124
5.1.1	Cell wall expansion in cell elongation	124
5.1.2	GA-regulated- root expressed XTH genes	128
5.2	Materials and Methods.	130
5.2.1	Plant material	130
5.2.2	Gene redundancy	131
5.2.3	Functional analysis of root development for <i>xth</i> mutants	132
5.2.4	amiRNA approach to study an <i>xth</i> quadruple mutant	132
5.2.5	Tissue-specific expression profiles of XTHs	135
5.3	Results.	135
5.3.1	Selection of GA regulated XTHs members	135
5.3.2	Tissue specific expression profiles of XTHs	138
5.3.3	Selected AtXTH mutants present a decrease in the primary root length	139
5.3.4	Double <i>xth</i> mutants present an additive effect	140
5.3.5	Growth rate is decreased in the double <i>xth</i> mutant <i>xth17 X xth18</i>	142
5.3.6	Meristem size is significantly decreased in the <i>xth17 xth18</i> double mutant	145

5.3.7	Number of cells in the meristem is not affected in the double mutant <i>xth17 xth18</i>	146
5.3.8	The transition from meristem to elongation zone happens in a more abrupt fashion in the double mutant <i>xth17 xth18</i>	147
5.3.9	Simultaneous downregulation of <i>AtXTH17</i> , <i>AtXTH18</i> , <i>AtXTH19</i> and <i>AtXTH20</i> leads to root with shorter lengths in a similar fashion as the double mutants	151
5.4	Discussion.	153
 CHAPTER 6: SUMMARY AND CONCLUSION		161
6.1	Summary	161
6.2	Conclusions	164
 REFERENCES		165
 APPENDICES		182

Abbreviations

$\mu\text{g/ml}$	microgram per millilitre
μl	microlitre
μg	microgram
μM	micromolar
bp	base pair
cDNA	complementary DNA
cm	centimetre
CPIB	Centre for Plant Integrative Biology
CPR	cell production rate
dag	days after germination
DEG	differentially expressed gene
DEPC	diethylpyrocarbonate
DEX	dexamethasone
dH ₂ O	distilled water
DNA	deoxyribonucleic acid
dNTP	deoxynucleoside triphosphate
DNase	deoxyribonuclease
dsDNA	double-stranded DNA
EDTA	ethylenediaminetetraacetic acid
EMS	ethyl methane sulphonate
EZ	elongation zone
Fig	figure
FC	fold change
FN	fast neutron
g	gram
g/l	gram per litre
GA	gibberellic acid
GFP	green fluorescent protein
GO	gene ontology
GR	growth rate
GUS	β -glucuronidase
Gy	Grey
h	hour
Kb	kilobase pair
L	litre
mg/l	milligram per litre
min	minute
ml	millilitre
mM	milimolar
MM	mismatch

mRNA	messenger RNA
MS	Murashige and Skoog
NASC	Nottingham Arabidopsis stock centre
ng	nanogram
ng/ μ l	nanogram per microlitre
NGS	next generation sequence
PBS	phosphate-buffered saline
PM	perfect match
QC	quality control
RMA	robust multiarray average method
RNA	ribonucleic acid
RNase	ribonuclease
rpm	revolutions per minute
RT-PCR	reverse transcription-polymerase chain reaction
sec	second
SD	standard deviation
SE	standard error
TXM	transcriptomics
v/v	volume to volume ratio
XTH	xyloglucan endotransglycosilase-hydrolase
w/v	weight to volume ratio

CHAPTER 1: GENERAL INTRODUCTION

1.1 *Arabidopsis thaliana*

The flowering plant *Arabidopsis thaliana* represents the most important model organism for plant biology and genetic studies. *Arabidopsis*, commonly known as mouse-ear cress, is a member of the mustard family (Brassicaceae) that includes cultivated plants such as cabbage and broccoli. Even though *Arabidopsis* has not any direct agronomic value per se, it provides numerous advantages for basic research and molecular biology as a model plant.

Arabidopsis was first described during the sixteenth century by the physician Johannes Thal, in Germany. Research on *Arabidopsis*, dates back to early 1900s, when the correct chromosome number was predicted; and the first collection of mutants was published in 1947 by E. Reinholz (Meyerowitz, 2001). Since then, a great deal of knowledge in, physiological, biochemical and developmental processes of *Arabidopsis* has been obtained.

Arabidopsis possesses a relatively small genome size of 125 Mbp organised in 5 chromosomes, allowing for easy genetic analysis and manipulation. On top of that, it has a rapid life cycle of ~ 6 weeks from germination to mature seed (Figure 1.1; Boyes *et al.*, 2001); producing thousands of seeds through self-pollination and can also be easily cross-pollinated for genetic studies. Due to its small size (40-45 cm high) *Arabidopsis* has very limited space and nutrient requirements, and thousands of plants can be easily grown in a greenhouse or indoor growth chamber either on soil or in tissue culture media. *Arabidopsis* transformation to obtain genetically engineered plants is also straightforward using

Agrobacterium tumefaciens (Clough and Bent, 1998). In addition, *Arabidopsis* seedlings and their roots are relatively translucent, facilitating light and confocal microscopy for phenotypic and genetic studies. The sequencing of the *Arabidopsis* nuclear genome was published in the year 2000 (The Arabidopsis Genome Initiative, 2000), facilitating genetic analysis and gene identification. The last version of TAIR (The Arabidopsis Information Resource, TAIR10, 2010) estimates that the *Arabidopsis* genome contains 27416 protein coding genes, 4827 pseudo genes or transposable element genes and 1359 ncRNAs. In addition, a large number of mutant collections and genomic resources have been made available (<http://arabidopsis.info/>). All the information and resources gained from *Arabidopsis* are helping to contribute to build up an information platform to our understanding of plant biology and also plants of economic and cultural relevance.

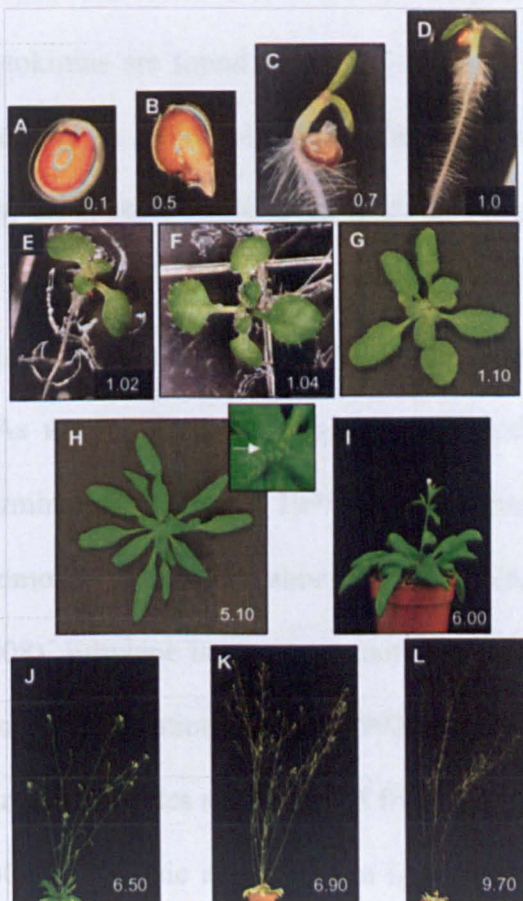


Figure 1.1 *Arabidopsis thaliana* Growth Stages. (A-C) Stage 0; Seed germination (3 to 5.5 dag). A) Seed imbibition B) Radicle emergence C) Hypocotyl and cotyledon emergence (D-G) Stage 1; Leaf development (6 to 25.5 dag). D) Cotyledons opened fully. E) Two rosette leaves F) four rosette leaves G) ten rosette leaves. (H) Stage 5; Inflorescence emergence (26 dag). First flower buds visible (indicated by arrow in inset). (I-K) Stage 6; Flower production (31.8 to 49.4 dag). I) first flower open. J) Midflowering. K) Flowering complete. (L) Stage 9; Senescence and seed harvesting (not determined). (dag) Days after germination. (Boyes *et al.*, 2001)

1.2 Plant hormones

Plant hormones play a key role controlling the growth and development of plants. They are responsible of the integration of environmental signals together with endogenous developmental programs to ensure plant survival. The main classes of plant hormones to date are auxins, cytokinins, gibberellins, ethylene, abscisic acid and brassinosteroids (Figure 1.2). These regulatory molecules represent relatively simple small organic compounds that exert distinct, often synergistic, sometimes antagonistic functions in the plant.

The major form of auxin, indole-3-acetic acid (IAA), was the first plant hormone identified (Went, 1928). IAA has been shown to participate in the regulation of basic growth processes such as cell division, elongation and differentiation (Buchanan *et al.*, 2000). Cytokinins are found at sites of active cell division in plants (Salisbury and Ross, 1992) and play an active role in promoting cell division. For example, together with auxin, they play an important role in the determination of cell-fate in the roots of *Arabidopsis* (Muraro *et al.*, 2012). Gibberellins represent a large class of compounds. The Gibberellic acid (GA3) is the most widespread and the first to be structurally characterised (Graebe, 1987). GAs are involved in many physiological processes such as in the stimulation of seed germination (Hilhorst, 1993), flower development (Wilson *et al.*, 1992)) and also in the promotion of root and shoot growth (Gallego-Bartolomé *et al.*, 2011, Ubeda-Tomás *et al.*, 2008). Ethylene is a gaseous hormone and is involved in the regulation of flowering and root hair formation (Abeles, 1992; Tanimoto *et al.*, 1995). It also stimulates the ripening of fruit and initiates abscission of fruits and leaves (Barry and Giovannoni, 2007; Yang *et al.*, 2008). Abscisic acid plays an important role in seed dormancy and in inhibition of cell

growth (Koornneef *et al.*, 2002, Finkelstein *et al.*, 2002). It is also plays an important role in the plant tolerance to drought and salt stress (Leung and Giraudat, 1998). Brassinosteroids are plant steroids playing essential roles in plants; they promote vascular differentiation (Yamamoto *et al.*, 1997), shoot elongation (Choe *et al.*, 2002, Oh *et al.*, 2012) and inhibit root elongation through the synthesis of ethylene (Arteca and Bachman, 1987).

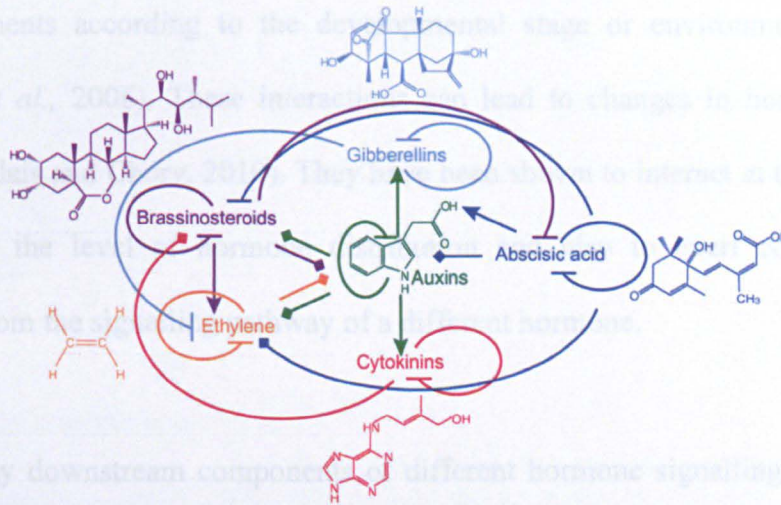


Figure 1.2. Phytohormone structures and functional interactions. Schematic representation of the main plant hormones and their interactions. Upregulation of hormone biosynthetic genes or downregulation of genes involved in hormone inactivation, are indicated by lines with arrowheads; downregulation of genes involved in hormone biosynthesis or upregulation of genes involved in inactivation of a hormone, are indicated by blocked arrows; changes in gene expression with uncertain outcome are indicated by diamond arrowheads (Jaillais and Chory, 2010).

growth and development.

To date, there is a great deal of understanding of the molecular mechanisms of hormone biosynthesis, transport and response. The biosynthetic pathways for most of the hormones have been well characterized (for example GA, ABA, and BR) or are currently being characterised (such as auxin and JA). Also, a diversity of hormone receptors have recently been largely described. Hormone receptors include receptor kinases in the plasma membrane (brassinosteroids; Li and Chory, 1997), histidine kinases receptors localized in the endoplasmic reticulum (ethylene; Chang *et al.*, 1993) or plasma membrane (cytokinins; Inoue *et al.*, 2001), and receptors of different classes found in the cytosol and nucleus

(abscisic acid, gibberellins and auxins) (Chow and McCourt, 2006). Protein degradation by the ubiquitin-dependent pathway plays a central role in hormone signalling. Although they may elicit non-genomic responses, hormone signalling generally leads to major changes in gene expression, to control cell division and expansion (Santner *et al.*, 2009).

Different signalling pathways interact in order to be able to rapidly respond to the different plant requirements according to the developmental stage or environmental conditions (Nemhauser *et al.*, 2006). These interactions can lead to changes in hormone levels or responses (Jaillais and Chory, 2010). They have been shown to interact at the level of gene expression, at the level of hormone distribution and also to exert control over key components from the signalling pathway of a different hormone.

Although many downstream components of different hormone signalling pathways have been identified, more work is needed to fully understand how these signalling pathways are integrated to control plant growth. Increased knowledge in hormone regulation of processes such as cell elongation, will contribute to gain global understanding of plant growth and development.

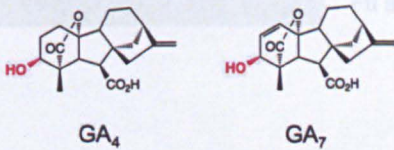
1.3 Gibberellins

1.3.1 General description

Gibberellins (GAs) are a large family of tetracyclic, diterpenoid growth regulators that act as essential endogenous signals regulating growth and developmental processes during the reproductive and vegetative plant life cycles (Richards *et al.*, 2001). Gibberellins were

originally identified on studies of the rice fungal phytopathogen *Gibberella fujikuroi* (foolish seedling) which causes stem over-growth in infected rice plants (Stowe and Yamaki, 1957). While 136 GAs have been identified in higher plants and fungi (MacMillan, 2002), only a few of them exhibit biological activity e.g., GA₁, GA₃, GA₄ and GA₇ (Figure 1.3) (Hedden and Phillips, 2000). In *Arabidopsis*, GA₄ is the main form of bioactive gibberellin (Hu *et al.*, 2008).

Non 13-hydroxylated Bioactive GAs



13-hydroxylated Bioactive GAs

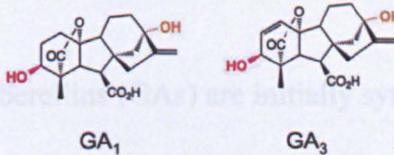


Figure 1.3. **Major Bioactive GAs from Plants and Fungi.** GA₄ is the major active GA in *Arabidopsis*. GA₃ is the most abundant GA made in fungi. The 3 β -hydroxyl groups are highlighted in red and the 13-hydroxyl groups are highlighted in orange (reproduced from Sun, 2008).

A variety of GA-related physiological roles have been determined by studies with external application of GA, inhibition of the GA biosynthetic pathway and a range of GA biosynthetic and signalling mutants (Sasaki *et al.*, 2003; Griffiths *et al.*, 2006; Peng *et al.*, 1997). In *Arabidopsis*, GA-deficient mutants have been described to exhibit several phenotypes during their life cycle such as non-germinating seeds, dark green compact rosettes, late flowering (under long-day conditions), male sterility, shorter roots and severe dwarfism (Figure 1.4) (Koornneef and Van der Veen, 1980, Wilson *et al.*, 1992 and Griffiths *et al.*, 2006, Ubeda-Tomás *et al.*, 2008). Hence GA is essential for seed

germination, root growth, leaf expansion, inflorescence stem elongation, flowering initiation, anther and petal development, as well as fruit and seed development (Tyler *et al.*, 2004).

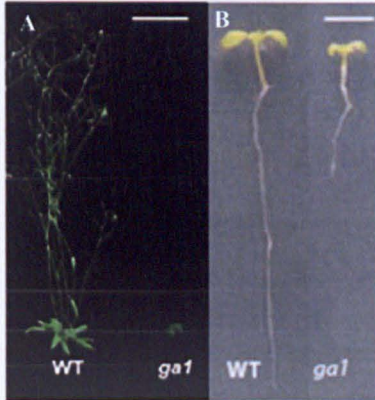


Figure 1.4. **GA-deficient mutant phenotypes.** Defects on GA signalling such as in the single mutant *gal(gal-3)* results in abnormal growth phenotypes. A) The single mutant *gal* shows a severe dwarf phenotype when compared to the size of the wild type. Bar = 10cm. B) 5-day-old primary seedling roots. *gal* mutant exhibits a root length significantly shorter than wild type. Bar = 5 mm. (Figure adapted from Fu and Harberd, 2003; Sun, 2008)

1.3.2 Gibberellins biosynthesis and deactivation

Gibberellins (GAs) are initially synthesized from geranyl geranyl diphosphate (GGDP) in a multi-enzyme pathway of intricate regulation. There are three major stages within the biosynthetic pathway of GAs involving three different classes of enzyme: terpene synthases (TPSs), cytochrome P450 monooxygenases (P450s), and 2-oxoglutarate-dependent dioxygenases (2ODDs) (Hedden and Phillips, 2000; Yamaguchi, 2008).

The first stage takes place in plastids, and result in the conversion of CGDP in *ent-kaurene* by the action of CPS and KS. Next, within the endoplasmic reticulum the conversion of *ent-kaurene* to GA₁₂ occurs through the action of two P450s. In the final stage of the pathway, GA₁₂ is converted to the bioactive form GA₄ through oxidations carried out by the action of two soluble ODD enzymes, GA 20-oxidase (GA20ox) and GA 3-oxidase (GA3ox), in the cytosol (Hedden *et al.*, 1997).

Deactivation of bioactive GA in the plant is a key regulated process to reduce the amount of active GA. In *Arabidopsis*, deactivation of bioactive GA is carried out by GA 2-oxidases (GA2oxs) that catalyse the β -hydroxylation of GA₄ (Figure 1.5).

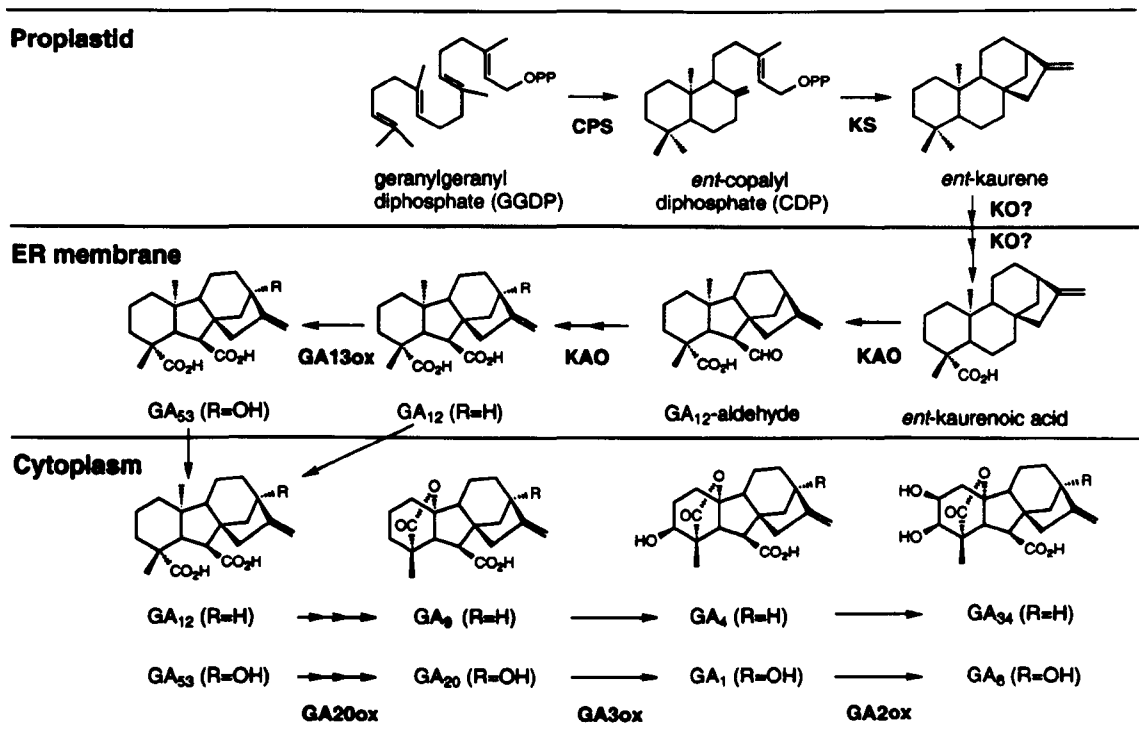


Figure 1.5. **Major GA Biosynthetic and Catabolic Pathways in Higher Plants.** The enzyme names are shown in boldface below or to the right of each arrow. GA₄ and GA₁ are the bioactive GAs, and GA₃₄ and GA₈ are their inactive catabolites. Abbreviation: CPS- ent-copalyl diphosphate; KS-Kaurene synthase; KO- Kaurene oxidase; KAO Kaurenoic acid; GA2ox- GA 2-oxidase; GA3ox- GA 3-oxidase; GA13ox- GA 13-oxidase; GA20ox- GA 20-oxidase (Olszewski *et al.*, 2002).

Many steps in the GA biosynthesis pathway are controlled by enzymes that are the products of small multigene families (Yamaguchi, 2008). Different gene family members have a specific pattern of expression (Phillips *et al.*, 1995). GAs auto-regulate their levels by repressing the expression of several genes whose products are involved in its biosynthesis and by promoting expression of genes involved in their inactivation (Zentella *et al.*, 2007). The levels of GA are additionally influenced by other hormones such as ethylene and auxin (Yamaguchi, 2008), as well as by environmental signals such as light.

GA also regulates its own biosynthesis via negative feedback regulation on transcripts encoding the GA20ox and GA3ox (Thomas *et al.*, 1999). GAs also regulate the level of transcripts encoding the deactivating GA2ox to decrease the levels of bioactive GA. Both these regulatory mechanisms interact to achieve GA homeostasis (Olszewski *et al.*, 2002; Middleton *et al.*, 2012).

1.3.3 GA signalling

1.3.3.1 GA binding to the GID1 receptor

GA signalling involves the binding of bioactive GA to the soluble receptor protein GID1 (GIBBERELLIN-INSENSITIVE DWARF1), which can then interact with DELLA repressor proteins, to induce their degradation via the E3 ubiquitin ligase SCF^{GID2/SLY1} (reviewed by Schwechheimer, 2008). The identification of the GA receptor was a key step in the understanding of how the interaction between GA and DELLAS takes place. The GA receptor GID1 was first cloned in rice (Ueguchi-Tanaka *et al.*, 2007). *gid1* mutants show a strong GA-insensitive dwarf phenotype as a result of the inability to degrade the rice DELLA protein SLR1. *Arabidopsis* contains three GID1 orthologues, AtGID1a, AtGID1b and AtGID1c (Nakajima *et al.*, 2006). GID1 is a soluble nuclear-enriched receptor and its distribution is not affected by GA. GID1s show sequence similarity to hormone-sensitive lipases (HSL), and contains the conserved HSL motifs (HGG and GX SXG). However, non enzymatic activity has been detected on GID1 (Ueguchi-Tanaka *et al.*, 2007).

Murase *et al.* (2008) showed that the GID1 receptor has a globular structure containing a pocket like structure, where the GA molecule is attached by its carboxylic acid group. Uniquely, GID1 has a loose strand at its amino-terminal end that interacts with the surface of the bound GA, so covering the pocket like a lid. DELLA protein is thought to interact with the surface of the lid to induce a conformational change that allows its recognition with the SCF complex (Figure 1.6).

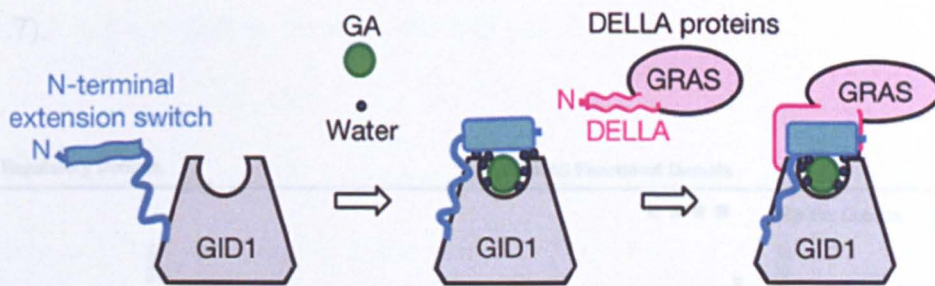


Figure 1.6. **A Model for the GA-GID1-DELLA Complex.** GID1 appears to contain the substrate binding pocket and lid, similar to those present in the bacterial HSLs. Active GAs bind to the substrate binding pocket with the aid of the lid. GA binding induces a GID1 conformational change in the N-terminal helical switch for DELLA binding, which promotes a conformational transition in the DELLA protein. (Reproduced from Murase *et al.*, 2008).

1.3.3.2 DELLA proteins are growth repressors

GA-induced growth response is associated with changes to the abundance of DELLA proteins. The presence of DELLA proteins leads to repression of the GA-induced growth. This restraint in GA-induced growth is relieved upon DELLA degradation. Other mechanisms such as hormone cross talk and environmental stimulus are thought to be involved in the regulation of this signalling pathway (Weiss and Ori, 2007).

The DELLA proteins are nuclear growth repressors belonging to the GRAS superfamily of putative transcription factors (Pysh *et al.*, 1999). DELLA proteins are characterised by two

highly conserved domains. The N-terminal DELLA domain is a regulatory domain conferring GA responses, whereas the C-terminal GRAS domain is thought to function to regulate transcription (Sun and Gubler, 2004). More specifically, in the N-terminal domain there is the “DELLA” motif and the TVHYNP motif that interact with the HSL-like “lid” of GID1. The C-terminal half of the protein is strongly related to the SCARECROW family of regulatory proteins (Schwechheimer, 2008) and includes domains like SG2-like and SAW which bind to transcription factors to suppress GA-regulated induced growth (Figure 1.7).

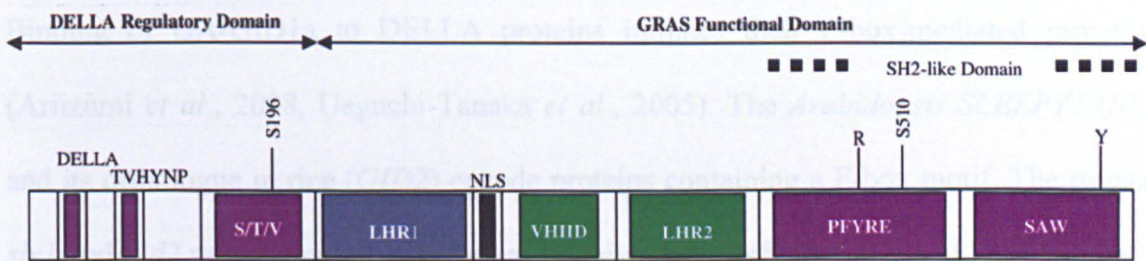


Figure 1.7 **Domain structure of a typical DELLA protein.** DELLA protein organization illustrating the conserved domains and subdomains involved in GID1 binding (purple), target binding (blue), nuclear localization (grey), and SLY1/GID2 binding (green). DELLA, TVHYNP, poly serine/threonine/valine (pS/T/V), Leucine repeat (LR), and VHIID repeats were named for the consensus amino acids. The DELLA and TVHYNP domains are specific for the DELLA repressor proteins, and all proteins containing these domains have been implicated in GA signalling (reproduced from Hauvermale *et al.*, 2012).

In *Arabidopsis*, DELLAs are encoded by the *GAI*, *RGA*, *RGL1*, *RGL2* and *RGL3* genes (Peng *et al.*, 1997; Silverstone *et al.*, 1998; King and Ben-Tal 2001). Genetic analyses have shown that each DELLA displays both distinct and overlapping functions in the regulation of plant development (Achard *et al.*, 2006). DELLA's gain-of-function mutations result in reduced GA response, whereas loss of function results in GA-constitutive phenotype, even when GA-biosynthesis inhibitors are present. Thus, indicating their key role as negative regulators in GA signalling (Richards *et al.*, 2001).

Yeast-two hybrid analyses have shown that interaction between GID1 and DELLAs occur in a GA-dependent manner. Interaction between the three AtGID1s and the five DELLAs proteins take place in all 15 possible combinations but with different affinities for each. Since the five DELLAs are differentially involved in GA-dependent process, it is likely that particular interactions between a specific AtGID1 and DELLA occur for the different GA-dependent processes (Ueguchi-Tanaka *et al.*, 2007).

1.3.3.3 DELLA degradation through the 26S proteasome

Binding of GA-GID1a to DELLA proteins initiates their F-box-mediated proteolysis (Ariizumi *et al.*, 2008, Ueguchi-Tanaka *et al.*, 2005). The *Arabidopsis SLEEPY1 (SLY1)* and its orthologue in rice (*GID2*) encode proteins containing a F-box motif. The recessive *sly1* and *gid2* mutants result in GA-unresponsive dwarfs (Steber *et al.*, 1998; Sasaki *et al.*, 2003).

These proteins act as part of the SCF (SKP1, CULLIN1, F-Box)-type E3 ubiquitin ligase complexes, conferring specificity for the DELLAs repressors. SLY1 and GID2 appear to activate GA signalling by targeting DELLA proteins, for ubiquitination and degradation through the 26S proteasome (Smalle and Vierstra, 2004). Therefore, by inducing the proteolysis of DELLA proteins, GA promotes the activation of DELLA-repressed/GA responsive genes and subsequently the release of growth repression (Figure 1.8) (Silverstone *et al.*, 2001).

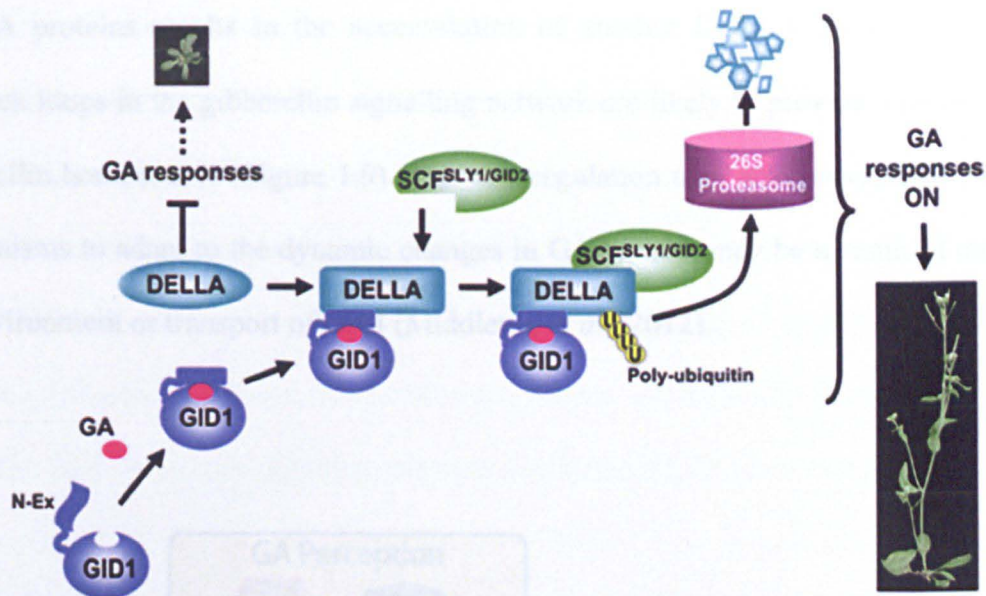


Figure 1.8. **GA signalling pathway.** GA binding to the GID1 receptor precedes the interaction with DELLA protein. This interaction may trigger a conformational change on DELLA that results in its recognition by SLY1 (a subunit of the SCFSLY1 complex). Once the interaction between the SCFSLY1 complex takes place, DELLA is polyubiquitinated and then degraded via the ubiquitin-proteasome pathway. Once DELLA is degraded, GA-induced growth response can take place (figure reproduced from Sun, 2010).

1.3.3.4 GA homeostasis

Positive and negative feedback control of transcription are mechanisms used to maintain GA signalling homeostasis (Middleton *et al.*, 2012; Willige *et al.*, 2007). First, GAs control their own synthesis by repressing the transcription of the rate limiting enzymes in their synthesis (such as the oxidases *GA3ox* and *GA20ox*), and by activating the transcription of the GA-inactivating catabolic enzyme *GA2ox*. Second, parallel to the GA-mediated DELLA degradation, GAs also promote DELLA protein transcription. Third, GA suppresses the transcription of the GID1 and SLY1 F-box protein genes. Thus, GA-induced DELLA protein degradation is readjusted by decreased GA biosynthesis, increased DELLA protein synthesis, and reduced GA sensitivity (reviewed by Schwechheimer, 2008). Another level of control is in the homeostasis of the levels of DELLA proteins. The stabilization of one of the DELLAs proteins is balanced by the reduction of another DELLA protein. Equally, the reduction in the levels of one of the

DELLA proteins results in the accumulation of another DELLA protein. The various feedback loops in the gibberellin signalling network are likely to provide a mechanism for gibberellin homeostasis (Figure 1.9). This autoregulation may also provide the plant with mechanisms to adapt to the dynamic changes in GA4 which may be a result of changes in the environment or transport of GA4 (Middleton *et al.*, 2012).

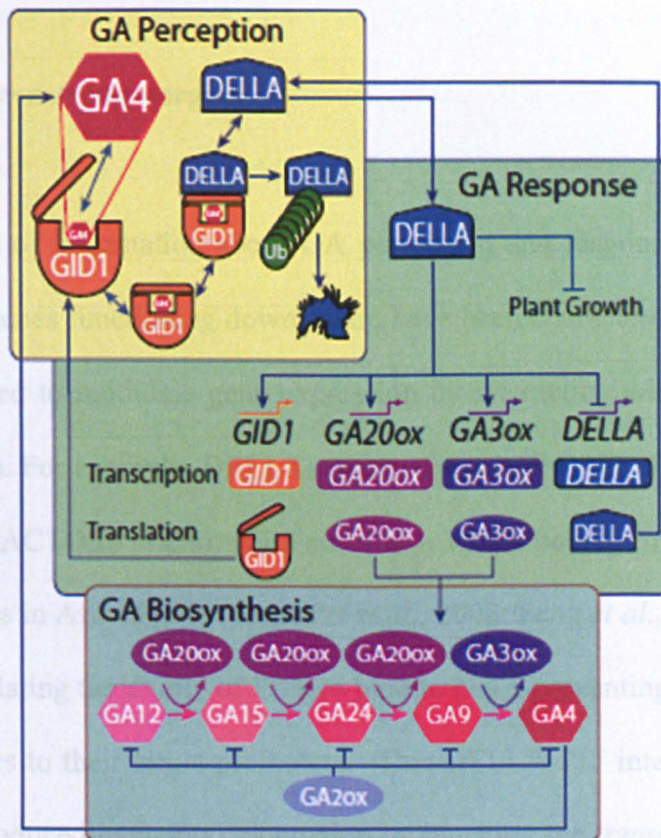


Figure 1.9. **Feedback look in the gibberellin signalling network.** The gibberellin signalling network is composed of three main modules. Perception: gibberellin (GA4) binds to the GID1 receptor, and this complex binds to DELLA proteins. The GA4–GID1 complex then mediates the ubiquitination (indicated by Ub) of the DELLA proteins. Response: DELLA proteins mediate transcriptional activation of the *GID1*, *GA20ox*, and *GA3ox* genes and the repression of *DELLA* transcription. Biosynthesis: the enzyme *GA20ox* converts GA12 to GA15, then to GA24, and finally, to GA9, which is subsequently converted to GA4 by the enzyme *GA3ox*. The various feedback loops within this modules help to provide a mechanism for GA homeostasis in order to maintain growth rates (reproduced from Middleton *et al.*, 2012).

At the biochemical level, it has been suggested that GA signalling is controlled by mechanisms different than GA-dependent protein degradation and transcription. O-GlcNAcylation modification of Ser and Thr residues by the enzyme OGT (O-linked N-acetylglucosamine transferase) often interferes with phosphorylation of nearby protein kinase sites (Slawson and Hart, 2003). SPY, a plant OGT, functions as a repressor of GA signalling (Filardo and Swain, 2003). Mutation of this protein results in partial suppression of the GA-biosynthesis or signalling mutants in which DELLA proteins accumulate.

1.3.3.5 DELLA downstream targets

Despite the wealth of information about GA perception and response pathways (fig 1.9) only a few of the genes functioning downstream have been characterised to date. DELLAs have been suggested to modulate gene expression by interacting with other transcription factors (Sun, 2011). For example, DELLAs interact physically with the PHYTOCHROME INTERACTING FACTORS (PIFs); PIF3 and PIF4, which belong to the family of bHLH transcription factors in *Arabidopsis* (de Lucas *et al.*, 2008; Feng *et al.*, 2008). DELLAs act by negatively regulating the ability of PIFs to bind to DNA preventing the binding of these transcription factors to their target promoters. This DELLA-PIF interaction results in the inhibition of PIF-induced hypocotyl elongation by blocking the transcription of PIF target genes. Light induced photomorphogenesis after germination is activated by transcription factors such as ELONGATED HYPOCOTYL5 (HY5), and the inactivation of other transcription factors that stimulate etiolated growth, like the PHYTOCHROME-INTERACTING FACTORS (Li *et al.*, 2010). GA appears to balance the effect of light by simultaneously negatively regulating HY5 protein levels and reducing the inhibitory effect that DELLAs have over PIFs (Alabadí and Blázquez, 2009).

In addition to PIFs, DELLA proteins have been found to interact with other members of the bHLH family. Arnaud *et al.*, (2010) showed that DELLAs can interact with ALCATRAZ (ALC) and prevent its function to control fruit development (Arnaud *et al.*, 2010). While Josse *et al.*, (2011) showed that DELLAs can interact with SPATULA (SPT) to control cotyledon expansion (Josse *et al.*, 2011). DELLAs have also been found to interact with another class of transcription regulators, the jasmonate ZIM-domain proteins (JAZs). In the absence of GA, DELLA binds JAZ1 and blocks its ability to bind and inhibit the transcriptional activator MYC2 (Chini *et al.*, 2007). The inactivation of MYC2 leads to shorter roots and the expression of JA and wound-induced genes. Therefore, DELLA acts as a positive regulator of JA response by blocking JAZ1 repressor action through protein-protein interaction (Hou *et al.*, 2010).

As well as this, chromatin immunoprecipitation (ChIP) experiments have shown that DELLAs interact directly with several promoters of its target genes (Zentella *et al.*, 2007; Zhang *et al.*, 2011). As shown in figure 1.9, several DELLA target genes are GA biosynthesis enzymes or GA receptors, supporting a role for DELLAs in maintaining GA homeostasis by feedback regulation of positive components in the upstream GA signalling pathway (Sun 2011) .

Other DELLA-induced target genes encode putative transcription factors/regulators, or RING-type ubiquitin E3 ligases (Zentella *et al.*, 2007). One of these DELLA targets is the E3 enzyme XERICO. In silico gene-expression analysis indicated that XERICO is induced by salt and osmotic stress and that promotes accumulation of abscisic acid that antagonizes GA effects (Ko *et al.*, 2006). Also, Zhang *et al.*, (2011) showed that expression of the SCARECROW-LIKE 3 (SCL3) protein is regulated by GA via DELLA protein

stabilisation. SCL3 is also a GRAS family member, but it does not contain the GA-responsive DELLA domain. SCL3, acts as a positive regulator of GA signalling and an attenuator of DELLA proteins (Heo *et al.*, 2011). Co-immunoprecipitation and transient expression assays showed that SCL3 antagonizes DELLA function in controlling target gene expression by direct protein–protein interaction (Zhang *et al.*, 2011). It appears that SCL3–DELLA interaction also is involved in maintaining GA homeostasis by regulating expression of upstream GA biosynthetic genes.

1.4 Root development in *A.thaliana*

1.4.1 Study of root development in *Arabidopsis thaliana*

Roots perform many essential functions including supplying water and nutrients, anchorage to the soil and establishment of biotic interactions in the rhizosphere. Roots are of special significance to agriculture; of particular interest is the present focus on improving roots with greater capacity to locate and use nutrients found in natural soils (Schiefelbein and Benfey, 1991). Modifications of root features such as radial patterning, distal patterning and root hair size and location could potentially modify root function, increasing its water/nutrient uptake. All these modifications together with an improved knowledge of processes such as cell expansion and lateral root development could lead to the creation of plants with improved roots able to perform better in particular soils.

The simplicity of the organization of the *Arabidopsis* root makes this model plant an excellent system to study different aspects of plant organogenesis, such as regulation of pattern formation, cell division, intercellular signalling and cell differentiation. The

Arabidopsis genome sequence has been completed and there are large numbers of root-mutant collections. On top of the genetic and molecular analyses advantages of using *Arabidopsis*, another major advantage is the small size and translucence of its roots, which allows growth of seedlings on agar plates where the roots can be easily visualised. This has made possible easy genetic screens for plants that exhibit abnormal root development.

1.4.2 Arabidopsis root structure

The *Arabidopsis* root has a simple structure with a characteristic radial pattern. There are highly organized cylindrical structures consisting of single layers of cells containing a fairly constant number of cells. Primary root tissues are organized in concentric cylinders of epidermis, ground tissue (cortex and endodermis), and stele (pericycle and vasculature) from outside to in (Dolan *et al.*, 1993). In the centre of the root, the vascular tissue has bilateral symmetry with water conducting xylem on the axis of symmetry and sugar transporting phloem on both sides of it. The pericycle is composed of an average of 12 cells surrounding the vascular tissues. Pericycle cells have the ability of initiate the formation of new lateral roots. The endodermis and cortex layers are both composed of a constant number of eight cells per ring. The outer layer, the epidermis, it is composed of two cell types, ones that form root hairs (trichoblasts) and others that do not form them (atrachoblasts). Near the root tip, there is also a layer of lateral root cap cells outside the epidermis and columella cells protecting the quiescent centre (QC) (Figure 1.10).

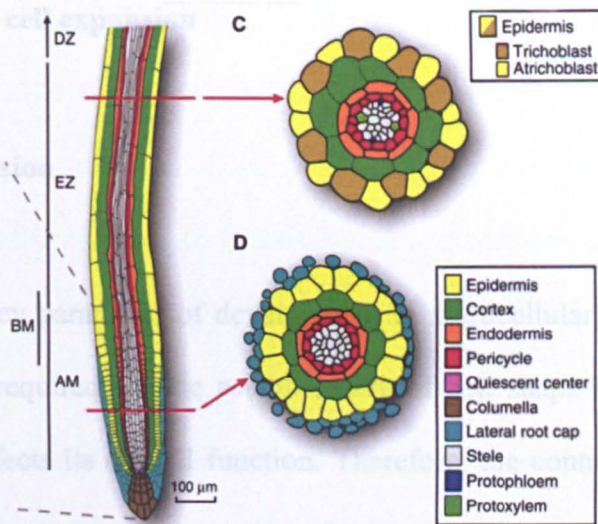


Figure 1.10. **Structure of the *Arabidopsis* root at tissue and cellular level.** a) Schematic representation of the proximal–distal organization of the root. Indicated on the left of the are the root apical meristem (AM), elongation zone (EZ), differentiation zone (DZ), and the basal meristem (BM). b) Cross section of root in the elongation zone showing the position of trichoblast and atrichoblast cell files. Also the location of the protoxylem and protophloem cells are indicated. c) Cross section of an immature root showing the radial organization of cell files (reproduced from Overvoorde *et al.*, 2010)

A developmental gradient is observed at the growing tip of roots. This gradient can be subdivided into 3 developmental zones. The apical tip belongs to the meristematic zone (apical and basal meristem) or zone of cell division. In this zone, cells continuously arise from the quiescent centre (QC) and undergo several rounds of divisions. (apical meristem). In the basal meristem the rate of cell division slows and gives way to the next zone, the elongation zone. The elongation zone is where cell division ceases and there is rapid growth by cell elongation. Then, there is the zone of differentiation or specialization, in which elongated cells from the different tissues mature into fully differentiated cells to assume their final fate. An increased length of epidermal cells demarcates the transition between the meristematic and elongation zones and the differentiation zone is made obvious by the manifestation of root hairs in the epidermis. The remaining part of the root belongs to the mature zone which is able to produce lateral roots.

1.5 GA regulation of cell expansion

1.5.1 Root cell expansion

Cell expansion is a key parameter of development in multicellular organisms. Regulation of cell expansion is required for the establishment of cell shape and polarity. The final shape of an organ affects its overall function. Therefore, the control of cell expansion in roots is a key factor to ensure the formation of a versatile root able to supply the required nutrients and adapt to the environment for the survival of the plant.

Due to the lack of cell movement during plant development, the final size and shape of the root is determined in major part by cell expansion. The sum of individual cell expansions taking place along a file of cells results in the anisotropic growth of the root.

Regulation of cell expansion in the root occurs in a way that the primary axis is usually parallel to the direction of growth, thus creating long cylindrical cells. Cell expansion in roots follows the cease in cell division. At the end of the root cap, the frequency of cell division decreases and cells increase in length (Green, 1976). Growth rates are consistently low across the meristematic region. Towards the elongation zone, growth is faster and more uniform and gradually decreases to zero at the end of this zone giving rise to the differentiation zone (Benfey and Scheres, 2000).

The direction and how far a cell expands are the two main determinants of a cell's final shape. Different types of cell expansion take place in different regions of the root. In order to produce cell files, initial cells and their progeny go through a continuous process of cell

expansion and division. At the beginning the expansion of the dividing root cells is quite slow and non-polar, so that their size remains rather constant. At the same time, formation of new cells from continuous cell divisions in the meristem move these cells upward in the cell file. Then a transition takes place to anisotropic cell expansion, which combined with cell division results in cells with radial dimensions longer than longitudinal dimensions. During this phase the final root radius is established. A second transition towards a highly polarized longitudinal expansion occurs in the beginning of the elongation zone. This expansion is fast and highly oriented in the longitudinal axis (Benfey and Scheres, 2000).

The regulation of this root growth is carried out by different hormones which regulates specific growth processes (cell proliferation, differentiation or expansion) in distinct tissues (Figure 1.11) (Ubeda-Tomás *et al.*, 2012).

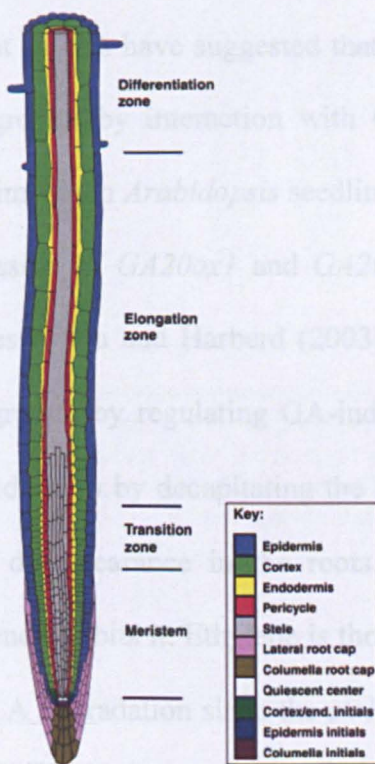


Figure 1.11. **Cell expansion in the root.** In the meristematic zone cells are generally isodiametric. As they traverse the elongation zone, radial expansion ends and rapid longitudinal expansion occurs (Ubeda-Tomás *et al.*, 2012).

1.5.2 Hormonal control of root cell expansion

The ability to rapidly increase root growth is particularly important for newly germinated seedlings in order to secure vital resources such as anchorage, water, and nutrients after emerging from their seed coat. Root growth is promoted by cell proliferation and cell elongation and the final root length is determined by the number of dividing cells and their final cell size (Beemster and Baskin, 1998). Phytohormones such as auxin, abscisic acid (ABA), brassinosteroids (BRs), cytokinin (CK), ethylene and gibberellins (GA) have shown to be involved in the regulation of the root growth and development (Perrot-Rechenmann, 2010). The signals of the different plant hormones are perceived by a range of different receptors that indirectly interact with transcription factors resulting in changes on gene expression and modifications to plant growth and development.

It has been described that both auxin and GA promote cell elongation in stems and roots. Recent studies have suggested that auxin derived from the shoot-apex promotes stem and root growth by interaction with GA metabolism and or signalling to some extent. In experiments in *Arabidopsis* seedlings, external application of auxin results in the increased expression of *GA20ox1* and *GA20ox2*, as well as *GA3ox* genes (Frigerio *et al.*, 2006). Studies by Fu and Harberd (2003) suggested that auxin appears to promote *Arabidopsis* root growth by regulating GA-induced degradation of RGA and GAI. Removing shoot-derived auxin by decapitating the seedlings decreases the ability of GA to promote GFP-RGA disappearance in the roots. While GA promotes root elongation, it seems that ethylene inhibits it. Ethylene is thought to inhibit GA-induced root elongation by blocking DELLA degradation since the *ctr1* (constitutive ethylene response) mutant shows delayed GFP-RGA disappearance in GA-treated roots (Achard *et al.*, 2006).

Recent studies have confirmed that different hormones control root growth by regulating specific growth processes in different tissues (Ubeda-Tomás *et al.*, 2012). GA promotes root elongation by regulating cell elongation and division in the endodermis (Ubeda-Tomás *et al.*, 2008; 2009). Auxin targets elongating epidermal cells during the gravitropic response and also regulates cell division in the meristem and stem cell niche (Swarup *et al.*, 2004; Blilou *et al.*, 2005). Cytokinin (CK) plays a role in the regulation of meristem size by antagonising the effect of auxin in cell division in the transition zone (Ruzicka *et al.*, 2009).

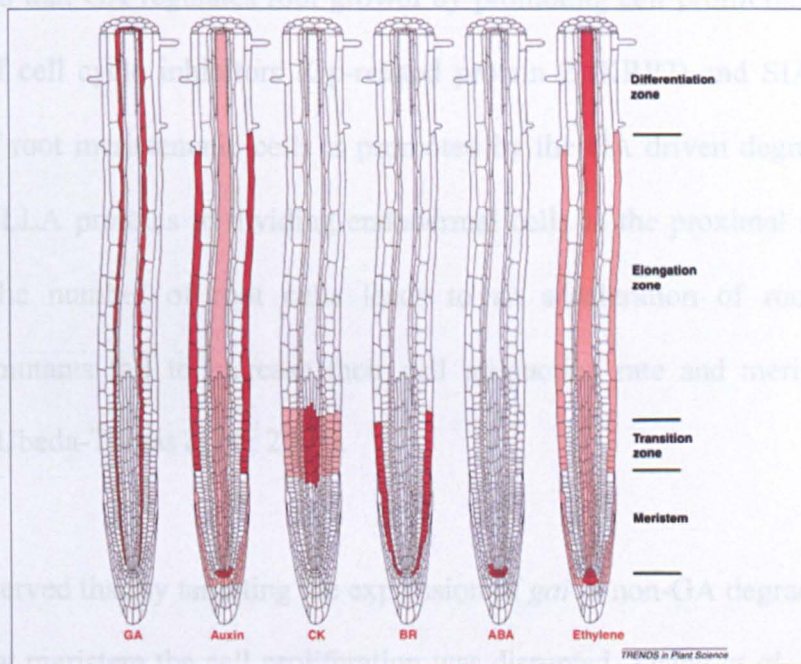


Figure 1.12. Schematic representation of hormone primary response tissues/regions in the Arabidopsis primary root. Red denotes tissues that are direct targets of designated hormone, whereas pink denotes indirect target tissues. From left to right each root represents the site of action of GA, Auxin, CK, BR, ABA and Ethylene respectively. On the right side of the root are indicated the different developmental zones of the root (reproduced from Ubeda-Tomás *et al.*, 2012).

CK is also involved in the differentiation of vascular tissue in the transition zone (Delo Ioio, *et al.*, 2007). Brassinosteroids target the epidermis in the meristem in the transition zone for the control of shoot and root growth (Savaldi-Goldstein *et al.*, 2007; Hacham *et*

al., 2011). In the case of ABA, it exerts its role in the root meristem acting in the QC and stem cells (Zhang *et al.*, 2010). Last, ethylene regulates cell division in QC and also auxin biosynthesis in columella cells (Swarup *et al.*, 2007). The novo-synthesised auxin is then transported to the epidermal cells of the elongation zone where it inhibits cell elongation and to increase ethylene sensitivity (Figure 1.12).

1.5.3 GA control of tissue-specific root cell expansion and division

At the level of cell proliferation, work by Archard *et al.*, (2008) and Ubeda-Tomás *et al.*, (2009) showed that GA regulates root growth by promoting cell proliferation through the modulation of cell cycle inhibitors Kip-related protein 2 (KRP2) and SIAMESE (SIM). Production of root meristematic cells is promoted by the GA driven degradation of GAI and RGA DELLA proteins in dividing endodermal cells in the proximal meristem. The increase in the number of root cells leads to an acceleration of root growth. GA biosynthetic mutants fail to increase their cell production rate and meristem size after germination (Ubeda-Tomás *et al.*, 2009).

They also observed that by targeting the expression of *gai* (a non-GA degradable mutant of *gai*) in the root meristem the cell proliferation was disrupted. Zhang *et al.*, (2011) showed that expression of the GRAS protein SCL3 is subject to regulation by GA via DELLA protein stabilisation. Mutant studies indicate that SCL3 plays a role in determining the timing of the root ground tissue divisions, acting downstream of SCR and SHORT-ROOT (SHR), both of which are key regulators for endodermis specification and stem-cell maintenance (Cui *et al.*, 2007).

Work by Heo *et al.*, (2011) suggests that SCL3 has a central role in coordinating GA-dependant cell elongation and is likely to form a conjugate with SCR, which modulates ground tissue cellular divisions. SCL3-DELLA interaction integrates GA signalling activities with the developmental program controlled by SCR and SHR. Expression of *gai* in dividing endodermal cells was sufficient to block root meristem enlargement (Figure 1.13).

However, expression of *gai* in the other tissues (either epidermis, cortical or stele) did not affect the root growth, thus indicating that the endodermis is the primary site of action of GA-regulated root growth (Ubeda-Tomás *et al.*, 2008).

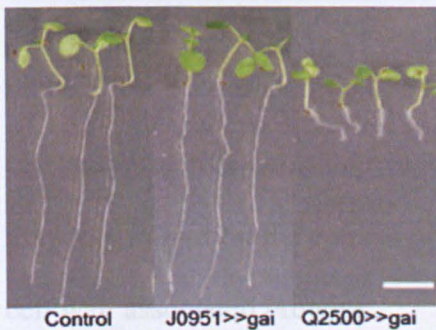


Figure 1.13. **Expression of *gai* in the *Arabidopsis* root.** Phenotype of 7 days-old seedlings. Expression of *gai* in the epidermis (J0951>>*gai*) does not result in a defect in root growth when compared to the control. On the other hand when *gai* is expressed in the endodermis there is a disruption in the root growth with a much shorter length than the control root. Bar= 5mm (figure adapted from Ubeda-Tomás *et al.*, 2008).

Based on the effect of the expression of *gai* in the endodermis, the authors concluded that endodermal cell expansion is a rate-limiting factor determining the elongation of other roots tissues, and hence of the entire root. Disruption of the endodermal anisotropic growth appears to cause a severe effect on the expansion of adjacent cortical and epidermal cells. The inability of the cortex cells to expand longitudinally results in a distinct radial expansion of these cells which cause the outer epidermal cells to buckle and bulge outwards (Figure 1.14).

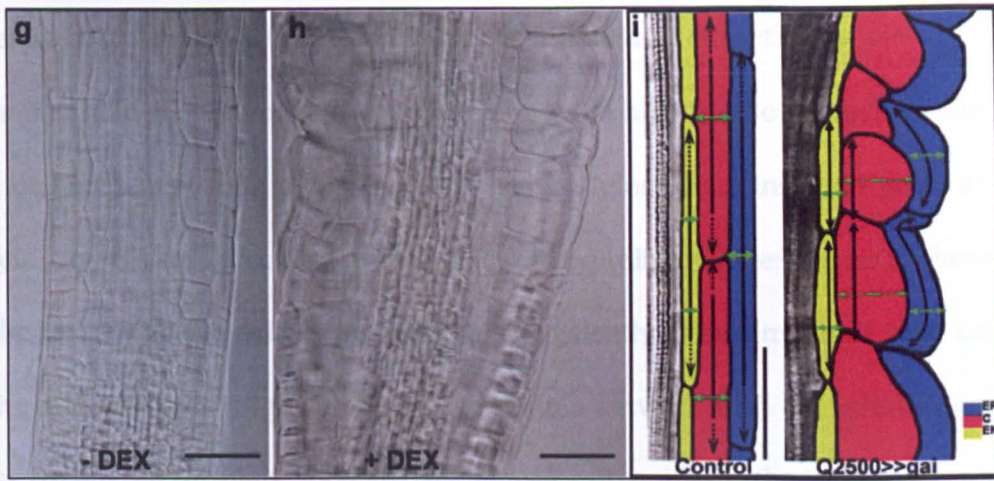


Figure 1.14. **Blocking of the GA response in the endodermis causes the adjacent tissues to bulge.** Seedlings growing in media without *gai* expression inducing-media (-DEX) or with inducing media (+DEX). Schematic diagram image of control (left) and Q2500>>*gai* (right) root cells, with a colour-coded key. GA induced degradation of DELLA repressor proteins in the endodermis promotes anisotropic growth of root cells in this tissue and surrounding root tissues. Anisotropic cell expansion (left, black arrows) usually predominates over radial cell expansion (green arrows). (Right) Disrupting the endodermal GA response by expressing the stabilised DELLA protein *gai* slows anisotropic cell expansion, causing cortical cells to expand radially and epidermal cells to bulge outwards (figure adapted from Ubeda-Tomás *et al.*, 2008).

Since it has been shown that cell expansion is directly associated with modifications of the cell wall properties, it is logical to assume that the regulation of endodermal cell elongation may rely in part on the control of GA over the cell wall extensibility and therefore over the cell wall associated proteins.

1.5.4 The plant cell wall

The plant cell wall is a complex biochemical network which has an important role in many aspects of the physiology of the plant. Amongst its functions, the plant cell wall provides mechanical strength, definition of cell shape, mediation in cell-cell communication processes, protection against pathogen attack and interaction with symbionts (Plomion *et al.*, 2001). The plant cell wall is attached to the middle lamella which acts as the interface between adjacent plant cells, ensuring the adhesion of a cell with its neighbours.

The plant cell wall consists of many layers of cellulose microfibrils associated by hydrogen bonds that hold the microfibrils together to provide high tensile strength. Interacting with these cellulose microfibrils can be found hemicelluloses, pectins and lignins as well as a discrete number of structural proteins (hydroxyproline-rich extensins), phenolic esters (ferulic and coumaric acids), ionically and covalently bound minerals (e.g. calcium and boron), and enzymes (Fig. 1.15) organized into a network with the cellulose microfibrils, the cross-linking glycans increase the tensile strength of the cellulose, whereas the coextensive network of pectins provides the cell wall with the ability to resist compression.

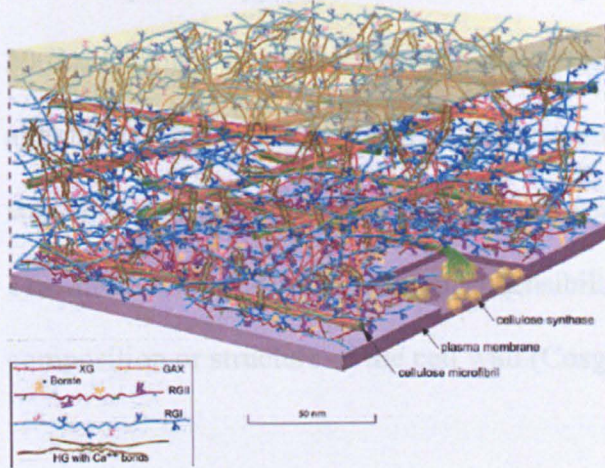


Figure 1.15. Structure of the primary cell wall. For clarity the proportion of cellulose in the cell wall has been reduced in the image. The amount of the various polymers is shown based approximately on their ratio to the amount of cellulose. The amount of cellulose shown was reduced, relative to a living cell (Fig. 1), for clarity. The main hemicellulose in plants is xyloglucan (shown in orange). Since the distance between microfibrils has been amplified, the hemicellulose cross-links [shown in dark orange (xyloglucan, XG) or light orange (glucuronoxylarabinoxylan, GAX)] are abnormally extended (Somerville *et al.*, 2004).

1.5.5 Root cell wall modifying enzymes

Cell expansion is primarily regulated by changes in the cell wall properties (Taiz, 1984). There is evidence that the plant cell wall regulates both the orientation and extent of cell expansion (Tsukaya and Beemster, 2006). It is believed that the polarity of the cell elongation is determined by the polarity of the arrangement and length of cellulose microfibrils (Wasteneys, 2004). Simultaneously, the orientation of cellulose microfibrils is

thought to be regulated by the arrangement of the cell cortical microtubules (MTs) (Baskin, 2005).

Plant cell enlargement is stimulated by the uptake of water into the vacuole, which rapidly expands to press against the cell wall. Cell-wall growth follows after the relaxation of the stress produced by the cell turgor, most likely by the modification of the mechanical properties regulating the cell wall extensibility. The control of this process relies in the regulated process of loosening and shifting of selected load-bearing linkages between cellulose microfibrils. The process of expansion has to be coupled with the process of cell wall component synthesis to avoid thinning of the wall during its expansion (Cosgrove, 2005). Changes on the cell wall during periods of slow cell growth are mainly due to alteration of the wall composition and cross-linking. On the other hand, changes on the cell wall due to rapid growth responses are associated to changes on cell wall extensibility. This modification on the cell wall extensibility does not result from modifications in the composition or structure of the cell wall (Cosgrove, 1993).

Relaxation of the wall stress (wall loosening) can be a consequence of the scission of a stress-bearing crosslink or from the sliding of such a crosslink along a scaffold. In both situations, the result is a reduction in the wall stress without a significant change in wall dimensions. As a consequence of wall relaxation, there is also a relaxation on the turgor pressure which leads in increased water uptake and further enlargement of the cell wall.

Currently, expansins, xyloglucan endotransglycolase/hydrolase, endo-(1,4)- β -d-glucanase and hydroxyl radicals have been proposed as wall loosening agents. Expansins are a group of non-enzymatic wall proteins that induce wall stress relaxation and extension in a pH-

dependent manner by disturbing the bonds that hold the microfibrils in place within the wall. The pH of the cell wall of growing cells is usually between 4.5 and 6, which is the range in which acidification activates expansin activity. Additionally, expansins appear to increase polymer mobility in the cell wall, allowing the structure to slide apart during extension (Whitney *et al.*, 2000).

Xyloglucans endotransglycolases/hydrolases (XTHs) are thought to act in this cell-wall loosening process by cleaving xyloglucan polymers and joining the newly generated end to another xyloglucan chain (xyloglucan endotransglucosylase, abbreviated XET, activity, (Figure 1.16) or to water (xyloglucan endohydrolase activity). Together with this wall loosening function, XTHs are also involved in trimming of xyloglucans at the surface of cellulose, wall strengthening, integration of new xyloglucans into the cell, xyloglucan hydrolysis (especially during xylem formation) and fruit softening have been reported for XTHs (Cosgrove 2005 , Miedes and Lorences, 2009). Expression analyses have shown that XTH gene expression is high in regions of active wall formation such as in elongation zones, and in regions where wall deposition continues after cell enlargement has ceased or where other forms of wall remodelling take place (Yokoyama *et al.*, 2004; Van Sandt, *et al.*, 2007)).

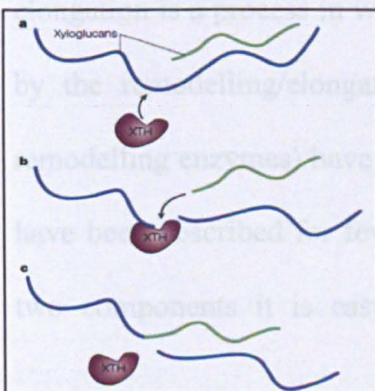


Figure 1.16. **The activity of xyloglucan endotransglucosylase/hydrolase (XTH) as an endotransglucosylase.** The enzyme performs two reactions, first a scission of a glycosidic bond in the xyloglucan backbone, followed by the re-formation of the bond with a second xyloglucan chain. a) Two xyloglucan chains are shown (blue and green). XTH binds to one of the chains. b) Upon cutting the xyloglucan backbone, one of the strands remains covalently attached to the catalytic site of the enzyme. The free end of a second xyloglucan moves into place for the second reaction. c) After ligation, a hybrid xyloglucan is formed, which is indicated as a xyloglucan of two colours and a xyloglucan fragment is released (Cosgrove, 2005).

Endo-(1,4)- β -D-glucanases also seem to have a role in the augment in wall extensibility by releasing trapped xyloglucans from the microfibrils. Some evidence of their role in the wall loosening process come from studies of over-expression of PopCel1 (enzyme from *Poplar*) in *A. thaliana*, which resulted in an increase of plant growth and cell wall extensibility. These results indicate that xyloglucan-cellulose interactions may play a key role in the mechanical and growth properties of the cell wall. It has also been proposed that hydroxyl radicals ($\cdot\text{OH}$) may, as non-enzymatic agents, increase wall extensibility by cutting wall polysaccharides (Cosgrove *et al.*, 2005).

In summary, in order for a cell to be able to expand its volume, a few key steps need to occur. First, a vacuole enlargement by the intake of water leads to an increase of turgor pressure, this is followed by the loosening of the cell wall. Finally, these two processes need to be complemented by the novo synthesis and reorganization of cell wall components. Cell wall remodelling enzymes are considered to be major players of these last two processes.

1.5.6 GA regulation of cell wall remodelling enzymes

As previously described, GAs play a key role in the regulation of cell elongation. Cell elongation is a process in which several factors are involved in and has to be accompanied by the remodelling/elongation of the cell wall. Several cell wall proteins (cell wall remodelling enzymes) have been identified to date and their roles on cell wall extensibility have been described for few of them. Therefore, because of this connection between the two components it is easy to think about a direct role of GAs over this cell wall

remodelling enzymes (CWRE). Some evidences that GAs regulate these certain cell wall proteins which control cell wall extensibility are described below:

At the level of regulating XTHs, Liu *et al.*, (2007) observed that the expression of *AtXTH21* (At2g18800), an *Arabidopsis* XTH gene that mainly expresses in roots and flowers, was induced by treatment with GA₃ but not other hormones. *AtXTH21* is involved in the maintenance of the thickness, integrity and strength of the cell wall during cell elongation. Study of loss-of-function mutants using T-DNA insertion lines for *AtXTH21* resulted in dwarf plants with short roots and thinner cell walls. On the other hand, study of with overexpression lines (35S::XTH21) showed plants with thicker cell walls. Thus, *AtXTH21* gene seems to play a key role in the growth of the primary roots by changing the deposition of cellulose and the elongation of cell wall. In rice, Jan *et al.*, (2004) demonstrated that *OsXTH8* (*Oryza sativa* XTH-related gene) expression in the leaf was up-regulated by GAs and there was very little effect of other hormones over its expression. Transgenic rice expressing an RNAi construct of *OsXTH8* exhibited reduced growth. These results indicate that *OsXTH8* is differentially expressed in rice leaf sheath in relation to gibberellin and potentially involved in cell elongation processes.

At the level of regulating XET, Cui *et al.*, (2005) showed that in the process of gravitropism in rice leaf sheath there is an asymmetric distribution of auxin and also of GAs. That could explain the differential cell growth detected in this process. At the level of regulating expression of expansins (EXP), Volger *et al.* (2003), showed that in the case of young stems in tomato plants, only specific EXP appear to be GA regulated. Regarding the regulation of pectin esterification, Derbyshire *et al.*, (2007) studying the hypocotyl of two GA mutants, *gal-3* and *gai*, and particularly the conditional rescue of cell elongation by

GA in the *gal-3* mutant, showed that active cell elongation is associated with a higher average level of pectin esterification. Therefore there has been a number of instances where GA has been shown to have a direct effect on cell wall remodelling enzymes.

1.6 OBJECTIVES OF THIS THESIS

Root elongation is a complex developmental process that is highly regulated at multiple levels. At the cellular level, cell expansion is a key developmental process for the establishment of an effective primary root that will lead to the formation of a successful plant root system. Root cell elongation is regulated by a complex network of signalling pathways where GA plays a key role. GA specifically contributes to the coordination of root growth by regulating cell elongation in the endodermis (Ubeda-Tomás *et al.*, 2008). However, the downstream targets and mechanisms for how this regulation is accomplished is unclear.

The aim of this present PhD project is to study how GA controls cell expansion in the root endodermis of *Arabidopsis thaliana*. In order to analyse the gene regulatory network targeted by GA in this tissue to promote root growth, forward and reverse genetic approaches have been pursued.

- 1) A forward genetic screen of a fast neutron mutagenized population using an inducible system that blocks the GA response in the endodermis (termed *SCR:gai-GR*) has been carried out. Screening of this mutated population was expected to uncover novel downstream components of the GA signalling pathway to help construct the regulatory network targeted by GA.

2) In parallel, a transcriptomics data set using the inducible *SCR:gai-GR* line has been produced in order to select candidate genes which may be key components of the GA-regulated root cell expansion. The main focus on the analysis of the transcriptomics data is to identify transcription factors and cell wall remodelling enzymes with the aim to reconstruct the gene regulatory network targeted by GA controlling endodermal cell expansion.

3) Finally, this project also intends to study how GA signalling controls cell wall properties to achieve cell expansion. Studies of mutated cell wall remodelling enzymes that appear to be regulated by GA have been carried out in order to identify components involved in this regulatory process.

CHAPTER 2: GENERAL MATERIALS AND METHODS

2.1 Plant material and physiological assays

2.1.1 Seed stock

Arabidopsis thaliana accessions Columbia (Col-0) and Landsberg *erecta* (Ler) were used as control lines in most of the experiments, unless otherwise specified. T-DNA insertion mutants were largely selected from the Salk collection (Alonso *et al.*, 2003) and obtained from the Nottingham Arabidopsis Stock Centre (NASC) except for some personal donations specified in the correspondent chapter. *SCR::gai-GR-YFP* seeds (Ubeda-Tomás *et al.*, 2009) and *RGR::GFP-RGR* seeds used for transcriptomics experiments were obtained from Dr. Susana Ubeda-Tomás.

2.1.2 Seed sterilisation and plating

Seed sterilisation was carried out in a laminar flow hood. Seeds were aliquoted into 1,5mL Microcentrifuge tubes and treated with a 5% (v/v) sodium hypochlorite solution for 5 minutes. After that time, the seeds were washed three times with sterile ddH₂O. Seeds were plated onto growth media in 12.1 cm square plates containing 65mL of growth media, using a P20 Gilson pipette and an Mltipipette tip (Barky Instruments International, Folkestone, UK).

2.1.3 Growth media

The growth media consisted of half- strength MS salts (Murashige and Skoog, 1962) [0.43% (w/v) MS salts (Sigma Aldrich Co., Dorset, UK), 1% (w/v) agarose (PGP, Park Scientific Ltd. Northampton, UK) and with the pH adjusted to 6.2 with KOH prior to autoclaving. Plates were sealed using micropore tape (3M, Bracknell, UK). For specific experiments, growth media was supplemented as required with Dexamethasone (1 μ M), hygromycin (50 μ g/mL), kanamycin (50 μ g/mL) or BASTA (10 μ m/mL) once it had cooled.

For transcriptomics studies, seeds were plated over a sterile 100 μ m nylon mesh (Lockertex, Warrington, UK) placed over the growth media to facilitate the dissection and collection of roots for RNA extraction.

2.1.4 Stratification

To optimise synchronised seed germination, seeds plated on the appropriate media, were incubated at 4°C in the dark for 2 days. The seeds were then transferred into constant light conditions (50 μ mol·m²sec⁻¹) at 22°C and grown vertically for length of time required.

2.1.5 Seed collection and cross pollination

When seed collection or cross pollination was required, seeds growing on plates (as described on 2.1.3) were transferred to soil after approximately 10 dag (days after germination). Individual seedlings were transferred to 9cm pots containing 3:1 mix of

compost (Levington M3) vermiperil (Silvaperl) and grown at 20°C under a 12-h light, 12-h dark regime in the greenhouse. Plants were covered with plastic disposable sleeves to prevent cross pollination.

Plants were ready for cross pollination once they had bolted and produced mature flowers. The receptive inflorescence had all the opened flowers removed. The remaining floral buds were emasculated using forceps under microscope (Leica, Microsystems GmbH Wetzlar, Germany). Then, a mature stamen from a flower from the donator plant was selected. This stamen was brushed onto the recipient stigma until pollen was visible on the stigma surface. The formed siliques were left to turn yellow on the plant before collecting and were left to dry for subsequent studies.

2.2 Physiological assays

2.2.1 Root growth assays and Image analysis

To assess basal root growth, root length of seedlings grown vertically was measured from hypocotyl to root tip for a period of days (from 3 dag to 5-8 dag). Analysis of the root length was done using NeuronJ plugin of the ImageJ 1.4.1j (<http://rsb.info.nih.gov/ij/>) software. Growth rates (GR) were measured as means of length of the root (mm)/time (hours). Unless differently stated, at least three biological replicates were performed for each root growth assays with at least fifteen seedlings per line. Data are presented as the mean +/- the standard error and two-tail Student *t*-tests were performed using Microsoft Excel software to check for significance (p-Value <0,05) were performed.

2.2.2 Confocal microscopy for root analysis

Confocal microscopy to image *Arabidopsis* roots was performed using a Leica SP5 confocal laser scanning microscope (Leica, Milton-Keynes, UK). For cell quantification and cell length measurements, seedlings were treated with propidium iodide (10 µg/ml; Sigma) to stain the cell walls.

Quantification and measuring of cells was performed with the Cell-o-Tape image analysis tool (French *et al.*, 2012). Cell Production Rate (CPR) was measured as the GR/average cell length (cell/hour). Unless differently stated, at least three biological replicates were performed for each root growth assays with at least ten seedlings per line. Data are presented as the mean +/- the standard error and two-tail Student *t*-tests to check for significance (p-Value <0,05) were performed using Microsoft Excel software.

2.3 Nucleic Acid isolation

2.3.1 Genomic DNA extraction

DNA was extracted from single leaves that were harvested and snap frozen in liquid nitrogen, these were then homogenised to a fine powder. When thawed, 600µl of DNA extraction buffer (0.2M Tris-HCl pH7.4, 0.025M EDTA, 0.25M NaCl and SDS 0.5% w/v) was added. Samples were vortexed vigorously for 30 seconds and were then centrifuged at 14000 x g for 5 minutes to remove cell debris. Supernatant was collected and the DNA was precipitated for 5 minutes on ice with 500µl of isopropanol (Fisher). Samples were centrifuge at 14000 x g for 5 minutes, and the DNA pellet was air dried for 30 minutes or

for 10 minutes under vacuum. The DNA was then re-suspended in 30µl of sterile water and stored at -20°C.

2.3.2 RNA extraction

mRNA was extracted using the QIAGEN RNeasy Mini kit (QIAGEN, West Sussex, UK). Roots from selected seedlings were snap frozen in liquid nitrogen and then ground to a fine powder. 350µl of Buffer RLT (containing 0.1 % (v/v) β-mercaptoethanol (Fisher Scientific UK Ltd, Loughborough, UK) was added to the homogenised tissue and mixed thoroughly. The lysate was transferred to a QIAshredder spin column and centrifuged for 5 minutes at full speed (13000 x g). The supernatant was transferred to a new microcentrifuge tube and 1:1 volume of 70% ethanol was added and mixed by pipetting.

The sample was then transferred to an RNeasy MinElute spin column placed in a 2 ml collection tube and centrifuged for 15 seconds at 10000 x g, discarding the flow-through. 350 µl Buffer RW1 was added to the RNeasy MinElute spin column and it was again centrifuged for 15 seconds to 10000 x g and the flow-through was discarded. This step was repeated and the flow-through and collection tube were discarded.

The RNeasy MinElute spin column was placed in a new 2 ml collection tube and 500 µl Buffer RPE was added to the spin column and centrifuged for 15 seconds to 10,000 x g to wash the spin column membrane, discarding the flow through. 500 µl of 80% ethanol was added to the RNeasy MinElute spin column. After centrifugation at 10000 x g for 2 minutes the flow-through and the collection tube were discarded. Then the RNeasy MinElute spin column was placed in a new 2 ml collection tube and with the lid opened

centrifuged at full speed for 5 min to dry the column, the flow-through was discarded. Then the column was transferred to a 1.5 ml microcentrifuge tube and 14µl of RNase-free water was added directly to the column membrane. The sample was centrifuged at 13000 x g for 1 min to elute the RNA. Samples were kept at -80°C.

2.3.3 cDNA synthesis

mRNA was reverse transcribed into cDNA using the Transcriptor First Strand cDNA Synthesis kit (Roche Diagnostics Ltd., Lewes, UK) following the manufacturer's protocol. 500ng of mRNA was made up to a volume of 10µL using RNase-free water and 50pmol Anchored-oligo (dT)₁₈ primer ((Roche Diagnostics Ltd., Lewes, UK) was added. The sample was incubated at 65°C for ten minutes and then transferred to ice. 1X Transcriptor RT reaction buffer (Roche Diagnostics Ltd., Lewes, UK), 20 U Protector RNase Inhibitor (Roche Diagnostics Ltd., Lewes, UK), 1mM dNTPs and 10U Transcriptor reverse transcriptase were added and mixed by pipetting. The sample was then incubated at 55°C for 30 min. The cDNA was stored at -20°C.

2.3.4 Polymerase chain reaction (PCR)

PCR (and RT-PCR) was carried out in 20µl reactions containing 20-200ng DNA, 0.5nM primers, 0.2 nM dNTPs, 2mM MgCl₂ and 10U Mango-Taq DNA Polymerase (Bioline USA Inc., USA) in 1x PCR buffer. The PCR machine used in all experiments was AB GeneAmp PCR System 9700 (Applied Biosystems, USA). A standard PCR programme was used for all the different reactions with the only variation of annealing temperature which was adjusted for each reaction to temperatures between 53°C and 57°C (Table 2.1).

Primers used for product amplification were designed with the Primer 3 design tool (<http://frodo.wi.mit.edu>).

	Initial denaturation	94°C for 2 min
35 Cycles:	{	Denaturation 94°C for 30 sec
		Annealing 53-57 °C for 30 sec
		Extension 72°C for 1 min
	Final extension	72°C for 10 min
		4°C ∞

Table 2.1. Standard PCR programme

2.3.5 Agarose gel electrophoresis

Visualisation and separation of DNA was done by agarose gel electrophoresis. 1% (w/v) agarose (GIBCO BRL.) was added to 0.5 X TBE buffer (10X TBE buffer: 1M Tris-HCL pH8, 0.9 Boric acid, 0.01M EDTA) and melted in a microwave. To the mix, 0.4 mg of ethidium bromide (Sigma Chemicals, Sigma-Aldridge Co., Dorset, UK) was added to 100mL. The mix was then poured into a gel tray (BIO-RAD) and left to solidify. For each DNA sample 10µl was loaded into each gel well. Gels were run at 90V in gel tank reservoirs filled with 0.5X TBE buffer. DNA bands were visualised using a UV trans-illuminator computer system (Syngene, Cambridge, UK).

2.3.6 DNA purification from gel

Gel bands were purified using the Qiagen MinElute Kit following manufacturer's instructions. The band of interest was cut from the gel and the weight recorded. Three volumes of Buffer QG were added to 1 volume of gel. The sample was then incubated at 50°C until the gel slice was completely dissolved. One gel volume of isopropanol was added to the sample and mixed gently by inverting the tube. Next the sample was transferred to a MinElute column placed in a 2 ml collection tube and centrifuged for 1 minute at 13000 x g. The flow-through was discarded. 500 µl of QG buffer were added to the sample and then it was centrifuged for another minute at 13000 x g. The flow-through was again discarded. Subsequently, after adding 750µl of buffer PE the sample was centrifuged for 1 minute at 13000 x g. The flow-through was discarded and the sample centrifuged for an additional minute to dry the column. After that, the MinElute column was placed in a clean 1.5mL microcentrifuge tubes. The DNA was eluted by adding 10µl of H₂O to the centre of the membrane letting it stand for 1 minute before centrifuging for 1 minute at 13000 x g.

2.4 Cloning

2.4.1 Restriction enzyme digestion

Restriction digestion of PCR products was carried out in 10µl volumes containing 1 x buffer (New England Biolabs, Hitchin, UK), 2.5 U restriction enzyme (New England Biolabs, Hitchin, UK) and 5µl PCR product. Bovine serum albumin (BSA) was added to a

final concentration of 0.1 mg ml^{-1} according to manufacturer's recommendations.

Reactions were incubated at the recommended temperature for 2 hours.

2.4.2 Ligation reaction

For the ligation reaction a ratio of 3:1 [insert]:[vector] (mol/mL) was used. A total of $10 \mu\text{L}$ of Ligation Mix consisting of $1.0 \mu\text{L}$ 10X T4 ligase buffer (50 mM Tris-HCl, 10 mM MgCl_2 , 1 mM ATP, 10 mM Dithiothreitol, pH 7.5 at 25°C), $7 \mu\text{L}$ of purified insert, $1 \mu\text{L}$ of purified vector and $1 \mu\text{L}$ T4 Ligase was used for each reaction. The Ligation Mix was incubated at room temperature overnight.

2.4.3 Preparation of *E.coli* DH5a chemically competent cells

A single colony of *E. coli* was inoculated in 2.5 ml of LB media without antibiotics and grown overnight in a shaker at $120 \times g$ at 37°C . Next day 250 ml of pre-warmed LB media without antibiotics were inoculated with the starter bacterial culture and incubated until the optical density (OD_{550}) reached 0.5 – 0.6; at that stage, the cell culture was placed on ice for 10 minutes and then centrifuged at $6000 \times g$ for 5 minutes at 4°C .

The supernatants were discarded and cells were gently re-suspended in 100 ml ice-cold TB I buffer (30 mM potassium acetate, 100mM rubidium chloride, 10 mM calcium chloride, 50mM manganese chloride, 15 % glycerol, pH adjusted at 5.8 with acetic acid). After incubating the cells on ice for 5 minutes, cells were centrifuged at $6000 \times g$ for 5 minutes at 4°C . The supernatant was carefully removed and the pellet was finally resuspended in 10 ml ice-cold TB II buffer (10 mM PIPES, 10 mM rubidium chloride, 75 mM calcium

chloride, 15% glycerol, pH adjusted at 6.5 with KOH). Aliquots of 50 μ l were dispensed and snap frozen in liquid nitrogen. Competent cells were kept at -80°C for further use.

2.4.4 Transformation of *E.coli* DH5 α competent cells

A total of 10 μ L of DNA (ligation product) were added to aliquots of 100 μ L of *E.coli* DH5 α competent cells for each reaction. Then the mix was incubated on ice for 20 minutes. After that time, the cells were heat shocked at 42°C for 40 seconds and put back to ice for 20 more minutes. After this time, 900 μ L of LB media were added to the cells and then they were incubated at 37°C with continuous shaking. Finally, 150 μ L of cells were plated with LB-agar plates containing the appropriate antibiotic.

2.4.5 Transformation of *Agrobacterium* competent cells

Electro-competent *Agrobacterium* GV3101 strain containing the pSOUP vector necessary for replication was used in this project (kindly provided by Dr. U. Voss).

For electroporation of *Agrobacterium* cells, 1.5 μ l (100ng/ μ l) of the vector of interest was added to 50 μ l of prepared electro-competent cells and kept on ice. The cells and the DNA were gently mixed before being transferred to a pre-chilled cuvette. Electroporation was carried out using Bio-Rad GenePulser with the following settings: 2.5 Kv, 25 μ FD, 400 Ohms. The cells were recovered by adding 1 mL of LB media and then transferred to a new microcentrifuge tube to incubate in a shaker at 28°C for 1 hour. After this inoculation time, aliquots of 50 μ l, 100 μ l and 200 μ l were plated on plates containing solid LB media and the correspondent selection antibiotic. Plates were incubated at 28°C up to 48 hours.

2.4.6 Colony PCR

To perform colony PCR, bacterial colonies from *E. coli* and *Agrobacterium* to be analysed were first individually subcultured in 1 ml of liquid LB medium supplemented with the appropriate antibiotics and incubated for 2 hours in a rotary shaker at 37 °C or 28 °C respectively. 2 µl of the liquid culture were then used as template to perform a routine PCR reaction as described in section 2.3.5. For the thermal cycle an initial denaturation of 5 minutes was used every time.

2.4.7 Plasmid DNA extraction

Minipreps were done using the Qiaprep Miniprep Kit (Qiagen). Minipreps were done on cell cultures which had been grown overnight in 5mL of LB with appropriate antibiotic from the positive colonies confirmed by Colony PCRs.

First, cells from the culture were precipitated by centrifuging them at 5000 x g for 3 minutes. The pellet was re-suspended with 250 µl of Buffer P1 and transferred to a 1.5 ml microcentrifuge tube. Then, 250 µl of buffer P2 was added and mixed by inverting the tube. To that mix, 350 µl L of buffer N3 was added and mixed again by inverting the tube. The whole mix was then centrifuged at 13000 x g for 10 minutes and the supernatant transferred to a QIAprep spin column. The column was centrifuged at 13000 x g for 1 minute and then added 500µl of buffer PB to centrifuge the column again for 1 minute. Next, the flow-through was discarded and the column washed with 750 µl of buffer PE by centrifuging the sample at 13000 x g for 1 minute, the flow-through was discarded and the sample was centrifuged for a further minute at 13000 x g to dry the column. The QIAprep

spin column was transferred to a clean 1.5 ml microcentrifuge tube and the DNA was eluted in a total volume of 50 μ l deionised water.

2.4.8 Arabidopsis floral dip transformation

A single *Agrobacterium* colony containing the construct of interest was propagated in a 5mL LB culture with the selective antibiotics (30 μ g/ml Gentamicin and 50 μ g/ml Kanamycin, Sigma Aldrich, Gillingham, UK), at 28°C with shaking at 200 x g overnight. Then, this first culture was inoculated into 95 ml of same medium and grown at 28°C until the OD600 was between 0.7-1. This culture was centrifuged at 3500 x g for 10 minutes to pellet the cells, which were resuspended in 100ml of a 5 % (w/v) sucrose solution. Before dipping into plant, Silwet L-77 (0.05% w/v) surfactant was added to the sucrose solution containing the re-suspended cell pellet. *Arabidopsis* plants grown in 8-9 plants per 9 cm pots were first allowed to flower before the first floral bolts were removed. Approximately 4-5 days later the plants had re-grown new floral bolts and were ready for transformation by floral dip method described by Clough and Bent (1998). After dipping the plants in the sucrose solution containing the re-suspended cells pellet, plants were covered in a sealed plastic sleeve for 48 hours before opening and left to grow and set seed.

CHAPTER 3: FORWARD GENETIC SCREEN TO IDENTIFY NOVEL GA MUTANTS TO STUDY ROOT CELL EXPANSION (STUDY OF THE FAST NEUTRON *SCR::gai-GR-YFP* POPULATION)

3.1 INTRODUCTION

With the completion of the Arabidopsis genome sequencing (The Arabidopsis Genome Initiative, 2000), the sequence of every gene is now available. However, DNA and protein sequence has not been enough to identify the function of the majority of the *Arabidopsis* genes. Several steps and experimental approaches have been developed to date to be able to make the conversion from gene sequence to gene function. Forward genetics has proved very successful in the process of associating a phenotype to the gene. Similarly reverse genetics can be useful in associating a gene sequence to a function. In both reverse and forward genetic approaches, the function of the gene can usually be deduced from phenotypic changes observed as a consequence of modification of the gene activity (Alonso and Ecker 2006).

Numerous chemical, physical and biological agents can be employed to induce genome wide mutations in Arabidopsis. Normally the efficiencies and the outcome of the nature of the genomic lesion depend on the dose and the type of the mutagen used. In forward genetics, chemicals such as ethyl methane sulfonate (EMS) or radiation with γ -rays are commonly used to create mutations throughout the whole genome (Alonso and Ecker, 2006). More recently, fast neutron bombardment has also been used for large scale mutagenesis (Belfield *et al.*, 2012).

EMS and γ -rays mutagenesis methods usually give rise to point mutations, such as single nucleotide insertion, deletion or substitution (Fieldman *et al.*, 1994). EMS studies have

lead to the identification of key components of the GA signalling pathway. The *Arabidopsis sleepy1 (sly1-2)* was recovered from the screen of an EMS mutagenised population of *abil-1* (abscisic acid-insensitive) on the basis of lack of ability of the seeds to germinate in presence of 3 μ M abscisic acid (Steber *et al.*, 1998). Map-based cloning and further DNA sequence analysis revealed that *sly1-2* has a 2-bp deletion (Cys-337 and Thr-338) causing a frameshift that eliminates the last 40 amino acids of the protein (McGinnis *et al.*, 2003). However, EMS mutagenesis induced mutations generally have little or no effect on the activity of the mutagenised protein and causes a silent mis-sense mutation. In contrast, fast neutron bombardment generally gives rise to deletions and therefore chances of getting a null allele are very high. Molecular characterization of *Arabidopsis gal-3* (Sun *et al.*, 1992) and tomato *prf-3* (Salmeron *et al.*, 1996) further confirmed that fast neutron bombardment induces deletion mutations. Therefore, fast neutron mutagenesis offers a more efficient method to give rise to null mutants.

Fast neutron (FN) is a form of ionizing radiation commonly produced by exposure to uranium-aluminium alloy fuel source. Exposure to fast neutrons has been shown to be a very effective mutagen in plants (Li *et al.*, 2001). Many phenotype-associated genes have been successfully identified and cloned through such screens (Meinke *et al.*, 2003). With the *Arabidopsis* genome containing about 25000 genes (*Arabidopsis* Genome Initiative, 2000), irradiating 2500 seeds with fast neutron at a dose of 60 Grey (Gy) to inactivate a gene once on average, it is estimated that about 10 genes will be randomly mutated in each line (Koornneef *et al.*, 1982). These genomic alterations can be characterized by molecular techniques. For example, gibberellin biosynthetic gene GA1 was first cloned using a fast neutron allele *gal-3* (Sun *et al.*, 1992).

For a long time it has been commonly accepted that FN mainly induced deletions larger than a Kb in *Arabidopsis* (Bruggemann *et al.*, 1996). However, recent studies carried out by Belfield *et al.*, (2012) found a higher frequency of single base substitution than deletion mutations. Based on their results, it is suggested that fast neutron mutagenesis promotes the formation of mutational covalent linkages between adjacent pyrimidine residues. In addition, they showed that FNs induced more single base changes than large deletions, and that these single base deletions were probably caused by replication slippage. Therefore, when cloning mutants isolated from a FN mutagenesis population an appropriate sequencing method able to identify these potential single base changes are needed in order to increase the chances of identifying the gene of interest.

As described in the general introduction of this thesis, the GA signalling pathway has been well characterised upstream of DELLA proteins. Also, a large range of GA associated functions have been identified mainly through GA biosynthetic mutants or GA signalling mutants at the level of DELLAs. However, little is known about components acting downstream of DELLAs and how they relate to each other.

Therefore, in order to further investigate the molecular mechanisms of GA signalling that control cell elongation and therefore root growth, a forward genetic approach using fast neutron mutagenesis was followed to identify novel mutants of the GA signalling pathway.

A smart screen was designed where a fast neutron *SCR::gai-GR-YFP* population was employed to screen for novel GA signalling mutants. Fusion of the DELLA *gai* negative mutant to the glucocorticoid receptor (GR) results in arrest of the protein to the cytoplasm. But in presence of the steroid dexamethasone, nuclear translocation of *gai* takes place and the GA response is blocked in the endodermis preventing the root to grow. Mutation of any

component of GA signalling pathway acting downstream of GAI is likely to result in resistance to DEX treatment and in the restoration of the root growth.

3.2 MATERIALS AND METHODS

3.2.1 Plant Material

Fast-neutron-treated *Arabidopsis thaliana* seeds (Landsberg *erecta*, *Ler*) of the *SCR::gai-GR-YFP* line (Ubeda-Tomás *et al.*, 2008) were used for this screen. A non-mutagenised version of *SCR::gai-GR-YFP* seeds was used as positive control. As negative control it was used the *RGA::GFP-RGA* (RGR3; Silverstone *et al.*, 2001) line, which is the parental line of the *SCR::gai-GR-YFP* lacking the ability to block the GA response in a DEX inducible manner.

3.2.2 Fast neutron mutagenesis

A mutant population of the inducible line *SCR::gai-GR-YFP* was created by fast neutron irradiation. A total of 5000 transgenic *A. thaliana* seeds were mutagenised using 55 Grey (Gy) of fast neutrons (KFKI Atomic Energy Research Institute, Budapest, Hungary) to cover all the *Arabidopsis* genome. The resulting mutagenised seeds were sown in 242 pools of 20 M1 seeds.

3.2.3 Root growth assay for selection of putative mutants

3.2.3.1 Screening of the mutagenised *SCR::gai-GR-YFP* M2 population

The fast neutron mutagenised *SCR::gai-GR-YFP* segregating M2 population was screened for the identification of putative mutants. For each of the 242 pools, a total of 500 seeds were sterilised, stratified and germinated on MS media in single square Petri dishes as described in section 2.1 of general materials and methods. With the purpose of inducing the transgene expression, the media was supplemented with 10 μ M of Dexamethasone (Sigma Aldrich Co., Dorset, UK). After 7 days of continuous growth, seedlings were observed for restoration of root growth.

3.2.4 Confirmation of the *SCR::gai-GR-YFP* transgene integrity

3.2.4.1 Confirmation of the transgene presence by PCR

PCRs were carried out to detect the presence of the *gai* transgene for *SCR::gai-GR-YFP* putative mutants to discount a malfunction of the transgene due to the FN bombardment itself. A combination of primers that amplified part of both *gai* and *GR* sequences were used in order to discriminate between the endogenous *gai* sequence and the non-degradable version from the transgene (Table 3.1).

Gene	Primer	Sequence (5'-3')	Product size (bp)
<i>gai-GR</i>	GAI-S2-F	CGGCGGTGAGGGTTATCGGG	686
	GR7-R	GACCTCCTTAGGAACTGAG	
YFP	YS1-F	CCGGTACCAGCAAGGGCGAGGAGCTG TTCACC	706
	YS2-R	CCGGTACCCTTG TACAGCTCGTCCATGCCGAG	
actin	ACT1C-F	GATGGAGACCTCGAAAACCA	382
	ACT2C-R	CTGGAAAGTGCTGAGGGAAG	

Table 3.1. Summary of primers used for amplification of the gDNA and cDNA of the putative mutants. Information about the primers sequence and expected size of the amplified products are given.

PCR were performed as described in section 2.3.4 of general materials and methods. Amplification was conducted in 20 μ L reaction using gene specific primers and *Taq* DNA polymerase (Promega) for one cycle of 2 min at 94°C, followed by 35 cycles of 94°C, 30 sec; 58°C, 30 sec; 72°C, 1 min and a final elongation cycle at 72°C for 10 min. Primers for *gai-GR* and *YFP* detection were kindly provided by Dr. Ranjan Swarup (University of Nottingham).

3.2.4.2 Confirmation of the transgene expression by RT-PCR

The primers to amplify *gai-GR* and *YFP* used for RT-PCR were the same as for the PCR. Also, a further RT-PCR with *ACTIN8* primers for was performed as control to check the quality of the cDNA. Information about primer sequences and product length is described in Table 3.1. mRNA extraction and cDNA synthesis were carried out following protocols described on sections 2.3.2 and 2.3.3 of general materials and methods. RT-PCR was performed as described in 2.3.4.

3.2.4.3 Sequencing of the *gai* negative mutation

A combination of three pair of primers was used in order to amplify the *gai* fragment from the *SCR::gai-GR-YFP* transgene (table 3.2). Three overlapping fragments were obtained and sent for sequencing. Genomic DNA was extracted from whole roots as described in section 2.3.1 of general materials and methods

Primer	Sequence (5'-3')	Product size (bp)
Sq-F1	TTCGAAAGGTGGAAGACGAC	609
Sq-R1	TTTTCTCATCGCTCCGATTT	
Sq-F2	GACTGTAGCGGAAGCTCTGG	650
Sq-R2	CCTGCTCAACCACAGTGAAA	
Sq-F3	TTCGATGCTTGAGCTTAGACC	606
Sq-R3	GCTTGCTGAATCCCTTTGAT	

Table 3.2 List of primers to sequence the *gai-GR-YFP* fragment from the *SCR::gai-GR-YFP* transgene.

Sequence of the *SCR::gai-GR-YFP* transgene with the deletion site causing the *gai* mutation as well as the primer hybridization sites used for genotyping and sequencing is shown in Appendix I.

3.2.5 Phenotypic characterization of putative FN mutants

3.2.5.1 Root length and growth rate assay

Restoration of root length was assessed by measuring the length of the primary root of the putative mutants and comparing them with the background line *RGA::GFP-RGA* (RGR3). Percentage of root growth was measured by assuming the length of RGR3 as 100 % of root

growth and comparing the lengths of the different putative mutants against it. The analysis of the growth rate (GR) was carried out as described in chapter 2.2.1

3.2.5.2 Root meristem and root cell analyses of putative mutants

High resolution images used for the analysis at the cellular level were obtained using confocal microscopy as described in section 2.2.2. Cell Production Rate (CPR) was measured as the GR/average cell length (cell/hour). Procedures and statistical analysis are described in section 2.2.2 of general materials and methods.

3.2.6 Next generation sequencing of putative mutants

Outcrosses between the FN putative mutants with Col-0 plants were carried out as specified in the section 2.1.6 of general materials and methods. Double homozygous mutants for the transgene (*SCR::gai-GR-YFP*) and the FN mutation were selected through bulk segregation analysis. Seedlings were first grown in presence of 50µg/mL of Hygromycin and resistant plants were then transferred to media containing DEX (10 µM). Sterilisation, media preparation and plating of the seeds were carried out as described in section 2.1 of general materials and methods. From each confirmed double homozygous FN putative line, 50 seedlings were pooled together and DNA extracted as described in section 2.3.1 of general materials and methods.

3.3 RESULTS

3.3.1 Root growth assay for selection of putative mutants

3.3.1.1 Screening of the mutagenised *SCR::gai-GR-YFP* M2 population

There are two functional germ line cells in *Arabidopsis* therefore, in the segregating M2 population a recessive mutation is expected to segregate in a 7:1 ratio (4:0 for one cell and 3:1 for the other cell). Since the M2 population is the result of pools of 20 M1 seeds, a single recessive mutation in a given pool is expected to segregate at 159:1. Hence, it was estimated that 480 seeds/pool (3 X Standard deviation) had to be screened to have a high statistical probability to identify a mutation in a given pool.

Out of the 242 pools of *SCR::gai-GR-YFP* mutagenised M2-seeds screened, a total of 30 pools showed seedlings that appeared to have restored root growth. The number of DEX resistant seedlings varied between the different pools (Table 3.3). These putative mutants were taken to the next generation to confirm their phenotype before further analysis.

Pool number	Number of resistant seedlings observed/pool
16, 25, 27, 32, 36, 45, 47, 64, 73, 80, 94, 119, 153, 157, 163, 177, 195, 211, 214, 215	1
4, 40, 49, 135, 187, 199	2
84, 159, 191, 211	3

Table 3.3. Preliminary screen: A summary of putative mutants identified from *SCR::gai-GR-YFP* FN population screen. On this table are described those pool numbers from the 242 pools screened where seedlings with root growth restored were identified. The different pools are grouped according to the number of putative mutants identified (1, 2 or 3).

3.3.1.2 Validation of the mutant phenotype

All the putative mutants were taken to the M3 generation and their phenotype rescreened for restoration of root growth. As expected most of the putative mutants failed to show restoration of root growth upon rescreen and were perhaps false positives and hence were not investigated further. 14 putative mutants from 9 pools were confirmed to show restoration of root growth in presence of DEX and were investigated further (table 3.4).

Pool number	Putative FN mutants
FN25	FN25
FN27	FN27
FN40	FN40-1, FN40-2
FN49	FN49-1, FN49-2
FN80	FN80
FN84	FN84-1 FN84-2 FN84-3
FN191	FN191-3
FN199	FNM199-2

Table 3.4. Mutants with validated phenotype on the M3.

The extent of root growth recovery was quantified for each of the 14 putative mutants and was compared with the control *RGA::GFP-RGA* (RGR3; figure 3.1). As shown in figure 3.1, a big variation in the level of root growth restoration in the different putative mutants is observed.

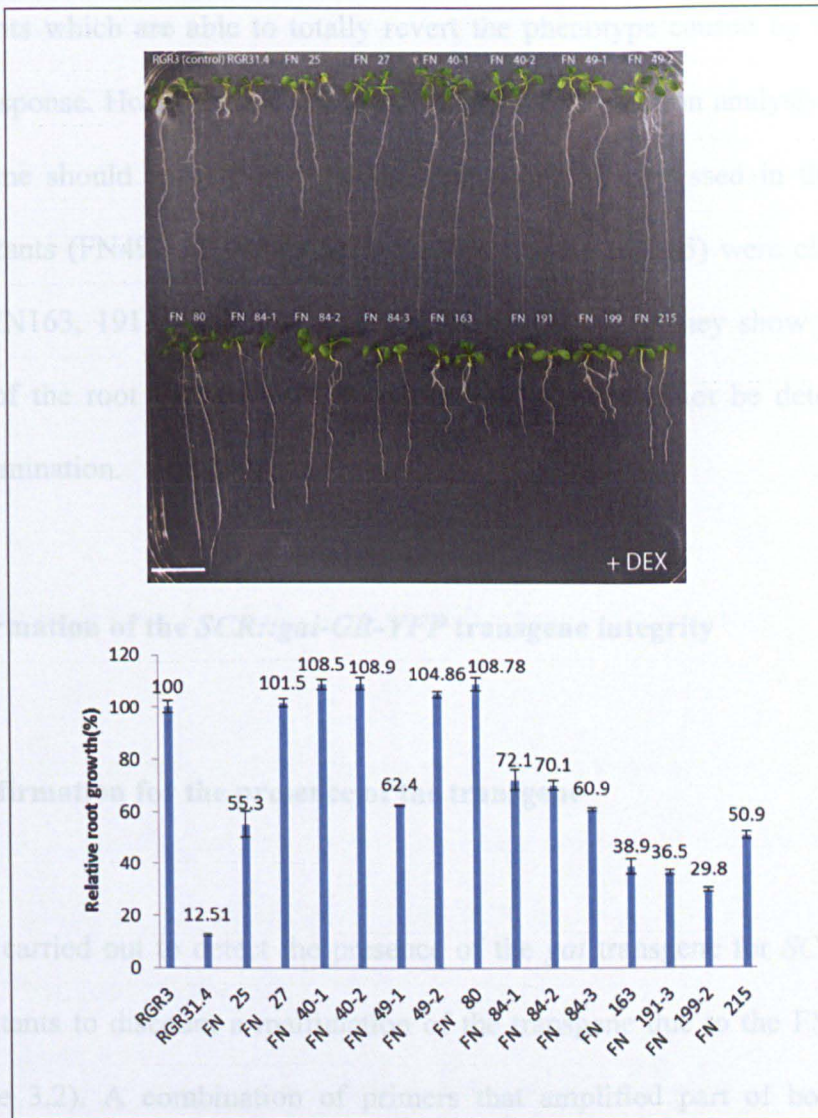


Figure 3.1. Putative FN mutants show different levels of root growth recovery phenotype. In the picture are shown two seedlings of each of the 14 FN putative mutant lines recovered from the screening of the M3 population grown in 1/2MS media containing dexamethasone. On the top left there is the control background line *RGA::GFP-RGA* (RGR3) and next to it the parental line of the mutagenised population *SCR::gai-GR-YFP* (RGR31.4). The graph represents the graphical quantification of relative root growth of each of the putative mutants when compared to the control line RGR3. The mean of the root lengths (mm) are shown with standard errors with vertical lines (Scale bar= 130mm).

On the basis of restoration of root growth phenotype of the different putative mutants, they were classified in three main categories; complete, partial or weak. A total of 5 putative mutants (FN27, FN40-1, FN40-2, FN49-2 and FN80) were classed as complete restoration of the root growth (with FN80 presenting roots larger than the control RGR3, figure 3.1).

This would imply that the lesion caused by the radiation is affecting a component or series

of components which are able to totally revert the phenotype caused by the lack of GA signalling response. However this is quite unlikely and expression analysis of the *gai-GR-YFP* transgene should show if the transgene is correctly expressed in these lines. Five putative mutants (FN49-1, FN84-1, FN84-2, FN84-3 and FN215) were classed as partial and three (FN163, 191-3, FN199-2) were classed as weak as they show partial to weak restoration of the root growth respectively. The FN25 could not be determined due to irregular germination.

3.3.2 Confirmation of the *SCR::gai-GR-YFP* transgene integrity

3.3.2.1 Confirmation for the presence of the transgene

PCR reactions were carried out to detect the presence of the *gai* transgene for *SCR::gai-GR-YFP* putative mutants to discount a malfunction of the transgene due to the FN bombardment itself (figure 3.2). A combination of primers that amplified part of both *gai* and GR sequences were used in order to discriminate between the endogenous *GAI* sequence and the non-degradable version from the transgene, *gai*.

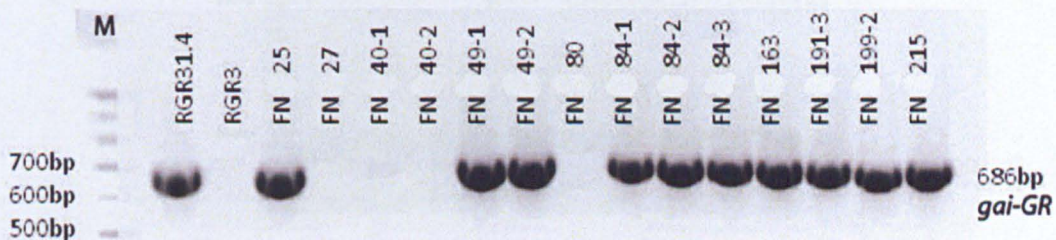


Figure 3.2. PCR reaction for detection of the *gai-GR* transgene. Electrophoresis photograph showing the results for the amplification of the *gai-GR* transgene. Amplification for the gDNA of all the putative mutants as well as the RGR3 and RGR31.4 control was performed. The first line on the left belongs to a 100bp DNA ladder. On the right, size of the expected band is mentioned.

PCR results clearly show that in most of the putative mutants (FN25, FN49-1, FN84-1, FN84-2, FN84-3, FN163, FN191-3, FN199-2 and FN215) the transgene can be detected. However, in four (FN27, FN40-1, FN40-2 and FN80) out of five mutants that showed complete restoration of root growth, no transgene band was detected. Interestingly, FN49-2, which also showed a complete recovery phenotype, did show positive results for amplification of *gai-GR* and hence expression analysis were done to ensure that the transgene is correctly expressed.

3.3.2.2 Confirmation of the *SCR::gai-GR-YFP* transgene expression

To investigate the expression of the transgene, RT-PCRs were performed in RNA isolated from roots. It is possible that the FN bombardment has caused a single base deletion or substitution, which is not identified on the PCR but which is enough to disrupt the expression of the gene (figure 3.3).

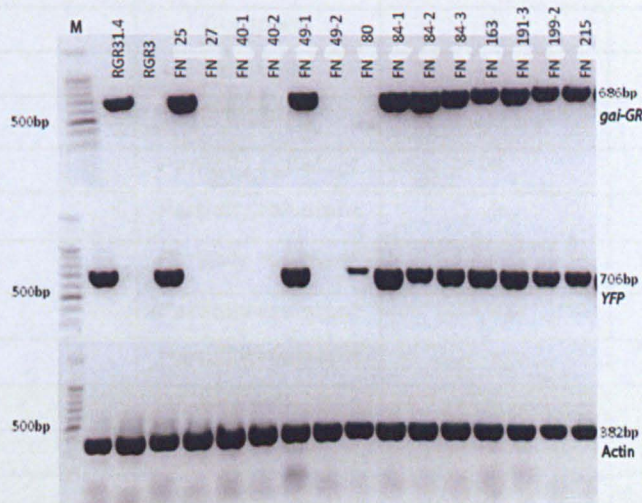


Figure 3.3. RT-PCR reactions for detection of the *gai-GR* transgene expression. Gel electrophoresis of RT-PCR reactions to detect the expression of *gai-GR* and *YFP* from the cDNA of the putative mutants. Two individual reactions to detect *gai-GR* and *YFP* respectively were performed to corroborate the integrity and expression of the whole transgene. A third reaction to amplify actin was carried out as control. First line on the top, shows the results of the amplification for *gai-GR*. The line on the middle shows the results of the *YFP* amplification. Bottom line corresponds to the control amplification with actin primers. The left of each line is the 100bp DNA ladder (M). On the right of each line the size of each expected band for the different amplifications is shown.

For completeness, RT-PCRs were also done in the cases where no transgene was detected. As expected no transgene expression was detected and these were used as negative controls. For FN80 there is a weak YFP band but this was ignored as false positive as PCR results show that the entire transgene cassette is missing in them.

Table 3.5 below summarises the genotyping of the 14 putative mutants. The different lines are first categorised based on their root growth recovery phenotype. Then, in the next column it is indicated whether these putative mutants still preserve the *SCR::gai-GR-YFP* transgene and finally if the transgene is expressed.

Line	Restoration of root growth	Result of PCR (<i>SCR::gai-GR-YFP</i> presence)	Result of RT-PCR (<i>SCR::gai-GR-YFP</i> expression)
RGR3 (Negative control)		Negative (-)	-
RGR31.4 (Positive control)		Positive (+)	+
FN27	Complete	-	-
FN40-1	Complete	-	-
FN40-2	Complete	-	-
FN49-2	Complete	+	-
FN80	Complete	-	-
FN25	(Irregular)	+	+
FN49-1	Partially resistant	+	+
FN84-1	Partially resistant	+	+
FN84-2	Partially resistant	+	+
FN84-3	Partially resistant	+	+
FN215	Partially resistant	+	+
FN163	weak	+	+
FN191-3	Weak	+	+
FN199-2	Weak	+	+

Table 3.5. **Characterisation of the 14 putative mutants pulled out from the FN mutagenised *SCR::gai-GR-YFP* population.** The different putative FN mutants are grouped in three color-code based on their root phenotype. In beige are those lines which a complete root growth recovery, in blue those ones with a partial phenotype and in green those one with weak root growth restoration. The first column refers to the name given to each mutant and the controls. The second one describes the root phenotype observed. Genotype of each mutant to confirm the transgene present was done by PCR (3rd column). Results for RT-PCRs to verify that the transgene was expressing are shown in the last column.

In summary, genotyping and the transgene expression analysis clearly show that in cases where there were partial or weak restoration of root growth the transgene appears to be intact and *gai* can be expressed in a normal fashion in these mutants to block GA response in the endodermis when induced with DEX. If this is indeed true, the phenotypes recovered are likely to be due to genes acting downstream of *gai* that have been affected by the mutagenesis.

3.3.2.3 Sequencing of the *gai* negative mutation

Even though RT-PCR results were positive in most cases, it is possible that the integrity of the transgene has been affected by the mutagenesis in a way that the *gai* gene was expressed but the protein was non functional. Therefore, all the putative mutants which have shown to express *gai-GR-YFP* were sequenced to corroborate the integrity of the transgene. The results suggested that none of the putative mutants showed any abnormalities. Therefore, it appears that a functional *gai* protein should form in each of the FN putative mutants thus blocking the GA response in the endodermis.

3.3.3 All the putative FN mutants are recessive mutations

In order to determine whether the different putative FN mutants isolated from the M3 population were recessive or dominant mutations they were backcrossed with the non mutated parental line *SCR::gai-GR-YFP*.

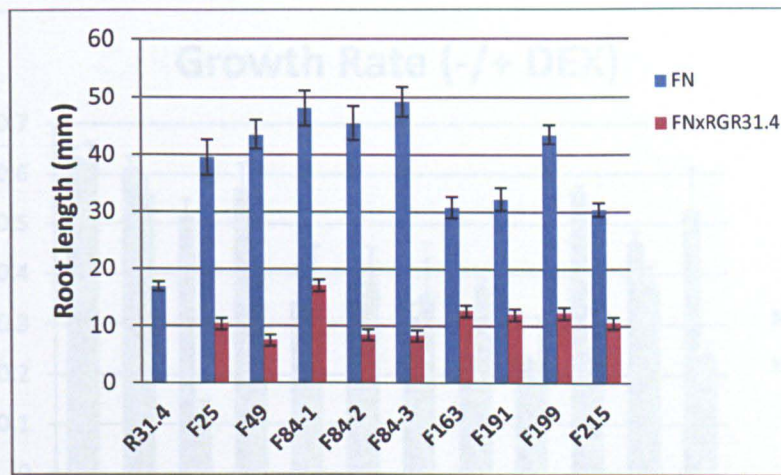


Figure 3.4. Analysis of the root growth recovery phenotype for the backcrossed FN putative mutants with the non-mutagenised parental line. The graph shows the overall length of the primary root for the FN putative mutants (F=FN, blue) together with the overall length of the F1 of crossing these mutants with RGR31.4 (red). The length of the parental line RGR31.4 is shown as control. Measures were taken at 9 dag. The mean of the root lengths (mm) are shown with standard errors with vertical lines.

As shown in figure 3.4, none of the 9 putative FN mutants are able to recover the root growth phenotype when backcrossed with the parental line. Therefore, it appears that the recovery phenotypes of all the FN putative mutants are caused by recessive mutations.

3.3.4 Phenotypic analysis

3.3.4.1 Growth rate analysis

Once the mutant phenotype was validated and shown that it was not due to some artefact in transgene rearrangement, detailed phenotypic characterization of these mutants was done. First, the growth rate of the different FN mutants in presence or absence of DEX was compared. If the mutation responsible for the recovery of the root growth is involved in the GA signalling acting downstream of DELLA, the growth of the roots in absence of the expression of *gai* should be similar to the non mutated parental line (RGR31.4).

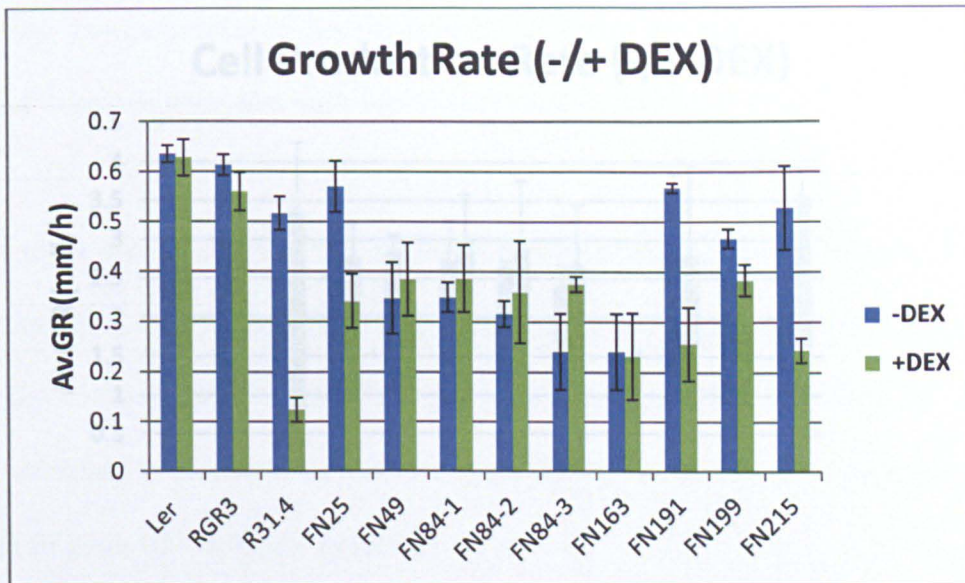


Figure 3.5. Analysis of the growth rate (GR) of the FN putative mutants. The GR (mm/h) for the roots of each putative lines was measured in both inducible (+DEX) and non inducible (-DEX) conditions. Landsberg *erecta* (Ler), RGR3 and the non-mutated parental line *SCR::gai-GR-YFP* (RGR31.4) were used as controls. Vertical lines in top of each bar indicate +/- SD.

From the results (figure 3.5) it can be observed that FN putative mutants can be classed in two major groups based on their growth rate phenotype in absence of DEX. FN25, FN191, FN199 and FN215 show a wild-type like growth rate in absence of *gai* expression and a reduced growth rate when the GA response is blocked in the endodermis. On the other hand, FN49, FN84-1, FN84-2, FN84-3 and FN163 appear to be insensitive to DEX thus showing a reduced growth rate in both presence and absence of the transgene expression.

3.3.4.2 Cell production rate analysis

To understand the cellular basis of the root phenotype associated with these mutants the cell production rate (CPR) was measured in inducible (+DEX) and not inducible conditions (-DEX).

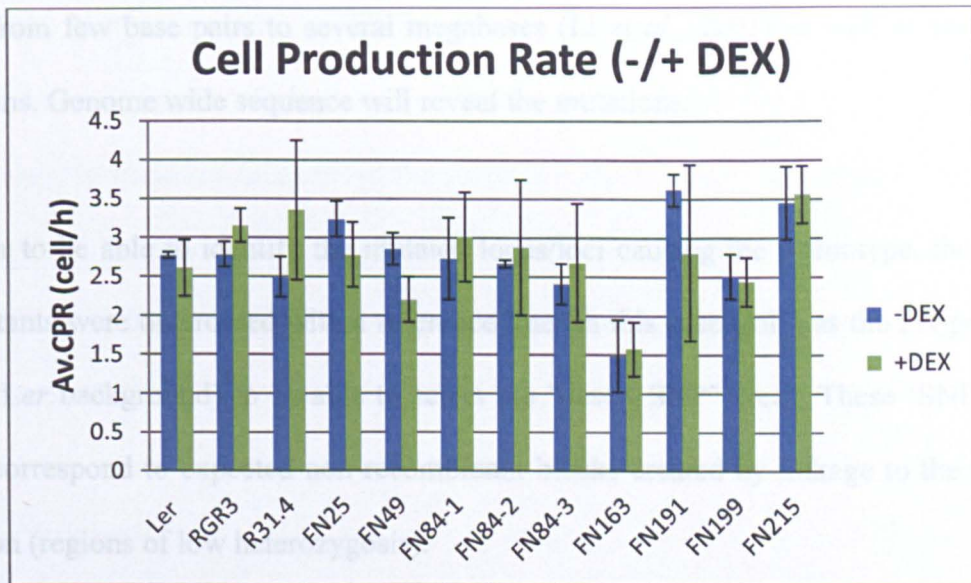


Figure 3.6. Cell Production Rate (CPR) measures for the FN putative mutants. The CPR (GR/mature cell length represented as cell/h) of each putative mutant was measured in both inducible (+DEX) and non inducible (-DEX) conditions. *Ler* (*Landsberg erecta*), RGR3 and the non-mutated parental line *SCR::gai-GR-YFP* (RGR31.4) were used as controls. Vertical lines in top of each bar indicate +/- SD.

As seen in figure 3.6, FN163 is the only line with reduced CPR, both in the presence and absence of DEX. This could be an indication that the mutation, which has been previously shown to act independent of the GA induced blocked response, could be affecting some component involved in the cell cycle.

For the rest of the FN putative mutants, the CPR is similar to those of the controls both under inducible and non inducible conditions suggesting that root growth is affected at the level of cell expansion for these mutants.

3.3.5 Next generation sequencing of putative mutants

In order to clone the genes responsible for the phenotype, a Next Generation Sequence (NGS) approach was used. FN mutagenesis can create DNA deletions in a wide range of

sizes (from few base pairs to several megabases (Li *et al.*, 2001) as well as single point mutations. Genome wide sequence will reveal the mutations.

In order to be able to identify the mutated locus/loci causing the phenotype, the putative FN mutants were outcrossed with a reference line (in this case Col – as the FN population was in *Ler* background) to be able to select the "desert SNP" areas. These 'SNP deserts' areas, correspond to expected non-recombinant blocks created by linkage to the recessive mutation (regions of low heterozygosity).

The progeny of the outcross of each line was then taken to the F2 generation and double homozygous lines carrying both the transgene (*SCR::gai-GR-YFP*) as well as the fast neutron induced mutation were selected. A bulk segregation approach was used to this end.

Identification of FN putative mutants carrying the transgene (*SCR::gai-GR-YFP*) were first selected on the basis of hygromycin resistance. A total of 30 hygromycin resistant seedlings were taken to the next generation (F3) to identify homozygous lines. Since all the FN putative mutants have been shown to carry recessive mutations, screening of the hygromycin resistant seedlings for the mutation in presence of DEX was carried out to identify those double homozygous lines for the FN mutation.

Once the double homozygous lines were confirmed, about 50 seedlings from the F3 population for each of the FN lines were pooled and DNA extracted for sequencing. This was done to dilute the background mutation from the population and preferentially select the mutations causing the phenotype.

NGS will identify 2 non-recombinant, mutation-harboring regions (one for the transgene that will be common for all the selected mutants and the other for every mutation). NGS uses a chi-squared statistics to quantify the relative contribution of the parental mutant and mapping lines to each SNP in the pooled F3 population. It then uses this information to objectively localize the candidate mutation based on its exclusive segregation with the mutant parental line (Robinson *et al.*, 2011).

3.4 DISCUSSION

In order to analyse the gene regulatory network targeted by GA to control the cell expansion in the endodermis of *Arabidopsis thaliana* roots, a forward genetic approach has been pursued. The screening of the fast neutron mutagenised population of the GA signalling mutant (*SCR::gai-GR-YFP*) was expected to uncover novel downstream components of the GA signalling pathway to help to construct the regulatory network targeted by GA.

Several components/factors are expected to be acting downstream of GAI on the GA signalling pathway. Therefore, any mutation affecting some of these downstream components of the GA signalling pathway is expected to partially overcome the root growth restraint produced by the *gai* negative dominant mutant.

As described previously this approach has resulted in identification of fourteen putative mutants. Indeed as in any screen, several false positives were also identified as revealed by genotyping and expression analysis. But for several putative mutants this study clearly showed that the molecular basis of the restoration of root growth phenotype is due to the

smart screen approach used. Sequencing analysis demonstrated that the sequence of the transgene had not been affected by the mutation and therefore the formation of a functional GAI protein takes place in all the rest of FN putative mutants. In summary, for all the 9 putative mutants with partial or weak restoration phenotype, the presence and expression of the *SCR::gai-GR-YFP* transgene were confirmed.

However, the possibility that in some cases recovery of the root growth phenotype is due to any random background mutation with no link to GA had to be ruled out. Hence, all the putative mutants were screened in absence of DEX on the media. The results of the growth rate in both inducible and non inducible conditions showed that some of the identified FN putative mutants (FN49, FN84-1, FN84-2, FN84-3 and FN163) appear to be insensitive to DEX. Therefore, it is possible that they may represent mutations independent from GA signalling.

The final size of *Arabidopsis* root is determined by cell division and cell expansion. GA has been shown to promote root elongation by regulating cell elongation in the endodermis (Ubeda-Tomás *et al.*, 2008). In order to disclose whether the root growth restoration phenotype of each mutant is related to cell expansion, their cell production rate (CPR) was analysed. For eight of the mutants (FN25, FN49, FN84-1, FN84-2, FN84-3, FN191, FN199 and FN215) it appears that root growth is affected at the level of expansion since the CPR levels are comparable to the ones of the controls. On the other hand, for one of the mutants FN163, it appears that the mutation responsible of the root phenotype is involved in cell division. However, this is not an unexpected result since GA has also been shown to regulate root meristem size by promoting cell proliferation (Ubeda-Tomás *et al.*, 2009).

Still, FN163 appeared to be insensitive to DEX, therefore it is unknown if this cell-cycle associated phenotype is GA regulated or related to another regulatory pathway.

Fast neutron mutagenesis has been widely reported to induce chromosomal deletions and rearrangements thus facilitating the rapid identification of the genomic location of the mutation using methods such comparative genomic hybridization (CGH; Carter, 2007) or microarrays based cloning. These two methods are able to detect changes, deletions and duplications. However, it has been recently shown that, in contrast to what was previously considered, FN radiation causes more base substitution than deletions mutations (Belfield *et al.*, 2012).

Several strategies have been developed to identify the genomic location of the mutation depending upon the nature of the lesion created. For example, in case of deletion mutants, high density microarray-based methods have proved successful as highlighted by the identification of a sodium overaccumulation mutant caused by a 523-bp deletion within the AtHKT1 (Gong *et al.*, 2009). Subtractive hybridization methods have also been successfully used for mapping deletion mutants as exemplified by the cloning of gibberellin biosynthetic *gal-3* (Sun *et al.*, 1992). For transposon based mutants, TAIL PCR (Marchant *et al.*, 1999) or inverse PCR approaches have been widely reported.

In contrast, point mutations and small deletions are normally identified by map based cloning. However map based cloning is slow, tedious and labour intensive. With the advances in genome sequencing, next-generation sequencing (NGS) methods are proving effective in mapping these mutations.

High-throughput next-generation sequencing platforms are powerful tools for the mapping of substitutions, deletions, insertions, polymorphisms, inversions, and translocations (Medvedev *et al.*, 2009). Therefore, a next generation sequencing approach will be used to identify the mutated gene causing the restoration of the root growth for each of the FN putative mutants.

Currently samples are being prepared for the sequencing and subsequent identification of the harbouring mutations. Future analysis of the data from the Next generation sequence hopes to unveil novel mutants involved in the GA regulation of root cell expansion to help to build up the GA regulatory network from which many components are still undisclosed.

Based on the phenotypic analysis of the different FN putative mutants, it is likely that cloning of some of the mutations may result in the identification of genes that are not directly regulated by GA despite playing a role in root growth. These mutants may be interacting with the GA signalling pathways through many of the hormone cross-talk phenomena reported (Ubeda-Tomás *et al.*, 2012) to regulate root growth.

CHAPTER 4: REVERSE GENETIC SCREEN TO STUDY GA REGULATED ROOT CELL EXPANSION

4.1 INTRODUCTION

4.1.1 Transcriptomics

The transcriptome is the complete set of all RNA transcripts in an organism or in a cell, for a specific developmental stage or physiological condition. It contains all the mRNAs that are being expressed in a given time. Analysis of the transcriptome is of major importance to expose the functional elements of the genome in order to understand the molecular basis of the developmental processes of cells and tissues. Even though mRNA is not the final product of a gene, transcription is the first step in gene regulation and information about the transcript levels is extremely useful in order to understand gene regulatory networks. (Brazma and Vilo, 2000).

Several technologies have been developed to infer and quantify the transcriptome, including sequence-based or hybridization approaches. Hybridization-based approaches usually involve incubating fluorescently labelled cDNA with custom-made microarrays or commercial high-density oligo microarrays (Wang *et al.*, 2009). Microarray experiments allow for comparison of gene expression profiles between two mRNA samples (e.g. treatment vs control, or treatment 1 vs treatment 2). Microarray-based technology provides the possibility to compare gene expression profiles from large data sets from different experiments giving another level of complexity to understand how certain genes relate to others such as at different time, location and environmental conditions.

When performing a transcript profiling experiment, it has to be taken into account the large sources of variability that may take place during the process. Variation may occur at biological (eg. genetic or environmental factors, growth factors and sampling time) and technical (systematic) level (eg. experimental variables introduced during the extraction, labelling and hybridisation of samples). It is important to check things like the quality of the RNA and dyes, to remove as much variation as possible before the hybridisation process. Normalization procedures are employed to minimise the amount of systematic variation in the data (Quackenbush, 2002). By minimising the amount of systematic variation, it is possible to focus on real biological changes during data analysis. After normalisation of the fluorescence intensities between experiments, it is possible to compare the data from one array experiment with another. Transcriptomics experiments produce very large data sets which need to be analysed by making use of statistical and bioinformatics tools.

4.1.2 The Affymetrix gene chip system

Affymetrix GeneChip® is one of the major transcriptomics technologies available for gene expression analyses (Affymetrix, Santa Clara, USA). Affymetrix is based on the use of oligonucleotides of around 20 nucleotides as probes of gene expression. Oligonucleotides are synthesized directly on the chip (in situ or in silico) through a process of photolithography, onto a glass support. There are pre-made oligonucleotide arrays available for a range of organisms, making it a simple system to use. Custom-made arrays can also be employed when Affymetrix arrays are not available for a particular organism of interest.

One difficulty of using oligo arrays is the possibility of cross-hybridization events of the oligo probes with several genes. To deal with cross-hybridisation and background signals, Affymetrix incorporates two forms of probe in its high-density oligonucleotide arrays, thus helping to improve the signal-to-noise ratios and the specificity of gene transcript identification.

The oligo arrays are designed with probes that form a perfect match (PM) and a mismatch (MM) with the target polynucleotide of interest. The PM oligo probe contains a segment of a wild-type allele (creating a perfect complementary match with a segment of the target gene of interest), while the mismatch oligo probe will be a copy of the PM oligo that has been altered by one base at a central position (Chudin *et al.*, 2001). MMs result in weaker hybridisation with signal intensities different to the PM signal intensities. Consequently, the MM probes serve as controls, helping to discriminate between a true hybridization signal and a signal produced by nonspecific hybridization. For each probe set, the representative value of the expression level of a specific gene would correspond to the average difference between the set of perfect match probes minus the set of mismatch probes.

The Affymetric GeneChip® Arabidopsis ATH1 Genome Array is used for the analysis of gene expression in *Arabidopsis thaliana*. The Arabidopsis ATH1 Genome Array contains more than 22,500 probe sets representing approximately 24,000 gene sequences on a single array (Affymetrix, 2012). Each of these probe sets consists of 11 PM probes and 11 mismatch MM probes. The length of each oligonucleotide probes is of 25 bp.

4.1.3 Transcriptomic experiments for root studies

Several transcriptomic experiments to study gene expression in *Arabidopsis* root at different levels and conditions have been reported. Birnbaum *et al.*, (2003) used a transcriptomic approach to elaborate a global map of gene expression within the *Arabidopsis* root. Gene expression was mapped to 15 different zones of the root corresponding to cell types and tissues at progressive developmental stages. The experiment offered the possibility to identify genes with coordinated expression in localized domains, thus relating gene activity to cell fate and tissue specialization.

In order to have a better understanding of the molecular mechanisms determining the properties of stem cells, Nawya *et al.*, (2005) followed a transcriptomic profile on quiescent centre (QC) cells from the *Arabidopsis thaliana* root meristem. While Brady *et al.*, (2007) carried out a detailed cell-type specific transcriptomic profile of the *Arabidopsis* root within a high-resolution set of developmental time points. Microarray expression profiles have also been carried out to study the development of lateral roots in *Arabidopsis thaliana* (Vanneste *et al.*, 2005; Centre for Plant Integrative Biology (CPIB), Nottingham, unpublished data).

Studies of the different roles of plant hormones in the *Arabidopsis* root have also been attempted by using transcriptomic approaches. Stepanova *et al.*, (2007) used a combination of physiological, genetic, cellular, and whole-genome expression profiling approaches to investigate the mechanisms of interaction between ethylene and auxin. Also, microarray studies of the role of GA within the different developmental zones of the *Arabidopsis* root have been performed (CPIB; Rothamsted Research; unpublished data).

Apart from the root, detailed transcriptomic analyses have been performed on other plant organs and tissues, such as on *Arabidopsis* stems (Minic *et al.*, 2009); in *Arabidopsis* sperm cells (Borges *et al.*, 2008) and for different stages of *Arabidopsis* development such as seed development (Penfield *et al.*, 2006; Carrera *et al.*, 2008).

Available root-specific transcriptomic data sets can provide us with information regarding different aspects of root development. For example, several of the available data sets can be used to compare the expression patterns of the different CWREs associated to cell elongation between different tissues, organs and stages of development, thus providing valuable biological information of the process of cell expansion.

4.1.4 Transcriptomic approach to dissect GA regulated root cell expansion

In this project a transcriptomics approach has been followed in order to study how GAs regulate root cell expansion. As mentioned above, various root transcriptomics data sets have been published to date, providing the opportunity to increase understanding of different aspects of root-related developmental processes. As the ultimate aim of this PhD project is to be able to elucidate those genes which are key components of the GA regulated root cell expansion in the endodermis, a more specific transcriptomic data set was designed to look at gene expression levels in a GA-related manner in these specific root tissues.

To achieve this, a new transcriptomic data set using an inducible system that blocks the GA response in the endodermis, the *SCR::gai-GR* system, has been generated as a time course experiment. This dataset will allow us to study the changes on the gene expression

when the GA response is blocked in the endodermis, in a time dependent manner. The comparison of this dataset with previous microarray data sets will allow the identification of genes involved in the GA regulatory network targeting endodermal root cell expansion. These candidate genes can be later functionally characterised to further understand their specific role in that process.

4.2 MATERIALS AND METHODS

4.2.1 Plant material and sample preparation

Seeds used for transcriptomics analysis were surface sterilised and grown over a square nylon mesh positioned on the top of the media. The use of this mesh was to act as mechanical support to facilitate the dissection of the root tip.

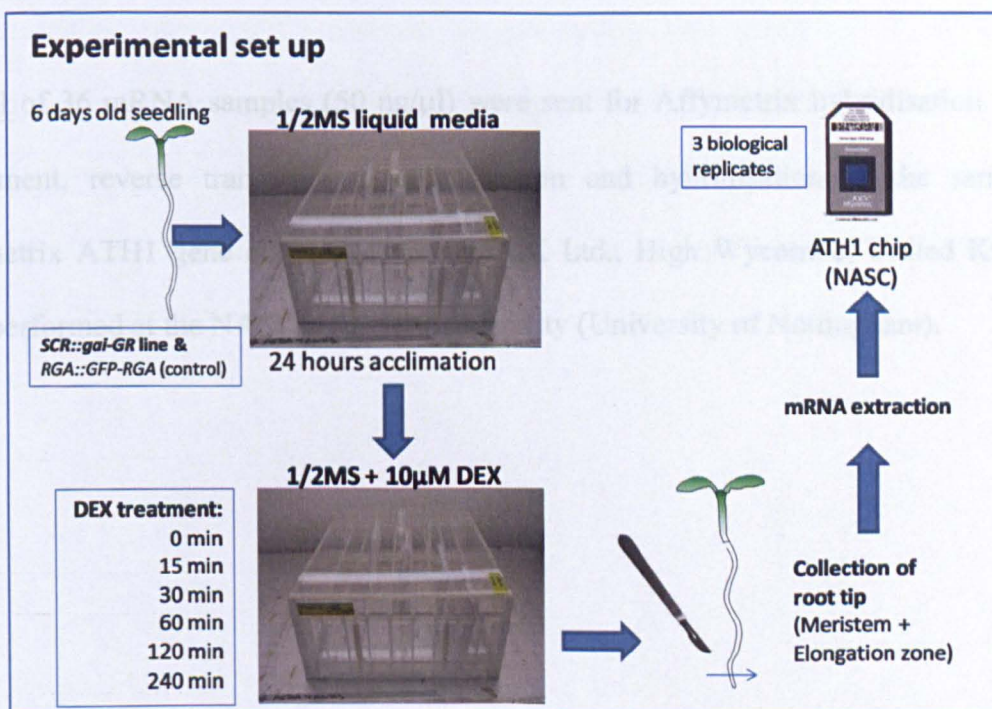


Figure 4.1 Summary of the experimental set up of the *gai-GR* microarray experiment.

As summarised in figure 4.1, plants were grown on the growth room shelves for 6 days in constant light. Then the lid of the plates was removed and plates transferred to a tank containing liquid ½ strength MS. Seedlings with their roots submerged on the liquid media were left there to acclimate for 24 hours. For the time point 0min, roots were dissected after the 24 hours in the ½ strength MS tank. For the rest of time points, plates were transferred to a new tank containing ½ strength MS liquid media supplemented with 10µM of DEX. Plates were kept there for the allocated period of time (30min, 60min, 90min, 120min and 240min) before dissecting the root tip. Dissection of the root tip was done using a scalpel under microscope (Milton-Keynes, UK). mRNA was extracted using the RNeasy micro kit (Crawley - West Sussex, UK) following protocol described on section 2.3.2 and sent for Affymetrix hybridisation. Three biological replicates were produced for each sample to allow for analysis of statistical significance.

4.2.2 Affymetrix hybridisation

A total of 36 mRNA samples (50 ng/µl) were sent for Affymetrix hybridisation. Quality assessment, reverse transcription, amplification and hybridisation of the samples to Affymetrix ATH1 gene chips, (Affymetrix UK Ltd., High Wycombe, United Kingdom) were performed at the NASC array service facility (University of Nottingham).

4.2.3 DEX-*SCR::gai-GR-YFP* Transcriptomics Data Analysis

4.2.3.1 Procedures for analysis of transcriptomics data

Bioconductor software (<http://www.bioconductor.org>) and R programming environment (www.r-project.org) were used to perform quality assessment of the Affymetrix Gene Chip DEX-*SCR::gai-GR-YFP* transcriptomics data and conduct analysis to determine differential gene expression of the arrays.

From the Affymetrix hybridization of the DEX-*SCR::gai-GR-YFP* transcriptomics (*gai-DEX*) samples a total of thirty-six .CEL files (one per array) were obtained. The Bioconductor software uses the R statistical programming language to analyse high throughput genomic data. It contains several packages that are designed to read the .CEL files containing data on the intensity at each probe on the GeneChip, along with other values. Quality control (QC) analysis, pre-processing, processing as well as statistical analysis of the samples were carried out by using available packages from the R software. Further analyses to create a list of differentially expressed gene, were conducted using Microsoft Excel. Figure 4.2 illustrates the sequence of steps that have been followed to analyse the *gai-DEX* transcriptomics data set.

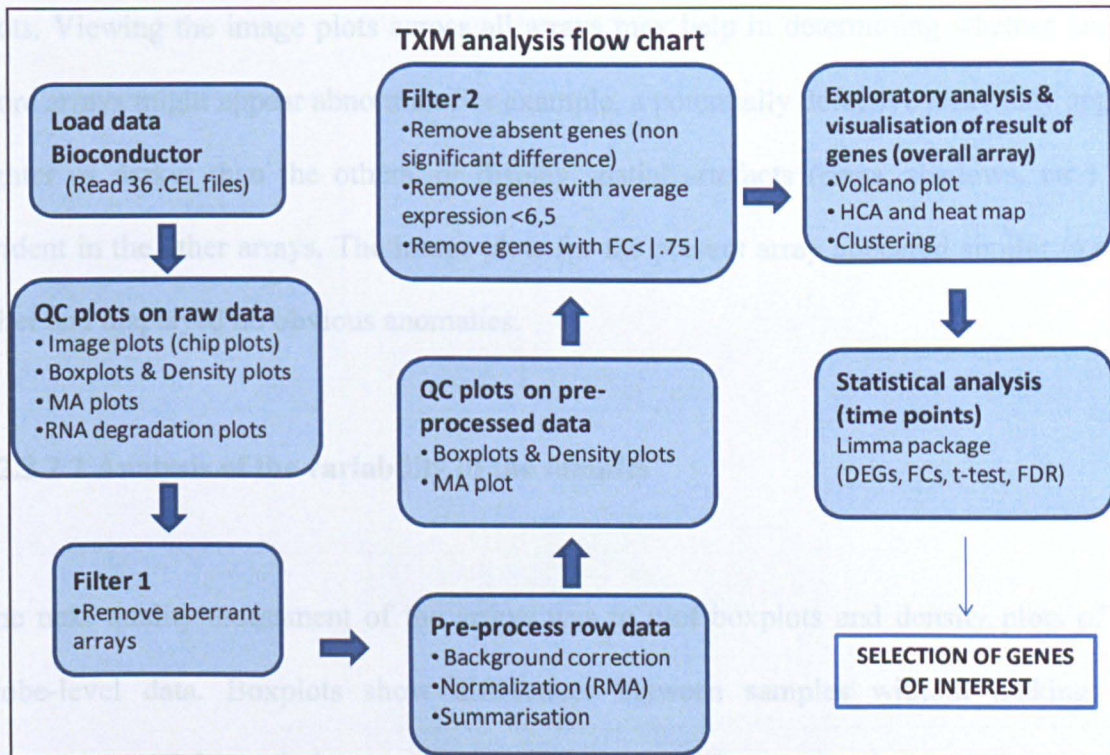


Figure 4.2. **Flow chart for the gai-DEX transcriptomics analysis.** Quality controls of the 36 .CEL files obtained from NASC were carried out prior further statistical analysis of the samples. Once aberrant arrays were removed, the data was normalised and new quality control assessments were performed on it. At this point, genes which were not present or had no significant expression on the array were removed to continue with the exploratory and statistical analysis of the data set for later selection of candidate genes of interest.

4.2.3.2 Quality assessment

Previous to the pre-processing of the Affymetrix array data, it was necessary to do a quality assessment of the array data to spot any abnormalities on the arrays. There are almost certain differences between the array signals caused not by genuine biological differences but by treatment or preparation artefacts.

4.2.3.2.1 Analysis of the integrity of arrays

A first step was to look at the image plots of the (PM and MM) probe-level data to determine if any anomalies existed. In general, we look for spatial artefacts such as scratches, drops or cover-slip effects or other non-homogeneous patterns in the image

plots. Viewing the image plots across all arrays may help in determining whether one or more arrays might appear abnormal. For example, a potentially defective array may appear lighter or darker than the others, or display spatial artefacts (rings, shadows, etc.) not evident in the other arrays. The image plots for the present array appeared similar to each other and displayed no obvious anomalies.

4.2.3.2.2 Analysis of the variability of the samples

The next quality assessment of the arrays was to plot boxplots and density plots of the probe-level data. Boxplots show differences between samples without making any assumptions of the underlying statistical distribution. The spacing between the different parts of the box are indicative of the degree of dispersion and asymmetry in the data. To determine the existence of potentially defective arrays, we looked for boxplots that stood out from the rest, by presenting for example different ranges or displaced boxes (interquartile ranges, IQR). The overall gene expression between arrays should not differ since only a small proportion of the total number of genes per array (sample) should be affected by the treatment (experimental conditions). Therefore, an overall evenness of all the boxplots for the 36 arrays was expected.

For the hybridised arrays of the *gai-DEX* experiment, the IQR, represented by the boxes in the box plots, overlap each other to a large extent, thus indicating a homogenous distribution of the samples (figure 4.3). Still, for array M0-R2, C15-R2 and C0-R3 the overall signal from the probe-level data is lower when comparing to the rest of arrays. On the other hand, probe-level signal seem to be higher for arrays M0-R1 and M0-R3. It is

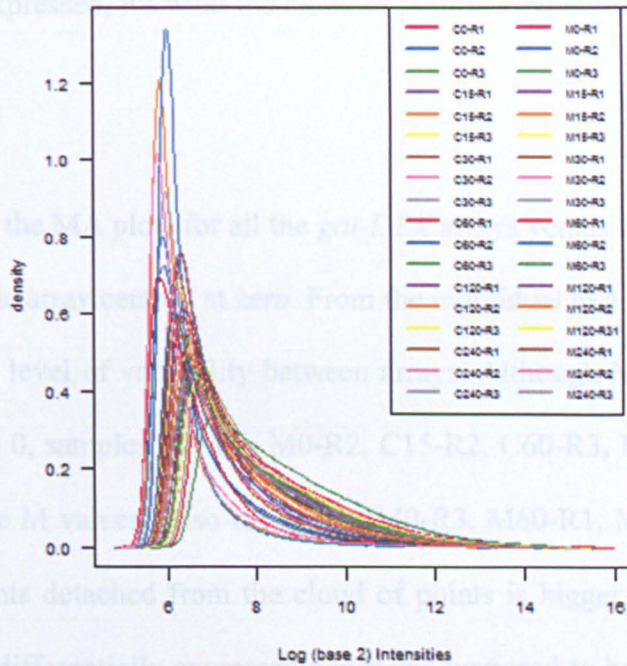


Figure 4.4. **Density plot of 36 arrays of the raw log₂-scale intensities of the *gai*-DEX experiment data.** This histogram shows the distribution and level of density of the probe-level data for the 36 individual arrays. The log intensity pick for the 36 arrays fall between values of 5 and 7. However, density values for the 36 arrays are proportionally wider expanding from around 0.5 and 1.5.

4.2.3.2.3 Analysis of the variability of probe intensities between arrays

MA plots are exploratory plots for quality assessment of the arrays probe-level data. MA plots are used for pairwise comparisons of all arrays in the experiment. When two microarrays are being compared, the differences of their log intensities for each probe on each gene (usually referred to ‘M’) are plotted against their average (usually referred to ‘A’). When comparison of more than two arrays is required, a synthetic array is created by taking the probe-wise medians across all arrays (Bolstad *et al.*, 2005). In a desired situation, the log-ratios M in a MA-plot should be evenly distributed around zero across all intensity values A. A loess regression line (smooth best fit curve) is added to the plot for better assessment of the log values. Quality problems are most obvious where the loess smoother oscillates a great deal or if the variability of the M values appears to be greater in one or more arrays relative to the others. For replicates and situations where most genes are

not differentially expressed, we want the cloud of points is expected to be around 0 and the IQR to be small.

Appendix II shows the MA plots for all the *gai-DEX* arrays versus the synthetic array, with the median synthetic array centred at zero. From the individual MA plots it is observed that there exists certain level of variability between arrays. Although M values for overall the arrays is centred to 0, samples M0-R1, M0-R2, C15-R2, C60-R3, M240-R2 present either positive or negative M values. Also for arrays, M0-R3, M60-R1, M120-R1 and M240-R1 the number of points detached from the cloud of points is bigger than expected from an experiment where differentially expressed genes are supposed to be a minority. Therefore, normalization of the intensities for all the arrays is needed before pre-processing the array data.

4.2.3.2.4 RNA degradation

Affymetrix's reverse-transcription step amplifies RNA from the 3' end of the gene. For every array, the individual probes are numbered sequentially from the 5' end of the targeted transcript. When RNA degradation is substantially advanced, PM probe intensities should be systematically increased at the 3' end of a probe set, when compared to the 5' end. The RNA degradation plot represents the average degradation effects calculated from all probe sets for a given array type. The higher the slope, the stronger is the effect of degradation. In addition, for a given experiment, arrays with slopes that clearly deviate from that of the bulk of arrays are likely to contain problematic data.

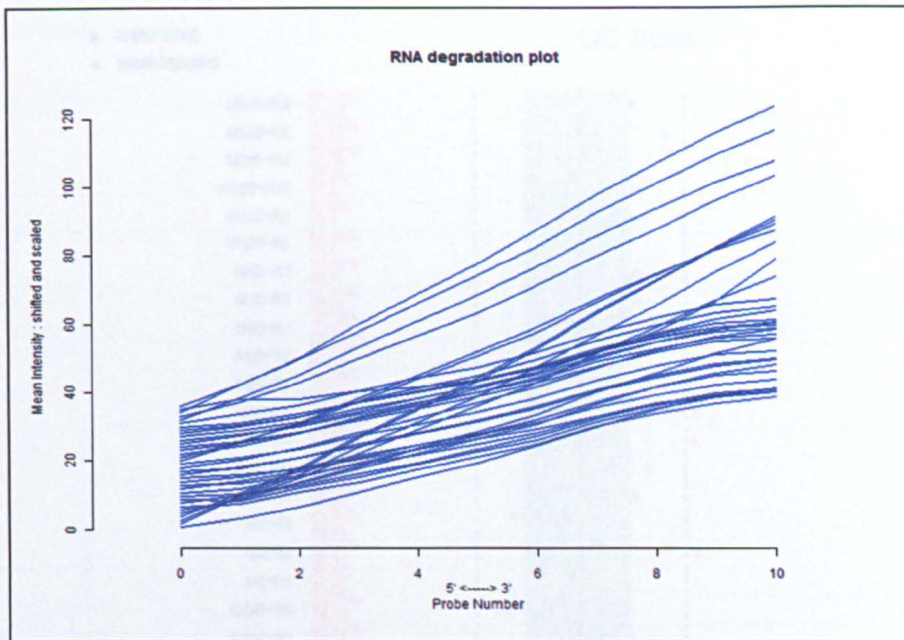


Figure 4.5. **RNA degradation plot for the *gai*-DEX experiment.** This figure illustrates the RNA degradation plot for the 36 individual arrays from the experiment. The y-axis represents the mean intensity of the PM probes. Probes are sequentially represented from their 5' to the 3' on the x-axis.

From the plot above (figure 4.5) we can observe that there are 4 arrays which their RNA degradation intensity profile is deviated from the rest. Additionally, 7 other arrays present steep slopes. Thus, from the observation of this plot we can infer that at least 11 of the 36 arrays from the *gai*-DEX experiment present some RNA-degradation related problem.

The QC plot we get with the Simpleaffy package from Biconductor shows the results of the statistical analysis of the RNA degradation (figure 4.6). The measures assessed in the analysis are the % present calls, average background, scale factors, and 3':5' ratios GAPDH and b-actin (control genes).

Arrays C30-R1, M30-R1, C60-R1, M60-R1, C120-R1, M120-R1, C240-R1, M240-R1, C0-R2, M0-R2, C15-R3, M15-R3 presented high levels of RNA degradation and therefore could not be considered for further analysis of the *gai*-DEX array experiment. The samples that failed the QC fell in pairs (Control vs Mutant for same time point and technical)

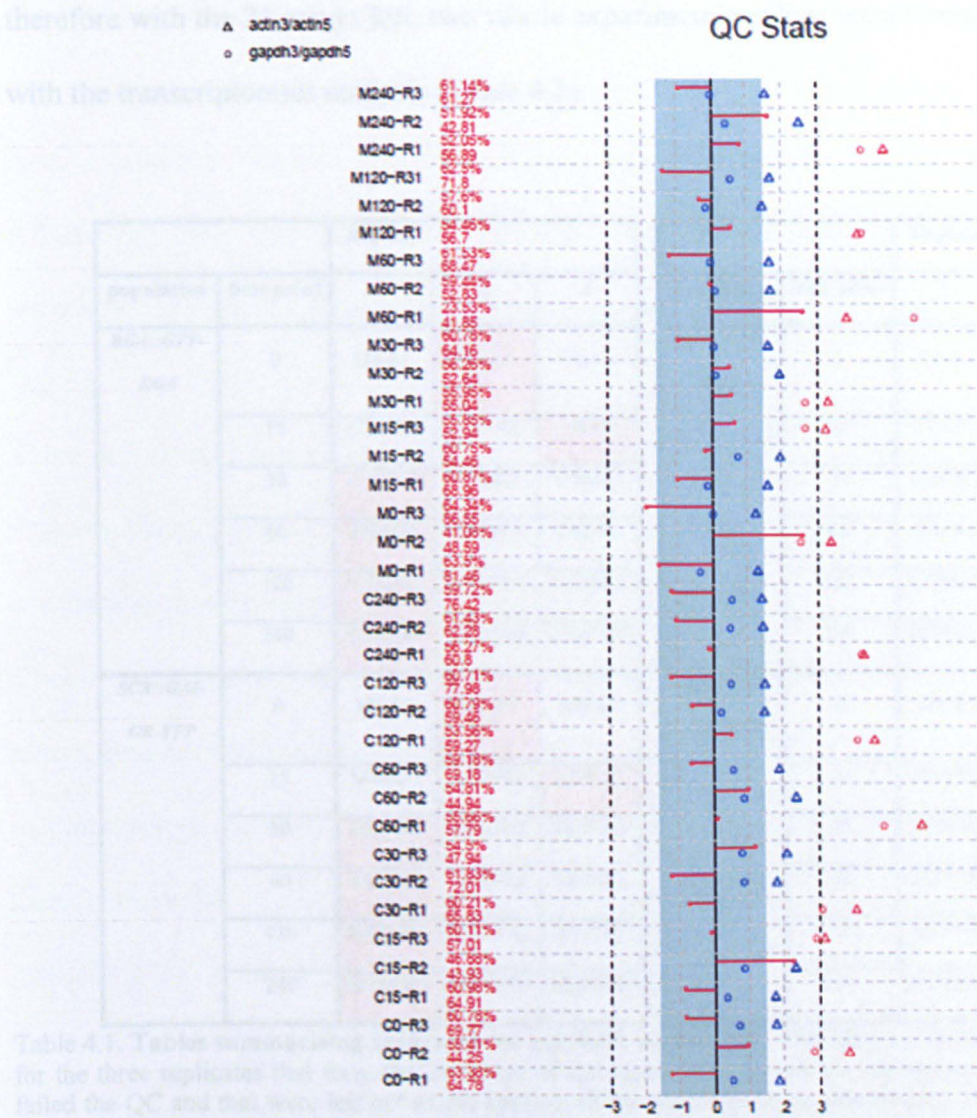


Figure 4.6. QC stats for the RNA degradation of the 36 *gai*-DEX arrays. The numbers next to the array name represent the % present call and average background values. Numbers in red indicate that there is considerable variation in these numbers between arrays. The blue surface represents the range in which the scale factor is within 3-fold of the mean of all arrays. For arrays of a same experiment, it is recommended that all arrays fall within this range. GAPDH 3':5' values are plotted as circles. Values below one (recommended) are given in blue, those above one in red. For b-actin 3':5' values are plotted as triangles. Values below three (recommended) are given in blue, those above three in red. For 12 of the arrays in the *gai*-DEX experiment (C30-R1, M30-R1, C60-R1, M60-R1, C120-R1, M120-R1, C240-R1, M240-R1, C0-R2, M0-R2, C15-R3, M15-R3) ratios are above the expected range for all the arrays.

Arrays C30-R1, M30-R1, C60-R1, M60-R1, C120-R1, M120-R1, C240-R1, M240-R1, C0-R2, M0-R2, C15-R3, M15-R3 presented high levels of RNA degradation and therefore could not be considered for further analysis of the *gai*-DEX array experiment. The samples that failed the QC fell in pairs (Control vs Mutant for same time point and replica) and

therefore with the 24 arrays left, two whole experiment-replicas were completed to proceed with the transcriptomics analysis (Table 4.1).

		Replica					Replica	
population	time point	1	2	3	population	time point	1	2
<i>RGA::GFP- RGA</i>	0	C0-R1	C0-R2	C0-R3	<i>RGA::GFP- RGA</i>	0	C0-R1	C0-R3
	15	C15-R1	C15-R2	C15-R3		15	C15-R2	C15-R1
	30	C30-R1	C30-R2	C30-R3		30	C30-R2	C30-R3
	60	C60-R1	C60-R2	C60-R3		60	C60-R2	C60-R3
	120	C120-R1	C120-R2	C120-R3		120	C120-R2	C120-R3
	240	C240-R1	C240-R2	C240-R3		240	C240-R2	C240-R3
<i>SCR::GAI- GR-YFP</i>	0	M0-R1	M0-R2	M0-R3	<i>SCR::GAI- GR-YFP</i>	0	M0-R1	M0-R3
	15	M15-R1	M15-R2	M15-R3		15	M15-R2	M15-R1
	30	M30-R1	M30-R2	M30-R3		30	M30-R2	M30-R3
	60	M60-R1	M60-R2	M60-R3		60	M60-R2	M60-R3
	120	M120-R1	M120-R2	M120-R3		120	M120-R2	M120-R3
	240	M240-R1	M240-R2	M240-R3		240	M240-R2	M240-R3

Table 4.1. Tables summarising arrays on the *gai-DEX* experiment. The table on the left show the samples for the three replicates that form the 36 arrays of the experiment. In red are highlighted those samples that failed the QC and that were left out of the analysis of the transcriptomics experiment. The table on the right summarises the new two replicas compiled from the samples that fulfilled the QC requirements for further downstream analysis of the data. Arrays for the *RGA::GFP-RGA* line are referred as arrays from the control (C), and arrays for the *SCR::GAI-GR-YFP* line as arrays from the mutant (M).

The rest of the differences for the *gai-DEX* arrays observed on boxplots, density plots and MA plots for will be normalised on the pre-processing of the data to make the arrays comparable in order to be able to carry out any downstream analysis.

4.2.3.3 Pre-processing of the microarray data

Before high level analysis such as differentially expressed genes and clustering can occur, the systematic error/artefacts components need to be removed from the arrays. It is

assumed that the overall signal should be similar over arrays since most of the genes will be unaffected by the experiment. Therefore, overall signal need to be the same for each array in order to expose true differentially expressed genes. The pre-processing of the Affymetrix data aims to adjust systematic effects that arise from variation in the experimental technology rather than from biological differences between RNA samples.

There are three main steps involved in the data pre-processing. Background correction removes background signal caused by non-specific hybridization. Normalization eliminate non-biological differences between arrays which can be caused by different efficiencies of reverse transcription, labelling, or hybridization reactions, physical problems with the arrays, reagent batch effects and laboratory conditions. It normalises expression intensities so that the intensities or log-ratios have similar distributions across a set of arrays, making them comparable. The last step involves the summarisation of the different probes values intensities into a single value for each gene/probe set.

Pre-processing of the *gai*-DEX microarray data was carried out by the Robust Multiarray Average method. This integrated function performs a convolution background correction, quantile normalisation and summarisation based on a multi-array model fit robustly using the median polish algorithm (Bolstad *et al.*, 2005). RMA only uses PM probes to produce expression level data. As a result of the RMA pre-processing, values of expression levels in log(base 2) scale are obtained for each gene.

4.2.3.4 Quality Control plots on pre-processed data

A new boxplot of expression values was carried out on the 24 arrays of the *gai-DEX* microarray in order to confirm the success of the normalization and summarisation. In figure 4.7, it can be observed that the arrays are accurately aligned. This is as a result of the aggressive quantile normalisation step in the RMA method.

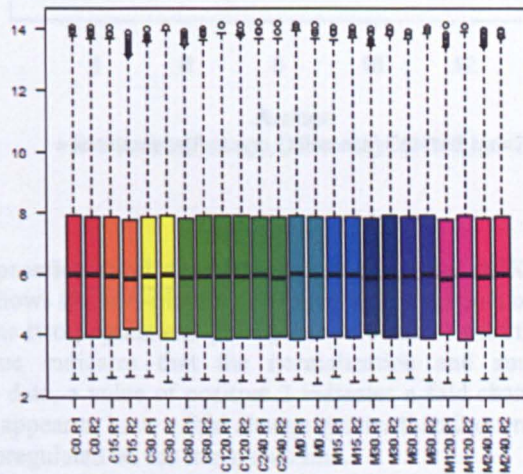


Figure 4.7. **Boxplot of expression level data of the 24 *gai-DEX* arrays from the RMA process.** The probe-level data displayed in the boxplots of these arrays are distributed from about 2–15 on the log (base2) scale. The boxplots of expression level values are nicely aligned following RMA transformation. The IQR of arrays is represented by the boxes in the boxplots. The bottom and top of the box represent the lower and upper quartiles respectively. The middle bar in the boxes is the median and the whiskers represent the lowest and highest values.

Once all the probe expression levels have been normalised, statistical analyses need to be performed in order to identify those genes which are differentially expressed between the control and the transgenic populations. The data from all of the genes (two biological replicates from each sample) were grouped into the experiment. *DESeq2* was combined to produce our data set for each time point. The *limma* package, which performs linear modelling of microarray expression values, was used to produce a list of differentially expressed genes. The *limma* package uses an

Also, an MA plot of the expression level data was performed to plot the differences of the average log (base 2) expression values between the two populations (transgenic vs control for all the time points). Figure 4.8 shows the MA plot between the two populations with the median centred at zero. The straight loess regression line indicates that the normalization and summarization procedures were satisfactory. Out of the 22810 genes of the ATH1 array, 16 appear to have a fold change greater than 2 for overall the time points. These could be candidate genes that are upregulated in the transgenic line.

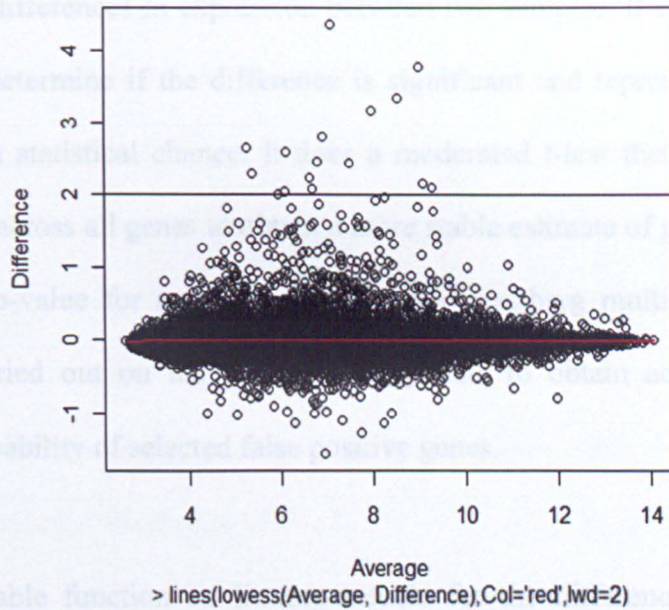


Figure 4.8. **MA plot of expression level data between the two *gai*-DEX array populations from the RMA process.** This figure shows the MA-plot for the expression level data of the differences of the average log(base2) values between the two populations (transgenic vs control) with the median centred at zero. The straight loess regression line indicates that the normalization and summarization procedures were satisfactory. For log (base 2) data, a value of positive 2 indicates a fold change of 4 to 1. Out of the 22810 genes of the ATH1 array, 16 appear to have a fold change greater than 2 overall the time points. These could be candidate genes that are upregulated on the transgenic line.

4.2.3.5 Statistical analysis of *gai*-DEX microarray data

Once all the probe expression levels have been normalised, statistical analyses need to be done in order to identify those genes which are significantly differentially expressed between the control and the transgenic lines. To generate a list of genes, two biological replicates from each sample were grouped into one experiment. Replicates were combined to produce one data set for each time point.

The limma package, which performs linear modelling of microarray expression values, was used to produce a list of differentially expressed genes. The limma package uses an

empirical Bayes method for assessing differential expression on each gene and produces estimates of the differences in expression between two samples. It also executes tests that are intended to determine if the difference is significant and represents a real biological effect rather than statistical chance. It does a moderated t-test that borrows information about variability across all genes to obtain a more stable estimate of gene specific variance. The result is a p-value for each gene. Benjamini-Hochberg multiple testing correction method was carried out on the *gai-DEX* array data to obtain adjusted p-Values thus reducing the probability of selected false positive genes.

From the top Table function on limma, a table for the difference in gene expression between the two populations can be compared. The table contains information about the average expression for each gene, the log fold change (FCs), t-statistics and associated p-value for the statistical test for differential expression and the adjusted p-value.

Before proceeding to the analysis of differentially expressed genes between the two populations for the each individual time point, exploratory analysis and visualisation of the genes was done for the two populations overall the time points. All the data for the different time points for each population was combined and statistically analysed to obtain the differentially expressed genes between the two populations without taking in account the different time points.

4.2.4 Selection of genes of interest

A selection of genes of interest to study the endodermal GA regulated root cell expansion was done from the DEX-*SCR::gai-GR-YFP* transcriptomics data set together with the analysis of two other available data sets. One of the available data sets used was a transcriptomics experiment carried out in CPIB (De Rybel *et al.*, 2012) where changes in gene expression were measured for 5 different developmental sections of the root; meristem, accelerating elongation, decelerating elongation, mature and rest of the root/ lateral root emergence zone (figure 4.9).

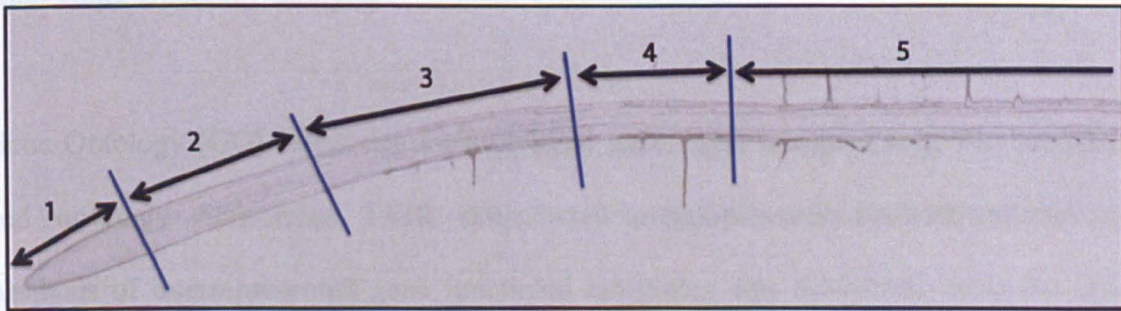


Figure 4.9 Image of root showing the five different developmental sections used for transcriptomics experiments. The first section belongs to the meristem (~350 μm), the second to the accelerating elongation (~900 μm), third to the decelerating elongation (~1.2 mm), fourth to the mature (~500 μm) and the fifth to the rest of root / lateral root emergence zone (~2.5 cm) (Figure provided by T. Holman, CPIB).

The other available transcriptomics data set used for the selection of candidate genes was from an experiment measuring tissue-specific gene expression (Mustroph *et al.*, 2009). Transcriptomics data was obtained from measuring the mRNAs in polysomes (translation complexes) from wild type seedlings.

To compare two samples (transgenic vs control) at a certain time point, two replicas were combined in a single experiment. After the statistical analysis performed with limma package (an application of Bioconductor), genes with an average expression values (RAM) higher than 100, a $FC > [0,75]$ and adjusted p-Value < 0.05 were selected.

All the genes that were successfully selected from the analysis of the 6 different time points were combined in a single list of genes. These selected genes were further filtered by comparing their expression with the data available from the datasets mentioned above. Genes which were significantly expressed on the elongation zone and also in the endodermis were selected as candidate genes to study potential members of the GA regulatory network within the elongation zone.

4.2.5 Gene Ontology analysis

Gene Ontology (GO) categories for individual genes were assigned from the annotation and ontology files from TAIR (<http://www.arabidopsis.org/tools/bulk/go/index.jsp>). Analysis of overrepresented gene functional categories was performed using the open-source software platform Cytoscape (<http://www.cytoscape.org>, Shannon *et al.*, 2003). The Biological Networks Gene Ontology tool (BiNGO) plugin was used to statistically assess the enrichment of a GO category of a set of genes. An Hypergeometric test with a Benjamini and Hochberg False Discovery Rate correction and an adjusted p-Values < 0.05 are performed in the set test cluster with respect to the overall Arabidopsis genome, and retrieves the relevant GO annotations in a context of GO hierarchy (Maere *et al.*, 2005).

4.2.6 Functional analysis of selected GA regulated genes

4.2.6.1 Identification of T-DNA insertion lines

Screening of T-DNA lines were carried out for those candidate genes selected from the transcriptomics analyses. The identification of T-DNA insertion lines for all the selected candidate genes was performed using *Arabidopsis* Ensembl genome browser from NASC, the European *Arabidopsis* stock centre home page, (<http://atensembl.arabidopsis.info/index.html>). Also, the *Arabidopsis* Information Resource (TAIR) database was used on the search (<http://arabidopsis.org>).

Salk homozygous T-DNA lines were selected for those genes which had available lines in which the insertion was located preferentially in an exon of the gene or in the promoter region as well as being homozygous lines.

4.2.6.2 Root growth assay

Seedlings for the different T-DNA lines were surface sterilised and growth on plates as described in sections 2.1 of general materials and methods. Basal root growth was assessed for the selected T-DNA lines to look for defects on the primary root length. Root measures were carried out as described in section 2.2.2 of general materials and methods.

4.2.6.3 Promoter analysis of *gai-DEX* regulated genes

Bioinformatics analysis of the promoter sequences of the selected candidate genes was carried out using the Plant Promoter and Regulatory Element Resources AthaMap (<http://athamap.de/>)

4.3 RESULTS

4.3.1 Experimental design of the *SCR::gai-GR* transcriptomics experiment

To complement the information already available from published microarray data sets and unpublished microarray experiments carried at CIPB, a new transcriptomics experiment was carried out. The line used to generate the new transcriptomics data set contained the *SCR::gai-GR-YFP* transgene; which enabled the steroid inducible disruption of the GA response in root endodermal cells (Ubeda-Tomás *et al.*, 2008).

The experiment was designed as a time course where plants were treated for a variable amount of time with the steroid dexamethasone (DEX), which triggers nuclear relocalisation of the expression of the *gai-GR-YFP* fusion protein. Transcripts were collected after 0min, 30min, 60min, 90min, 120min and 240min after treating the seedlings with DEX. The last time point of 240min was determined according to the fact that after this period of time the root growth phenotype associated with the expression of *gai* is already visible (Ubeda-Tomás *et al.*, 2008). As a control the parental line of *SCR::gai-GR-YFP*, a line only expressing *RGA-GFP* (*RGA::RGA-GFP*) was used. Gene expression for the control line was monitored for the same time points and conditions as

the *SCR::gai-GR-YFP* line in order to compare both data sets, and thus enabling the identification of differential expressed genes (DEG) due to the expression of *gai* and the subsequent inhibition of the GA response at the given time points. Although we were interested in observing the changes happening in the elongation zone, tissue was collected from the root tip of *Arabidopsis* roots, which includes both the meristem and elongation zone. The whole root tip was taken due to the technical difficulty involved in dissecting the elongation zone from the rest of the root, as well as to facilitate the collection of sufficient mRNA material for hybridisation.

4.3.2 Exploratory analysis & visualisation of result of genes

4.3.2.1 Identification of *SCR::gai-GR* regulated genes

To identify the genes which were differentially expressed in root tips excised from *SCR::gai-GR* versus WT DEX treated lines, a volcano plot was employed (figure 4.10). It plots the negative $\log_{10}(\text{p-value})$ versus the difference in log expression values between the two samples. From a biological point of view, the genes of interest are the ones that have both a low probability value (moderated t-test) and high absolute log-fold change. This plot is a way to visualise the genes that fulfil both parameters.

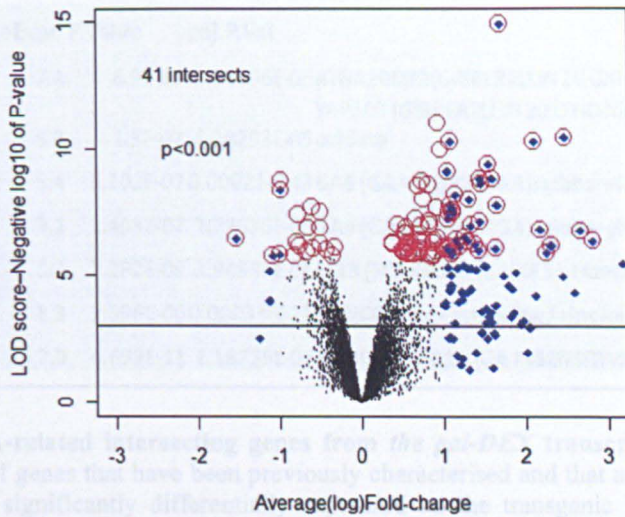


Figure 4.10 Graphical representation of the top genes which are more significantly differentially expressed. The volcano plot above shows the 100 genes with the lowest p-values (highly significant) as open circles (red) and the 100 genes with the highest absolute log-fold changes as diamonds (blue). A total of 41 intersecting genes that fulfil both parameters are observed in the plot. On the right of the graph are located those genes which are upregulated on the transgenic line when compared with the control and in the left those which are downregulated.

From this plot a total of 41 genes that possess simultaneously high (log) fold changes and low probability values were identified (Appendix III). Of the 41 intersecting genes, only 4 appear to be significantly downregulated while 37 are significantly upregulated in the transgenic line. So, we can conclude from this analysis that the predominant effect in terms of gene expression of blocking the GA response in the endodermal cells of the roots, is the stimulation of gene expression of several genes that otherwise are not expressed.

Table 4.2 show a list of reported GA related genes identified from the 41 intersecting genes obtained from the analysis.

AGI	logFC	AveExpr	P.Value	adj.P.Val	
AT5G51810	4.3	7.1	6.9E-09	8.81196E-06	ATGA200X2 (GIBBERELLIN 20 OXIDASE 2)
AT5G07200	2.6	5.3	1.5E-07	8.28293E-05	YAP169 (GIBBERELLIN 20 OXIDASE 3); gibberellin 20-oxidase
AT4G25420	2.3	5.4	6.102E-07	0.000214143	GA5 (GA REQUIRING 5); gibberellin 20-oxidase
AT1G15550	2.223	9.1	1.408E-07	7.77636E-05	GA4 (GA REQUIRING 4); gibberellin 3-beta-dioxygenase
AT1G50420	1.4	8.1	2.282E-09	3.94985E-06	SCL3 (SCARECROW-LIKE 3); transcription factor
AT2G04240	1.1	8.3	1.396E-06	0.000338811	XERICICO; protein binding / zinc ion binding
AT3G63010	1.1	7.0	4.699E-11	2.18736E-07	ATGID1B/GID1B (GA INSENSITIVE DWARF1B); hydrolase

Table 4.2. List of GA-related intersecting genes from the *gai-DEX* transcriptomics experiment. This table shows a number of genes that have been previously characterised and that are known to be regulated by GA. These genes are significantly differentially expressed on the transgenic line when compared to the control line overall the time points. The AGI code, the log FC (Fold Change) value, the average expression and the P-Value and adjusted P-Value are shown for each of the genes.

On top of the list there are three genes encoding for a gibberellin 20 oxidase (Atg51810, At5g07200, and At4g25420) and a fourth gene that encodes for a gibberellin 3 oxidase (At1g15550). As mentioned in the introduction, these are enzymes that catalyse the last steps of the synthesis of bioactive GAs. The lack of a GA response in the DEX induced *gai* expression could be interpreted by the plant as a lack of bioactive GA. The upregulation of these genes may be an indication of the plant responding to this apparent lack of available GA in the system. At1g50420 encodes a SCARECROW-LIKE 3 protein (SCL3) that is also highly upregulated in the transgenic line. Previous microarrays studies (Zentella *et al.*, 2007) found this gene to be a GA-repressed and DELLA-induced gene. SCL3 is a GRAS protein like DELLA, but it does not contain the GA-responsive DELLA domain. In the primary root, SCL3 mRNA is mainly expressed in the endodermis and it has been shown that SCL3 antagonizes DELLA function in modulating downstream GA responses (Zhang *et al.*, 2011). Therefore, given that in the *SCR::gai-GR-YFP* line DELLA protein is accumulated in the endodermis, the upregulation of SCL3 in our data is expected. Also, XERICICO (At2g04240), a small protein with an N-terminal trans-membrane domain which

is induced at a transcriptional level by DELLA proteins and repressed by gibberellins, appears to be significantly upregulated in the *gai*-DEX data set. The fact that the GA receptor *GID1B* (At3g63010) also has been identified amongst the intersecting genes, is another indication of the lack of GA sensing in the *gai*-DEX system.

4.3.2.2 Hierarchical Clustering revealed associations between functional classes of genes in the GA dataset

A heatmap is a two dimensional graphical representation of data where individual values are represented as colours in the form of a rectangular matrix. They are used to display the level of gene expression of many genes across a number of comparable samples. The value of the corresponding entry in the matrix determines the colour scale of each rectangle. The rows and columns of a heatmap can be ordered such that rows with similar values are placed next to each other and similar columns placed next to each other (Alvord *et al.*, 2007).

The hierarchical clustering approach aims to assemble a set of genes into a tree in a way that similar genes/arrays will be joined by very short branches and with longer branches as their similarity decreases. The clusters that are obtained (for the intersecting genes and for the arrays) can be combined with a heatmap to add extra information on the relation of the genes of interest versus arrays.

Figure 4.11 shows a heatmap of the forty-one intersecting genes that have simultaneously high (log) fold changes and low probabilities values that were displayed in the volcano plot (figure 4.10). The dendrograms at the top and the sides were created with and

agglomerative complete linkage algorithm, using a Euclidean distance measure (Kaufman *et al.*, 1990). The dendrograms connect the arrays and genes with similar expression levels.

The arrays from the same population (*RGA::GFP-RGA* or *SCR::GAI-GR-YFP*) for the different time points cluster tightly together indicating that the expression level values for these arrays on the intersecting genes are similar. Only one of the control samples at time 240 minutes replica 1 (C240-R1) seems to cluster more closely to the mutant (M) counterparts.

The dark blue shades indicate relatively higher gene expression levels, whereas dark red shades indicate relatively lower gene expression levels. The higher expression levels observed for the transgenic arrays correlates with the information shown on the volcano plot where most of the genes of interest presented a positive log-fold. Also for *SCR::GAI-GR-YFP* line (M) note the red section matching to those intersected genes that appeared to be downregulated (negative log-fold change, when compared to the level of expressions of the control line).

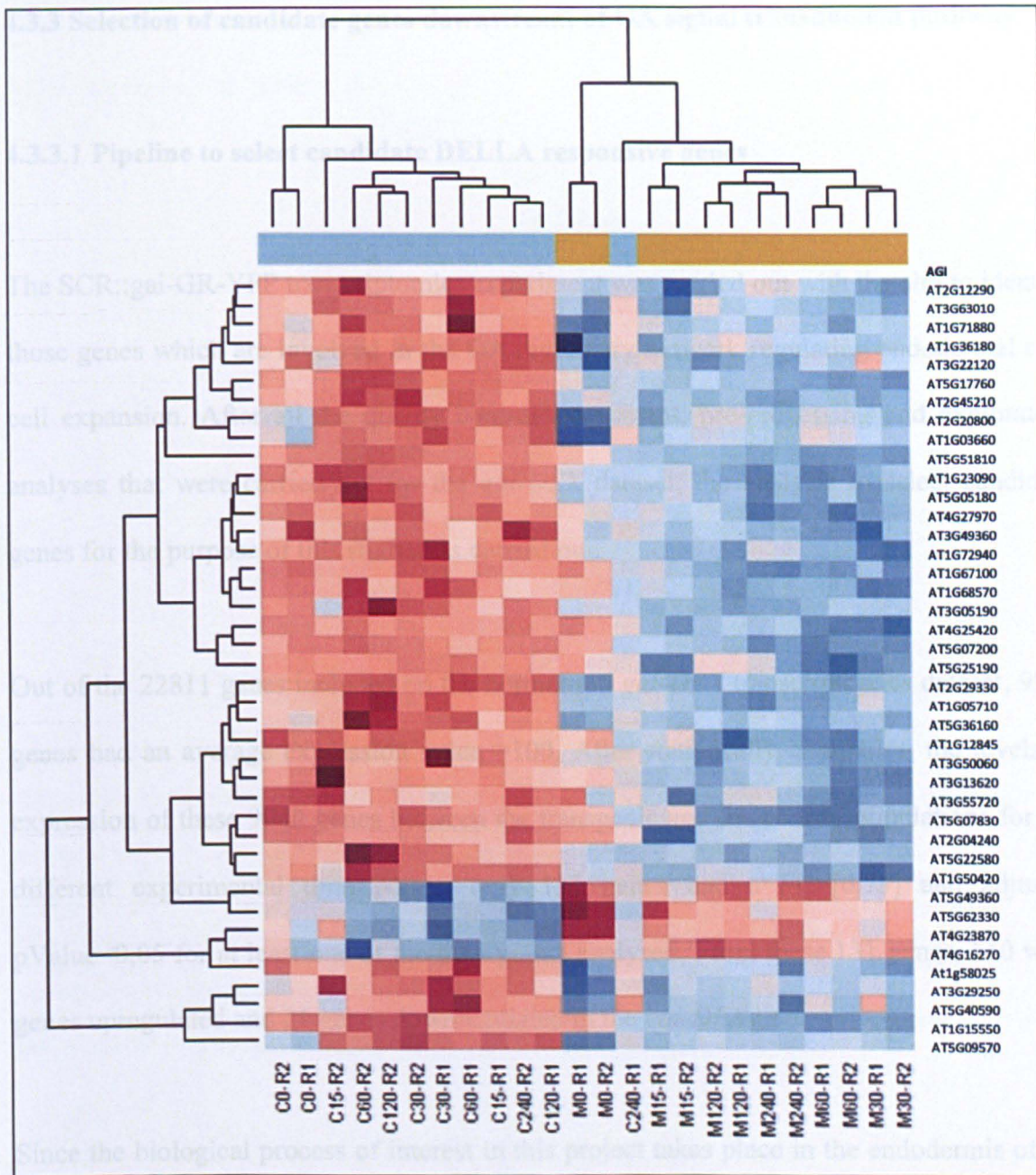


Figure 4.11. **Hierarchical clustering of the 41 intersecting genes of the *gai*-DEX experiment.** Graphical representation of the clustering of the gene expression levels for the intersecting genes between the different arrays. The bar on top is the colour code for the control *RGA::GFP-RGA* arrays (C-blue) and the *SCR::gai-GR-YFP* arrays (M-orange). Note that all the arrays for the control line, except for C240-R1, are grouped together on the left and the *SCR::gai-GR-YFP* arrays cluster together on the right. A strong blue color-grade is observed on the right representing the majority of the intersected genes for the different arrays that are overexpressed on the *SCR::gai-GR-YFP* arrays line when compared to the control. A group of genes highlighted in red are observed clustered together in the right of the heatmap corresponding to the intersecting genes which are downregulated in the the *SCR::gai-GR-YFP* at the different time points.

4.3.3 Selection of candidate genes downstream of GA signal transduction pathway

4.3.3.1 Pipeline to select candidate DELLA responsive genes

The SCR::*gai-GR-YFP* transcriptomics experiment was carried out with the aim to identify those genes which are involved in the GA regulatory network regulating endodermal root cell expansion. After all the quality control assessment, pre-processing and exploratory analyses that were carried out for the *gai-DEX* dataset, the analysis to select candidate genes for the purpose of this study was carried out.

Out of the 22811 genes included on the normalised *gai-DEX* transcriptomics dataset, 9940 genes had an average expression value >100. After statistically comparing the levels of expression of these 9940 genes between the transgenic and the control populations for the different experimental time points, only 131 genes had a $FC > [0,75]$ and adjusted $pValue < 0,05$ for at least one of the time points analysed. From these 131 genes, 110 were genes upregulated and 21 genes downregulated in the *gai-DEX* line.

Since the biological process of interest in this project takes place in the endodermis of the elongation zone of the root, in order to restrain the candidate genes to a further level of site specificity, the list of 131 differentially expressed genes was cross-referenced with a list of differentially expressed genes specific for the elongation zone EZ and a list of endodermal specific differentially expressed genes. Out of the selected 131 differentially expressed genes 63 were also significantly expressed in the EZ and 101 in the endodermis. A total of 60 genes fulfilling the three characteristic were selected as candidate genes (figure 4.12).

From these 60 candidate genes, 48 are genes induced on the *gai-DEX* line and 12 genes which are repressed (table 4.3).

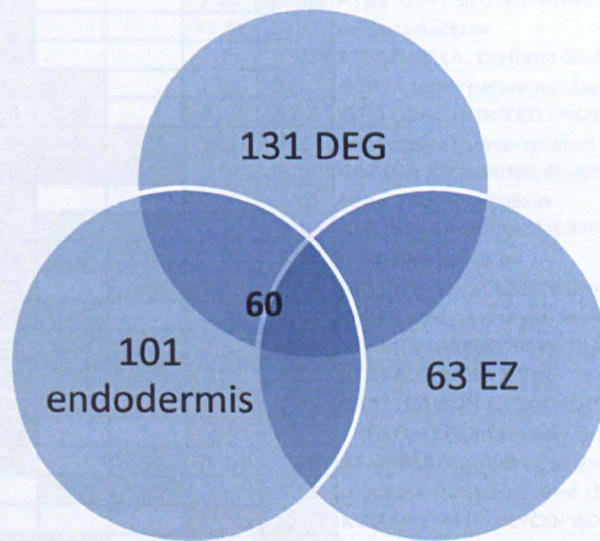


Figure 4.12. Venn diagram for the pipeline selection of candidate genes from the *gai-DEX* dataset. A total of 131 genes were found to be significantly differentially expressed in the *SCR::gai-GR-YFP* line when compared to *RGA::GFP-RGA* line for at least one of the six different time points carried out on the *gai-DEX* experiment. These 131 differentially expressed genes (DEG) were cross-referenced with a published tissue specific data set (Mustroph *et al.*, 2009) to select those genes which are significantly expressed in the endodermis (101 candidate genes). At the same time, to narrow the list of candidate genes to a set of genes which are likely to be related to the biological process of interest in this thesis, the 131 DEG were also cross-referenced with a transcriptomics data set for the different developmental zones of the Arabidopsis root (De Rybel *et al.*, 2012), to identify those genes which are significantly expressed in the elongation zone of the root. A total of 60 candidate genes that fulfilled the three parameters were selected for further analysis.

Table 4.3 List of selected *SCR::gai-GR* regulated genes significantly expressed in the root elongation zone and endodermis. Colour code list of candidate genes with associated expression levels. Genes which were further analysed are highlighted in grey. The blue column gives the values of the average expression of each gene in the dataset. Fold changes (FC) are highlighted in green for upregulated genes and in red for those genes which are downregulated. Column EZ2 show the levels of expression of each gene in the elongation zone of the root (yellow). The SCR2 column show the expression levels of the 60 genes in the endodermis.

AGI	AveExpr	FC-15	FC-30	FC-60	FC-120	EZ2	SCR2	TAIR description	
AT1G43910	7.31	2.12	2.28	1.65		8.32	7.72	AAA-type ATPase family protein	
AT5G28020	7.45		0.96	1.46		8.76	9.59	ATCYS2 (Arabidopsis thaliana cysteine synthase D2)	
AT2G04240	8.34	1.80	1.45	1.29	1.00	7.03	8.88	XERIC0; protein binding / zinc ion binding	
AT3G59140	7.04	0.97	1.32	1.47	0.94	7.96	7.76	ATMRP14 (multidrug resistance-associated protein 14)	
AT1G54120	8.56	0.96	0.99	0.98		8.81	8.36	unknown protein	
AT2G36460	9.30	2.25	2.38			7.49	10.19	fructose-bisphosphate aldolase, putative	
AT1G17170	8.23	2.51	2.33			7.20	11.30	ATGSTU24 (GLUTATHIONE S-TRANSFERASE (CLASS TAU)	
AT3G29250	9.37	1.95	1.82			11.42	12.34	oxidoreductase	
AT1G17180	9.27	2.55	2.84			7.79	10.23	ATGSTU25 (A. thaliana Glutathione S-transferase (class tau) 25)	
AT3G22370	8.97	2.27	2.49	1.94		7.98	10.07	AOX1A (alternative oxidase 1A); alternative oxidase	
AT5G13750	8.05		0.99	1.17		8.22	9.86	ZIFL1 (ZINC INDUCED FACILITATOR-LIKE 1)	
AT5G36160	7.84		1.39	1.85	1.30	8.68	9.77	aminotransferase-related	
AT1G15550	9.08		3.04	3.31	2.63	8.08	8.11	GA4 (GA REQUIRING 4); gibberellin 3-beta-dioxygenase	
AT5G54100	10.05	1.63	1.25			7.55	7.60	band 7 family protein	
AT5G07830	8.42		1.29	1.52	1.33	7.19	9.22	ATGUS2 (ARABIDOPSIS THALIANA GLUCURONIDASE 2)	
AT1G12845	7.92		1.23	1.42	1.61	6.51	6.94	unknown protein	
AT5G67480	7.18	0.90	0.95		0.94	8.47	6.89	BT4 (BTB AND TAZ DOMAIN PROTEIN 4)	
AT3G13620	7.28	1.88	1.62	1.39		6.82	7.42	amino acid permease family protein	
AT2G38290	7.39		0.85	0.99	1.01	7.57	8.40	ATAMT2 (AMMONIUM TRANSPORTER 2)	
AT4G08930	7.36		1.06	1.22	1.29	8.58	8.30	ATAPRL6 (APR-LIKE 6)	
AT2G38170	8.67		0.98	1.25	1.01	9.77	9.85	CAX1 (CATION EXCHANGER 1)	
AT1G78340	8.04	2.56	2.53			10.11	9.17	ATGSTU22 (Glutathione S-transferase (class tau) 22)	
AT3G62700	8.38		1.00		1.08	7.14	9.05	ATMRP10 (multidrug resistance-associated protein 10)	
AT2G45180	10.91			1.45	1.67	7.97	7.59	protease inhibitor/seed storage/lipid transfer protein (LTP)	
AT2G47000	9.74	1.39				10.96	10.42	MDR4/PGP4 (P-GLYCOPROTEIN4)	
AT2G31750	9.04		1.00	1.19		9.02	9.75	UGT74D1 (UDP-GLUCOSYL TRANSFERASE 74D1)	
AT1G28110	9.40			1.52	1.19	9.07	9.42	SCPL45; serine carboxypeptidase	
AT5G61820	6.72	1.36				10.17	12.74	unknown protein	
AT1G62380	8.72	0.82				8.91	11.08	ACO2 (ACC OXIDASE 2)	
AT2G23700	7.77		1.05	0.85		6.84	8.63	unknown protein	
AT1G08930	9.06			0.83	0.87	7.37	9.68	ERD6 (EARLY RESPONSE TO DEHYDRATION 6)	
AT5G11420	8.82		1.52	1.51		8.91	8.03	unknown protein	
AT5G40540	8.36		0.90	1.14		7.48	7.75	protein kinase, putative	
AT2G46700	7.62		1.26	1.14		6.84	7.87	calcium-dependent protein kinase, putative / CDPK, putative	
AT1G58440	8.77		0.87	0.90		9.75	10.29	XF1 (SQUALENE EPOXIDASE 1); oxidoreductase	
AT1G78050	7.32		1.13	1.14		6.98	8.00	phosphoglycerate/bisphosphoglycerate mutase family protein	
AT3G55720	7.27	1.57				6.84	8.10	unknown protein	
AT3G25250	7.61	1.62				6.99	8.14	AGC2-1 (OXIDATIVE SIGNAL-INDUCIBLE1); kinase	
AT3G23800	7.13			1.37		6.67	8.40	selenium-binding family protein	
AT4G09510	7.40			1.05		6.63	6.89	beta-fructofuranosidase, putative / invertase, putative	
AT3G11930	6.74				1.70	6.89	8.82	universal stress protein (USP) family protein	
AT1G20190	8.73			0.99		8.56	9.16	ATEXPA11 (ARABIDOPSIS THALIANA EXPANSIN A11)	
AT5G03610	7.96			1.04		8.68	8.92	GDSL-motif lipase/hydrolase family protein	
AT4G03210	8.36			1.04		7.14	8.58	XTH9 (XYLOGLUCAN ENDOTRANGLUCOSYLASE/HYDROLASE 9)	
AT3G12800	8.11	1.02				7.74	8.55	short-chain dehydrogenase/reductase (SDR) family protein	
AT3G14310	10.09			0.97		10.41	11.19	ATPME3 (Arabidopsis thaliana pectin methylesterase 3)	
AT5G01620	8.00			0.95		8.25	8.12	unknown protein	
AT5G44730	7.98				1.22	6.95	7.97	haloacid dehalogenase-like hydrolase family protein	
AT5G62330	6.95	-1.61				-1.86	9.54	8.55	unknown protein
AT3G54220	8.39			-1.24	-1.50	7.50	9.90	SCR (SCARECROW); transcription factor	
AT5G62340	11.04	-0.85				9.03	8.89	invertase/pectin methylesterase inhibitor family protein	
AT5G17310	8.69	-0.71				9.77	9.18	UTP--glucose-1-phosphate uridylyltransferase, putative	
AT5G49360	7.32		-1.32			9.80	7.73	BXL1 (BETA-XYLOSIDASE 1)	
AT3G51660	6.84	-1.13				6.70	6.81	macrophage migration inhibitory factor family protein	
AT1G48110	7.77				-0.78	7.45	8.08	ECT7 (evolutionarily conserved C-terminal region 7)	
AT3G47220	7.49				-0.89	7.26	7.61	phosphoinositide-specific phospholipase C family protein	
AT2G41660	8.61				-0.78	8.83	10.63	MIZ1 (MIZU-KUSSEI 1)	
AT5G24800	7.39		-1.14			7.90	7.51	ATBZIP9/BZO2H2 (BASIC LEUCINE ZIPPER O2 HOMOLOG 2)	
AT1G06040	9.80		-0.85			8.67	8.67	STO (SALT TOLERANCE); transcription factor/ zinc ion binding	
AT1G11380	7.28		-1.06			7.56	8.09	unknown protein	

4.3.3.2 Gene ontology analysis of candidate genes

Gene Ontology (GO) descriptions are employed to associate attributes to a gene using standardised language. To see which main cellular components, biological processes and molecular functions are affected when the GA response is blocked in the endodermis, selected differentially expressed genes from the *gai-DEX* experiment were categorised according to GO descriptions.

The first analysis was to associate each single gene of the 60 candidate genes to a GO functional category to see how they distribute between different categories. First, GOs were assigned for the cellular component category (figure 4.13). The whole Arabidopsis genome is distributed in a total of 16 GO cellular component categories. The 60 candidate genes are dispersed in a total of 15 functional categories, thus indicating that genes affected by the disruption of the GA response in the endodermis is not affecting genes localised to an unique or few cell components but there are widely distributed within the cell and extracellular sites. However, note that an 8.64% of the candidate genes are annotated as cell wall components which may correspond to genes associated with cell wall expansion.

Second, GO annotations in terms of biological function were assigned to the 60 candidate genes. 13 out of the 14 GO Biological categories associated to the whole Arabidopsis genome are represented for the candidate genes. Developmental processes and signal transduction categories account for the 4.75% and 3.72% respectively of the total biological processes annotated for the regulated genes. These two groups may include

genes which may be directly involved in the regulation of endodermal cell expansion acting downstream of GAI.

Last, the distribution of GO for Molecular function categories amongst the candidate genes, was analysed. In this occasion, the number of Molecular function categories represented by the genes was 11 of 15 annotated for the whole Arabidopsis genome. However, there are still represented a wide range of GO categories likely to include candidate genes with a role in the GA regulation of cell expansion.

Genes included in the DNA or RNA binding, transcription factor activity and protein binding categories, represented by a 2.45%, 1.84% and 8.58% respectively of all the genes, may play a direct role in the GA signalling pathway regulating cell expansion. On the other hand, genes included in the hydrolase activity (17.17%), other enzymatic activity (12.88%) and transporter activity (11.65%) categories could include genes that play a role in the process of cell expansion by modifying and delivering material to the cell wall as well as in hormone transport.

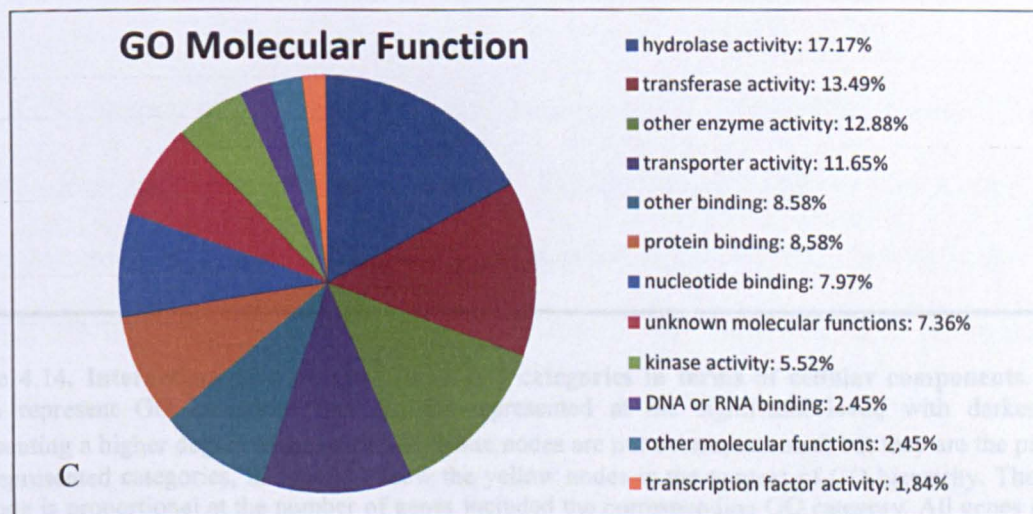
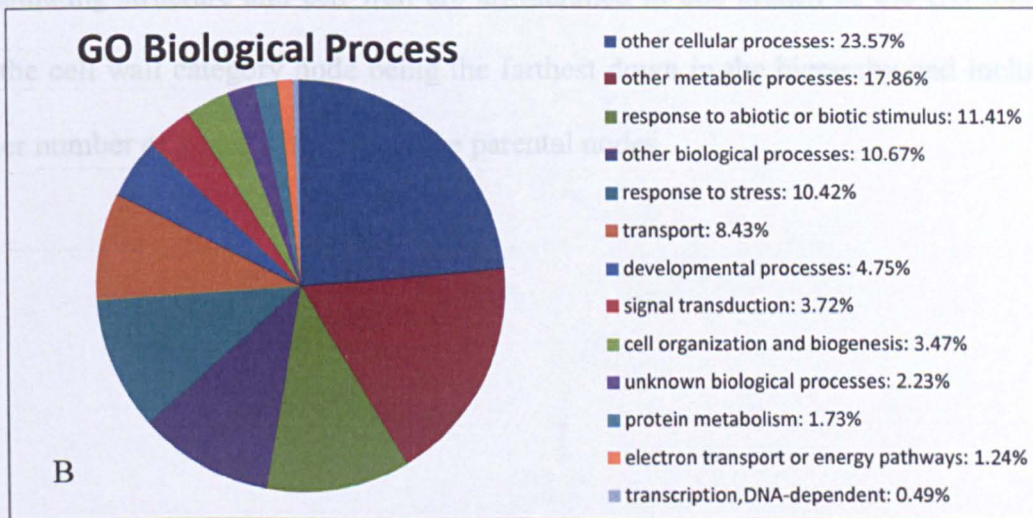
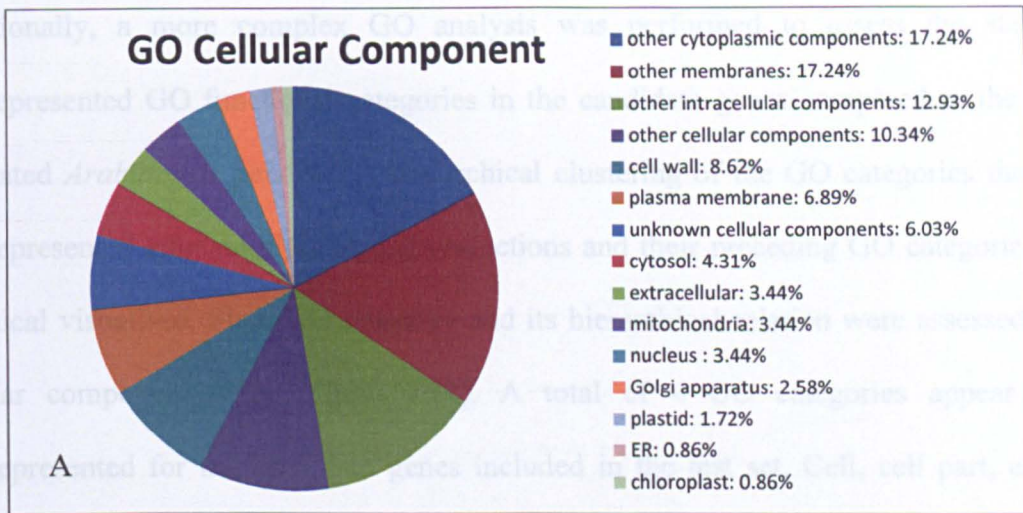


Figure 4.13. Gene Ontologies for cell component, biological process and molecular function categories. Gene Ontologies (GO) descriptions were assigned to all the selected candidate genes (upregulated and downregulated genes) from the *SCR::gai-GR-YFP* line. The percentages of the different GO categories present within the candidate genes for each GO description are shown in this chart. A) GO-cellular component B) GO-Biological Process C) GO-Molecular function

Additionally, a more complex GO analysis was performed to assess the statistical overrepresented GO functional categories in the candidate genes compared to the whole annotated *Arabidopsis* genome. A hierarchical clustering of the GO categories that were overrepresented after multiple testing corrections and their preceding GO categories were graphical visualised. First, GO ontology and its hierarchical relation were assessed at the cellular component level (figure 4.14). A total of 4 GO categories appear to be overrepresented for the candidate genes included in the test set. Cell, cell part, external encapsulating structure and cell wall are all included in one branch of the GO hierarchy, with the cell wall category node being the farthest down in the hierarchy and including a smaller number of genes with respect the parental nodes.

Figure 4.14. Interactions of overrepresented GO categories in terms of cellular components. Yellow nodes represent GO categories that are overrepresented at the significant level, with darker colour representing a higher degree of significance. White nodes are not overrepresented, but they are the parents of overrepresented categories, included to show the yellow nodes in the context of GO hierarchy. The area of the node is proportional at the number of genes included the corresponding GO category. All genes included in one category are explicitly included in all parental categories. A total of 4 linked nodes are highlighted in the network. Based on the nodes size, the two higher overrepresented nodes, cell and cell part include the larger number of candidate genes. Also, it appears that all the genes from the cell wall node are included in the external encapsulating node, representing a small portion of the candidate genes included in the cell part.

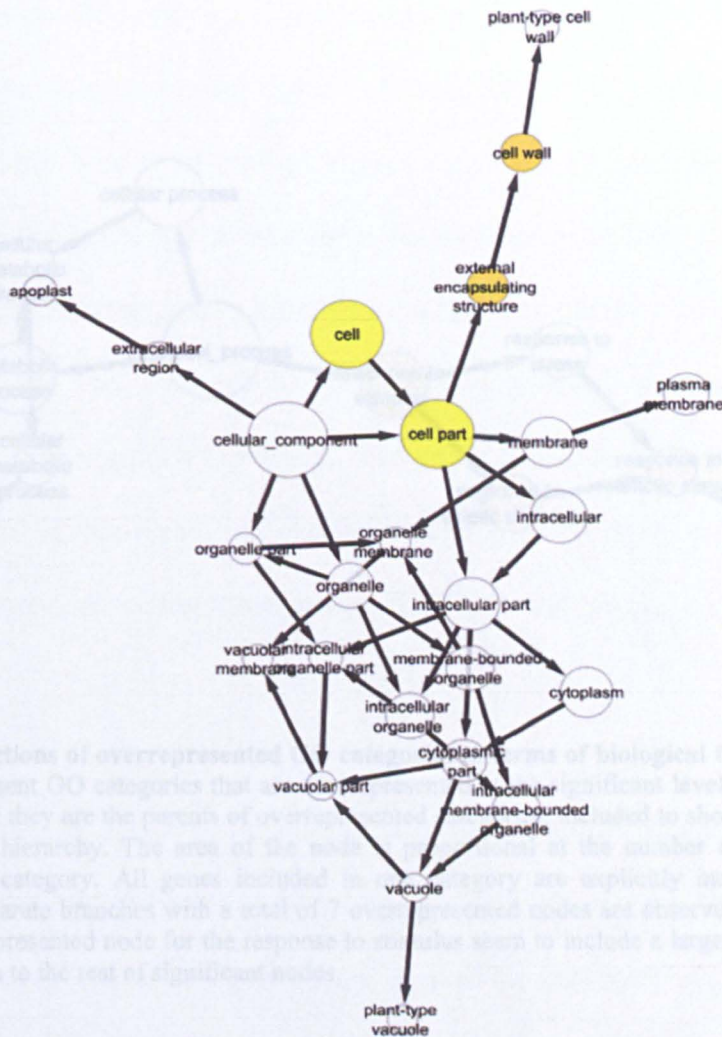


Figure 4.15: Interactions of overrepresented GO categories in the context of biological function comparisons. Yellow nodes represent GO categories that are overrepresented, but they are the parents of overrepresented nodes. The size of the nodes is proportional to the number of genes included in the corresponding GO category. All genes included in the analysis are explicitly included in all parental categories. Two separate branches with a total of 7 overrepresented nodes are observed in the network. The significantly overrepresented node for the response to stimulus seems to include a larger number of candidate genes in comparison to the rest of significant nodes.

4.3.4 Functional analysis of selected GA regulated genes

Also, GO ontology overrepresentation and its hierarchical relation were assessed based on the biological function of the genes (figure 4.15). A total of 7 GO categories appear to be

4.3.4.1 Analysis of differentially regulated genes that may be directly involved in the GA regulation of root cell expansion

related GO functional categories were observed. In one hand, we have the response to

stimulus, response to abiotic stimulus, response to osmotic stress and response to salt stress

categories. On the other hand the overrepresented nodes are for secondary metabolic

process, toxin metabolic process and toxin catabolic process. Based on their nodes areas,

carried out. T-DNA lines from selected candidate genes were screened with the aim to

the response to stimulus node is the one including a larger number of genes in comparison identify putative mutants with a reduced root length to the rest of overrepresented nodes.

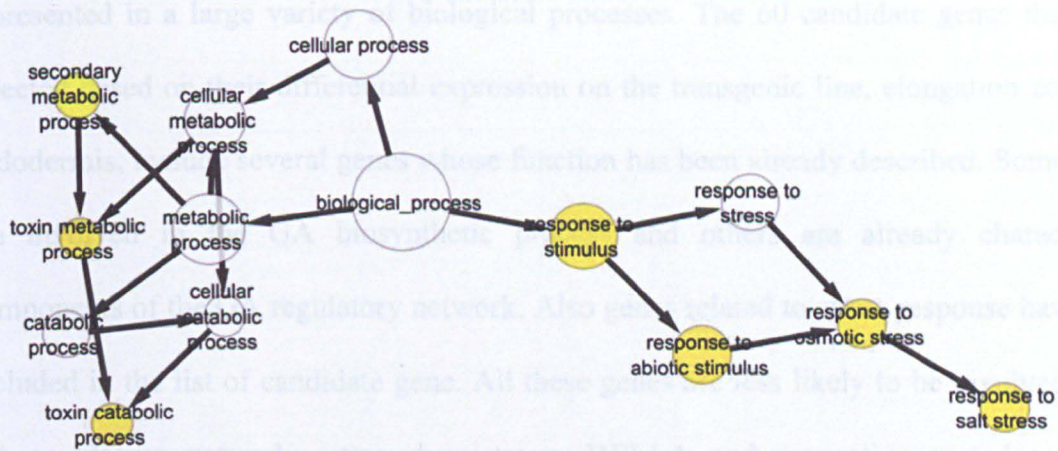


Figure 4.15. Interactions of overrepresented GO categories in terms of biological function components. Yellow nodes represent GO categories that are overrepresented at the significant level. White nodes are not overrepresented, but they are the parents of overrepresented categories, included to show the yellow nodes in the context of GO hierarchy. The area of the node is proportional at the number of genes included the corresponding GO category. All genes included in one category are explicitly included in all parental categories. Two separate branches with a total of 7 overrepresented nodes are observed in the network. The significantly overrepresented node for the response to stimulus seem to include a larger number of candidate genes in comparison to the rest of significant nodes.

4.3.4 Functional analysis of selected GA regulated genes

4.3.4.1 Analysis of differentially regulated genes that may be directly involved in the GA regulation of root cell expansion

As a first step to identify potential components of the GA regulatory network regulating GA to promote cell expansion, and therefore root elongation, root length analyses were carried out. T-DNA lines from selected candidate genes were screened with the aim to identify putative mutants with a reduced root length.

As observed from the GO analyses, a wide range of biological processes are represented within the differentially expressed genes selected from the *gai-DEX* experiment are represented in a large variety of biological processes. The 60 candidate genes that were selected based on their differential expression on the transgenic line, elongation zone and endodermis, include several genes whose function has been already described. Some genes are involved in the GA biosynthetic process and others are already characterised components of the GA regulatory network. Also genes related to stress response have been included in the list of candidate gene. All these genes are less likely to be involved in the GA regulatory network acting downstream DELLA and promoting endodermal cell expansion.

Therefore, in order to optimise the identification of potential components of the GA regulatory network regulating GA to promote cell expansion, and therefore root elongation, only certain classes of genes were selected for functional analysis.

Annotated transcription factors for which a function has not been established, and differentially expressed genes of unknown function at 15 min, 30 min and 60 min (as potential transcription factors) were selected with the aim to identify key signalling genes acting downstream of DELLA. Also, since cell expansion is an important process necessary for the elongation of the cells, all genes that coded for a cell wall associated genes were selected for functional studies.

A total of 22 candidate genes were finally selected for functional characterisation (table 4.4). T-DNA lines were available for the three transcription factors selected (table 4.5). From the 9 unknown genes selected, 8 had available T-DNA lines for screening of root

phenotype. Finally, a total of 10 CWREs were taken forward for functional characterisation and seven of them had T-DNA available.

	AGI	AveExpr	FC-15m	FC-30m	FC-60m	FC-120m	EZ2	endodermis	TAIR description
Transcriptor factor	AT5G67480	7,17	0,90	0,95		0,94	8,47	6,89	BT4 (BTB AND TAZ DOMAIN PROTEIN 4)
	AT5G24800	7,38		-1,14			7,90	7,51	ATBZIP9/BZO2H2 (BASIC LEUCINE ZIPPER O2 HOMOLOG 2)
	AT1G06040	9,8		-0,85			8,67	8,67	STO (SALT TOLERANCE)
Unknown	AT1G54120	8,55	0,96	0,99	0,98		8,81	8,36	unknown protein
	AT5G62330	6,95	-1,61			-1,86	9,54	8,55	unknown protein
	AT1G12845	7,91		1,23	1,42	1,61	6,51	6,94	unknown protein
	AT5G61820	6,71	1,36				10,17	12,74	unknown protein
	AT2G23700	7,76		1,05	0,85		6,84	8,63	unknown protein
	AT5G11420	8,82		1,52	1,51		8,91	8,03	unknown protein
	AT3G55720	7,27	1,57				6,84	8,10	unknown protein
	AT5G01620	8			0,95		8,25	8,12	unknown protein
	AT1G11380	7,27		-1,06			7,56	8,09	unknown protein
Cell wall remodelling enzymes	AT2G36460	9,3	2,25	2,38			7,49	10,19	fructose-bisphosphate aldolase, putative
	AT5G07830	8,42		1,29	1,52	1,33	7,19	9,22	ATGUS2 (ARABIDOPSIS THALIANA GLUCURONIDASE 2)
	AT2G31750	9,04		1,00	1,19		9,02	9,75	UGT74D1 (UDP-GLUCOSYL TRANSFERASE 74D1)
	AT5G62340	11,039	-0,85				9,03	8,89	invertase/pectin methylesterase inhibitor family protein
	AT5G17310	8,68	-0,71				9,77	9,18	UDP-glucose pyrophosphorylase, putative
	AT5G49360	7,31		-1,32			9,80	7,73	BXL1 (BETA-XYLOSIDASE 1)
	AT4G09510	7,39			1,05		6,63	6,89	beta-fructofuranosidase, putative
	AT1G20190	8,73			0,99		8,56	9,16	ATEXPA11 (ARABIDOPSIS THALIANA EXPANSIN A11)
	AT4G03210	8,36			1,04		7,14	8,58	XTH9 (XYLOGLUCAN ENDOTRANSGLUCOSYLASE/HYDROLASE 9)
	AT3G14310	10,09			0,97		10,41	11,19	ATPME3 (Arabidopsis thaliana pectin methylesterase 3)

Table 4.4. List of candidate genes for functional analyses. On this table are shown the genes that were selected from the analysis of the gai-DEX transcriptomics experiments split in three categories. First, there are three transcriptor factors, then a list of 9 unknown selected genes and at the bottom a list of 10 CWREs. The first column next to the gene name corresponds to the average expression value of the gene in the array. Next to them are shown the fold changes which are statistically significant at the different time points. Following FC columns are the EZ2 column, showing the expression values of the gene in the elongation zone of the root and the endodermis column with the correspondent values of the genes in this specific tissue. Finally, the TAIR description column shows the given description for each individual genes.

	AGI	T-DNA line	Insertion site	TAIR description
Transcriptor factors	AT5G67480	SALK_015577C SALK_079615C	exon exon	BT4 (BTB AND TAZ DOMAIN PROTEIN 4)
	AT5G24800	SALK_093416C SALK_111899C	exon exon	ATBZIP9/BZO2H2 (BASIC LEUCINE ZIPPER O2 HOMOLOG 2)
	AT1G06040	SALK_067473C	intron	STO (SALT TOLERANCE)
Unknown	AT1G54120	SALK_080235C	promoter	unknown protein
	AT5G62330	SALK_092085	exon	unknown protein
	AT1G12845	none available		unknown protein
	AT5G61820	SALK_034861C SALK_058742C	exon exon	unknown protein
	AT2G23700	SALK_119196 SALK_119150	prom prom	unknown protein
	AT5G11420	SALK_038436C SALK_094931C	exon prom	unknown protein
	AT3G55720	SALK_037792 SALK_038678	exon prom	unknown protein
	AT5G01620	SALK_007072	intron	unknown protein
	AT1G11380	SALK_022353 SALK_027015	prom prom	unknown protein
	Cell wall remodelling enzymes	AT2G36460	SALK_118067 SALK_118076	prom prom
AT5G07830		SALK_094246C SALK_095797	exon prom	ATGUS2 (ARABIDOPSIS THALIANA GLUCURONIDASE 2)
AT2G31750		salk_004870 SALK_109631	exon exon	UGT74D1 (UDP-GLUCOSYL TRANSFERASE 74D1)
AT5G62340		none available		invertase/pectin methylesterase inhibitor family protein
AT5G17310		SALK_015923 SALK_007967C	exon prom	UDP-glucose pyrophosphorylase, putative
AT5G49360		SALK_054483C SALK_012090C	exon exon	BXL1 (BETA-XYLOSIDASE 1)
AT4G09510		SALK_088756	prom	beta-fructofuranosidase, putative
AT1G20190		none available		ATEXPA11 (ARABIDOPSIS THALIANA EXPANSIN A11)
AT4G03210		SALK_023274 SALK_101024	prom exon	XTH9 (XYLOGLUCAN ENDOTRANSGLUCOSYLASE/HYDROLASE 9)
AT3G14310		none available		ATPME3 (Arabidopsis thaliana pectin methylesterase 3)

Table 4.5. List of selected T-DNA lines for functional characterisation of candidate genes. As in table 4.14, the list of candidate genes are split in three categories (Transcription factors, Unknown and CWREs). Next to each gene are shown the T-DNA selected (two of them when possible) and the insertion site in the gene of the T-DNA. Note that for the Unknown category, AT1G12845 does not have any T-DNA available as well as for AT5G62340, AT1G20190 and AtTG14310 from the CWREs category.

4.3.4.2 Genes upregulated in the *gai-DEX* transcriptomics assay show defects in root length

All T-DNA lines from selected candidate genes were screened with the aim to identify putative mutants with a reduced root length in order to identify potential components of the GA regulated root endodermal cell expansion.

Figure 4.16 shows the primary root length analysis done for selected T-DNA lines available at the time of the experiment for the selected candidate genes.

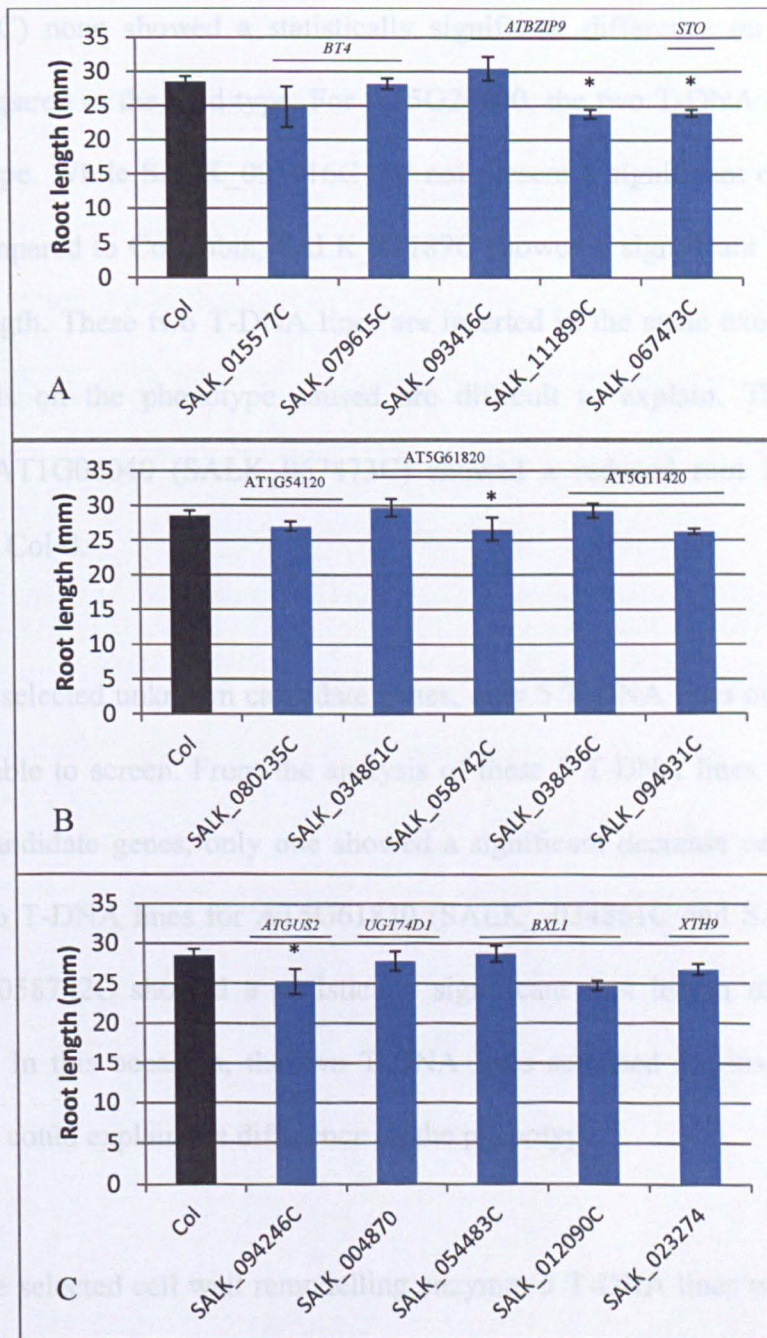


Figure 4.16. **Root length analysis of selected transcription factors, unknown and CWREs mutants.** Primary root length was measured for the different T-DNA lines obtained for the selected candidate at 7 days after germination (dag). A) transcription factor, B) unknown genes and C) CWREs. The mean of the root lengths (mm) are shown with standard errors as vertical lines. Asterisks indicates that the difference of the root lengths between Col-0 and the correspondent T-DNA line is statistically significant (Student's t-test, pValue<0.05)

As shown in figure 4.17 A, from all the T-DNA selected to screen the mutants of the three known selected transcription factors, two T-DNAs showed a significant decrease in their root length. For the two T-DNA lines available for AT5G67480 (SALK_093416C and SALK_111899C) none showed a statistically significant difference on the root length phenotype compared to the wild type. For AT5G24800, the two T-DNA selected differed on the phenotype. While SALK_093416C did not present a significant difference on the root length compared to Colombia, SALK_11189C showed a significant 16.4% reduction on the root length. These two T-DNA lines are inserted in the same exon of the gene so different results on the phenotype caused are difficult to explain. The only T-DNA available for AT1G06040 (SALK_067473C) showed a reduced root length of 15.8% compared with Col-0.

Regarding the selected unknown candidate genes, only 5 T-DNA lines out of the possible 13 were available to screen. From the analysis of these 5 T-DNA lines corresponding to three of the candidate genes, only one showed a significant decrease on the root length. Out of the two T-DNA lines for AT5G61820 (SALK_034861C and SALK_058742C), only SALK_058742C showed a statistically significant root length reduction of 6.5% respect Col-0. In this occasion, the two T-DNA lines screened are inserted in different exons and that could explain the difference on the phenotype.

Finally, for the selected cell wall remodelling enzymes 5 T-DNA lines were also screened and only one showed a significant root length reduction. SALK_094246C shows an 11.3% reduction on the root length compared to the wild type and is one of the two t-DNA available for AT5G07830. The second T-DNA line remains to be screened to see if we observed a constant phenotype.

However, further genotypic analysis needs to be performed on these T-DNA lines to confirm homozygous lines and to analyse mRNA expression before final conclusions based on their phenotypes can be reached.

4.3.4.3 Promoter studies of genes where T-DNA mutation caused a root growth defect

Promoter analyses were carried out for the candidate genes to get insights into their possible role as transcription factors for the unknown genes and to look for associated GA responsive motifs for both unknown and annotated transcription factors from the list of candidate genes.

First, the enrichment of cis-acting elements that are shared between the three candidate transcription factors (AT5G67480, AT5G24800, AT1G06040) in the 1000 bp upstream region that precedes the transcription start site was analysed (table 4.6).

Factor	Number of genes	Family	Sum of TFBSs in total	Theoretical number of TFBSs	Ratio (occurrence/theoretical)
ALFIN1	3	HD-PHD	10	14.43	0.69
ATHB1	3	HD-ZIP	4	1.76	2.28
AtSPL8	3	SBP	6	3.88	1.55
DOF2	3	C2C2(Zn) Dof	67	48.63	1.38
GT1	3	Trihelix	46	38.04	1.21
HAHB4	3	HD-ZIP	5	2.4	2.08
HOX2a_HOX2a	3	- other	4	4.67	0.86
HVH21	3	HD-KNOTTED	11	13.92	0.79
ID1	3	C2H2(Zn)	6	4.14	1.45
P	3	MYB	7	5.55	1.26
RAV1(1)	3	AP2/EREBP	13	8.21	1.58
TEIL	3	AP2/EREBP	15	15.91	0.94
TSS	3	- other	4	0.65	6.11
ZmHOX2a(1)	3	HD-HOX	17	19.96	0.85
ZmHOX2a(2)	3	HD-HOX	9	13.09	0.69

Table 4.6 Selected transcription factors contain 15 shared transcription factors binding sites (TFBSs). The table summarises the identified TFBSs that are common within the 1000bp upstream of the transcription starting site. Individual factors and the family they belong to are described as well as the number of times these TFBSs occur in total for all three genes. The theoretical number of TFBSs, as well as the ratio between the occurrence/theoretical numbers are also shown.

Secondly, the enrichment of cis-acting elements that are shared between all the candidate unknown genes was analysed (AT1G54120, AT5G62330, AT1G12845, AT5G61820, AT2G23700, AT5G11420, AT3G55720, AT5G01620, AT1G11380) in the 1000 bp upstream region that precedes the transcription start site (table 4.7).

Factor	Number of genes	Family	Sum of TFBSs in total	Theoretical number of TFBSs	Ratio (occurrence/theoretical)
ALFIN1	9	HD-PHD	34	43.28	0.79
DOF2	9	C2C2(Zn) Dof	179	145.88	1.23
GT1	9	Trihelix	154	114.12	1.35
HVH21	9	HD-KNOTTED	37	41.75	0.89
RAV1(1)	9	AP2/EREBP	22	24.63	0.89
TEIL	9	AP2/EREBP	49	47.74	1.03
ZmHOX2a(1)	9	HD-HOX	43	59.87	0.72
ZmHOX2a(2)	9	HD-HOX	29	39.28	0.74

Table 4.7 Selected candidate unknown loci contain 8 shared transcription factors binding sites (TFBSs). The table summarises the identified TFBSs that are common within the 100bp upstream of the transcription starting site. Individual factors and the family they belong to are described as well as the number of times these TFBSs occur in total for all three genes. The theoretical number of TFBSs, as well as the ratio between the occurrence/theoretical numbers are also shown.

Promoter analyses of both transcription factor and unknown genes have shown a number of shared transcription factors binding sites (TFBSs). Amongst the most represented in the two categories are the DOF 2, GT1 and TEIL domains.

According to the literature (Sakai *et al.*, 2000), the promoters of genes induced by GAI are enriched in the ARR1 (NGATT) and in the Dof (AAAG) binding sites (Yanagisawa, 2004). ARR1 has been shown to mediate the control of root meristem size in response to GAs through the up-regulation of ARR1 expression by DELLA proteins (Moubayidin *et al.*, 2010). However, ARR1 TFBSs were not identified amongst the promoter of our selected candidate genes. On the other hand, DOFs domains occur in multiple sites of the

analysed promoters. Dof proteins have been implicated in the regulation of GA signalling and biosynthesis in *Arabidopsis* and barley, most likely in the DELLA-mediated feedback regulation of the GA pathway (Gabriele et al., 2010). For the rest of identified TFBSs no link between them and GAs has been established yet.

From the selected unknown genes, screening of the T-DNA insertion for AT5G61820 resulted in plants with reduced root length. In order to get an insight in whether this unknown gene could be potentially regulated by GAI, we analysed the promoter region to try to identify associated GAI responsive motifs (table 4.8).

Factor	Number of genes	Family	Sum of TFBSs in total	Theoretical number of TFBSs	Ratio (occurrence/theoretical)
ATHB1	1	HD-ZIP	2	0.59	3.42
DOF2	1	C2C2(Zn) Dof	10	16.21	0.62
GAMYB	1	MYB	3	2.78	1.08
GT1	1	Trihelix	15	12.68	1.18
HOX2a_HOX2a	1	- other	5	1.56	3.21
HVH21	1	HD-KNOTTED	9	4.64	1.94
TGA1a	1	bZIP	8	1.25	6.39
ZmHOX2a(1)	1	HD-HOX	7	6.65	1.05
ZmHOX2a(2)	1	HD-HOX	4	4.36	0.92

Table 4.8 The unknown selected locus AT5G61820 contains at least one GAI response element The table summarises the identified TFBSs that occur in the 1000bp upstream of the transcription starting site. Individual factors and the family they belong to are described as well as the number of times these TFBSs occur in total for all three genes. The theoretical number of TFBSs as well as the ratio between the occurrence/theoretical numbers are also shown.

Detailed analysis of the promoter region of AT5G61820 resulted in the identification of the Dof binding site domains with multiple occurrence v (10). Also GT1, which was common for the selected transcriptionfactors and all the selected unknowns is represented in the promoter region of AT5G61820.

4.4 DISCUSSION

To date, there is a great deal of understanding about the GA biosynthesis, GA perception and DELLA degradation. At the level of GA signalling, recent studies have shown that DELLA proteins interact with other DNA-binding transcription factors to modify their activity (Zentella *et al.*, 2007). DELLAs appear to control gene transcription through protein interaction with specific transcription factor targets such as PIFs (de Lucas *et al.*, 2008; Feng *et al.*, 2008). However, a lot remains to be done before full understanding of GA signalling can be accomplished. Identification of those unknown components that interact with or are regulated by DELLAs is crucial to understand how GA control regulates the diverse developmental processes.

Several transcriptomics studies have been carried out with the aim to identify those components using different physiological and developmental conditions including roots (Nawya *et al.*, 2005; Brady *et al.*, 2007; Vanneste *et al.*, 2005), seed germination and seedling and floral development (Ogawa *et al.*, 2003; Cao *et al.*, 2006; Nemhauser *et al.*, 2006; Zentella *et al.*, 2007, Hou *et al.*, 2008). The analysis and comparison of all the available data sets has resulted in the identification of various DELLA early response genes. But further characterization of these components is needed to establish their precise role within the GA regulatory network.

In this chapter, a transcriptomics experiment was pursued to identify GAI targets that are directly involved in GA regulation of endodermal root expansion to try to build the gene regulatory network involved in the process. Several genes which respond to expression of a non-degradable form of DELLA *gai* have been identified and their role functionally characterised during root cell expansion.

4.4.1 DEX-*SCR::gai-GR-YFP* TXM Data Analysis

Analysis of the DEX-*SCR::gai-GR-YFP* microarray data has generated a large amount of information from which can be inferred multiple types of analysis to obtain biological information of interest.

From the list of intersecting genes (Appendix III), three of them encoded an *ATGA20OX* (*GIBBERELLIN 20 OXIDASE*; *ATGA20OX1*; *ATGA20OX2* and *ATGA20OX3*) and one a GA4 (GA REQUIRING 4)/ *ATGA3OX1* (*GIBBERELLIN 3-BETA-HYDROXILASE 1*). These are enzymes that catalyze the last step in the formation of bioactive GA. To find these genes amongst the most upregulated ones on the arrays provides an indication that the inducible *gai* system has successfully disturbed GA homeostasis, a key aim if we are to identify new components of the GA response pathway.

The volcano plot illustrates the genes that interact for both higher differential expression values and lowest p-Values. This list of genes could be pointing out those genes in which the expression of *gai* in the endodermis has had a big impact, and therefore could be related to the GA-regulated cell expansion. On the list of intersecting genes (table 4.2), there are found genes such as *ATGA20OX* (mentioned above), *XERICO* and *SCARECROW 3* which have already been described to have a GA related role (Zentella *et al.*, 2007). Of great interest in this search for key components on the GA-regulated endodermal cell expansion, are the cell wall remodelling enzymes. In the list of top differential expressed genes there are included 4 cell wall related proteins. This supports the fact that cell wall modification is a key process during regulation of cell expansion (Vissenberg *et al.*, 2000).

The second set of statistical analysis of the data was done comparing the gene expression between the control and the transgenic line at each individual time point. From the statistical analysis with limma, summary tables (topTables) including information regarding the expression levels of the different genes for each time point were obtained. This information was used to select the most significantly differentially expressed genes for each time point and to filter genes with higher FC or smaller adjusted p-Value to obtain a list of most representative genes at each time point. From them, gene classifications such as between early and late response genes can be done. They also give information about the trend of each individual gene over time (expression pattern) and so can help on gene clustering analysis to help to build up the gene network regulating cell expansion. From this approach a list of genes of interest for functional analysis was obtained.

4.4.2 Selection of candidate genes

After all the statistical analysis to normalise the data and obtain expression values for each gene, a list of 9940 significantly expressed genes from the 22811 included in the array was obtained. Once these genes were filtered for their fold change and adjusted pValue, the list was shortened to only 131 differentially expressed genes. This number can be quite low, however, the expression of the *SCR::gai-GR-YFP* transgene was targeted only in the endodermis but the mRNA was collected for all tissues of the root tip which were not directly affected.

The list of candidate genes was further reduced to 60 after filtering the 131 genes for their significant expression on the elongation zone and the endodermis with the aim to narrow

down the potential putative DELLA downstream signals involved in the endodermal cell expansion.

GO analysis of the selected candidate genes revealed that the blocking of the GA response in the endodermal cells caused a change in genes expression to overall the cell components. Further GO analysis to identify those overrepresented GO functional categories, show that cell wall was specifically overrepresented amongst other cell wall compartments/categories. This could be interpreted as the high regulation towards the cell wall modification needed to regulate cell expansion. On the overrepresented categories regarding the biological processes it can be observed that response to stimulus is the category including a higher number of genes. As observed on Ubeda-Tomás *et al.*, (2008) the lack of GA response in the endodermis prevents the cells in this tissue to expand and to the adjacent cell tissues to bulge. This is for sure to cause pressure on the cell walls that targeting also genes involved in stress responses as observed from the GO analysis.

4.4.3 Functional characterisation of candidate genes.

The key aim of this transcriptomics experiment was to identify components of the GA regulatory network targeting endodermal root cell expansion. Therefore, from the analysed data set there were selected several genes based on their expression profile and function which were thought to be potential components of the GA response network.

Several genes have been identified which are either up-regulated or down-regulated in response to the expression of *gai*. Those genes which are up-regulated in the absence of GA response in the endodermis are genes which are likely to act as growth repressors. On

the other hand, *gai* downregulated genes may be growth activators which are normally repressed by DELLAs.

Out of the three transcription factors selected, the expression of BT4 (AT5G67480) is enhanced in the absence of a GA signalling response. Screening of the two T-DNA lines for this locus did not result in a defect on the root length, which can support a role for these genes as growth repressor. According to its potential function as growth repressor, overexpression of this gene should result in a growth defect in the roots even though the DELLAs were normally degraded. BT4 has been reported as target of the DELLA protein RGA (Zentella *et al.*, 2007). Expression of a non degradable form of *rga*, resulted in down-regulation of *BT4* similar to our results and up-regulation in *gal-3* mutants treated with GA. The Arabidopsis genome encodes a small subfamily of five BTB AND TAZ DOMAIN (BT) protein. These proteins are characterised by an N-terminal BTB domain, a transcriptional adapter zinc finger (TAZ) domain and a C-terminal calmodulin binding (CaMB) domain. BT proteins have been found to interact with the potato calmodulin 6 in a calcium-dependent manner, and BT1, 2 and 4 were found to bind to bromodomain transcriptional regulators (Du and Poovaiah, 2004). Functional analyses of some BTB proteins carried out in yeast and *C. elegans* showed that these proteins probably act as scaffold proteins and are part of CULLIN3 (CUL3)-containing E3 Ubiquitin ligases (Furukawa *et al.*, 2003; Geyer *et al.*, 2003; Moon *et al.*, 2004; Pintard *et al.*, 2004). Analysis of single null or loss of function mutants result in plants with wildtype appearance suggesting the functional redundancy between BT members. Study of double and multiple mutants revealed a role for these proteins in reduced seed set and shortened siliques (Robert *et al.*, 2009). It appears that BT1, BT2 and BT3 act redundantly during

gametophyte development. The role of BT4 has not been established in this process and its function is still not known.

The other two selected transcription factors ATBZIP9 (AT5G24800) and STO (AT1G06040) are downregulated by the expression of *SCR::gai-GR-YFP*. Analysis of the T-DNA lines of these two genes resulted indeed in a reduction on the root length, thus revealing a potential role of these two genes GA regulated root cell expansion.

ATBZIP9, also named BZO2H2 (BASIC LEUCINE ZIPPER O2 HOMOLOG 2) is a member of the basic region/leucine zipper motif (bZIP) transcription factors. They have been involved in the regulation of processes such as pathogen defence, light and stress signalling, ABA response, seed maturation and flower development (Lee *et al.*, 2006; Tajima *et al.*, 2008; Yang *et al.*, 2009; Alonso *et al.*, 2009). In *Arabidopsis* there are annotated 75 distinct members of the bZIP family which are divided into 10 groups of homologues (Jakoby *et al.*, 2002). ATBZIP9 is included in group C which has three other genes (AtbZIP10/Bzo2h1;AtbZIP63/Bzo2h3 and AtbZIP25/Bzo2h4). These four members are homologous to the maize Opaque-2 (O2) locus (Vincentz *et al.*, 2003). O2 expression is restricted to the developing endosperm where it controls storage protein gene expression and the carbon to nitrogen balance (Cireri *et al.*, 1999). The O2-related function does not appear to be much conserved in *Arabidopsis*. In the case of AtbZIP63, it is poorly expressed in seeds and not much is known about its function. AtbZIP10 and AtbZIP25 are thought to interact with the regulatory factor ABI3 to control the activity of the At2S1 albumin gene promoter (Lara *et al.*, 2003). With respect to AtbZIP9, Silveira *et al.*, (2007) reported that AtbZIP9 mRNA accumulation was repressed by glucose and induced by abscisic acid and cytokinin. The expression of a fusion between the VP16 transcriptional

activator domain and AtbZIP9 resulted in significant changes in leaf development and in the structure of the vascular bundle. However, ATbZIP9 target genes are still unknown.

At this stage, we cannot be sure whether the reduction observed in the single T-DNA mutant for ATbZIP9 is related to a defect in the structure of the vascular bundle or it is an independent phenotype associated with the GA regulated endodermal cell expansion. Detailed analysis of the mutant roots at the cellular level would provide this information.

Regarding the identification of potential CWREs involved in the GA regulated endodermal root cell expansion, a list of 10 genes representing a diversity of CWREs families. Out of the 10 candidate genes, only three of them have currently been characterised. So far, only a loss-of-function mutant in ATGUS2, a glucuronidase gene, expressed in roots, exhibited a significant decreased length.

ATGUS2 encodes a protein with several post-translational modification sites including O- β -GlcNAc attachment sites and serine-, threonine- and tyrosine-phosphorylation sites, suggesting that this protein is extensively modified post-translationally. Previous studies suggested that GUS activity influences the sugar composition of chains of arabinogalactan proteins (AGPs). Also, work by Eudes *et al.*, (2008) assessing the phenotype of *atgus2* loss-of-function showed a reduction in both hypocotyls and root lengths. On the other hand, overexpression of ATGUS2 results in plants with increased hypocotyls and root lengths. This data is consistent with the phenotype observed from our screening and suggests an important role of ATGUS2 in the cell growth. More work needs to be done to try to identify the components downstream of GAI, that regulate the action of this enzyme on its role on the endodermal cell expansion.

Since the regulation of cell expansion is a complex process in which different kinds of enzymes are needed to modify the different molecules forming the cell wall, it is expected that future analysis of the rest of the identified CWREs pinpoint further enzymes complementing the work of ATGUS2.

In summary, several putative DELLA regulated genes have been identified in an inducible transcriptomic time course dataset. Functional studies provide preliminary evidence that their gene products play a role regulating root growth. Further studies are required to integrate them into the GA response pathway.

Chapter 5: ANALYSIS OF MEMBERS OF THE XYLOGLUCAN ENDOTRANSGLYCOSYLASE FAMILY IN THEIR ROLE IN GA REGULATED CELL EXPANSION

5.1 INTRODUCTION

5.1.1 Cell wall expansion in cell elongation

The regulation of cell expansion plays a key role controlling root growth (Ubeda-Tomás *et al.*, 2012). Cell expansion is primarily controlled through modification of the properties of the plant cell wall (Somerville, 2006). The plant cell wall consists of a complex network of polysaccharides of cellulose microfibrils associated by hydrogen bonds that hold the microfibrils together to provide high tensile strength. These cellulose microfibrils are embedded within a pectin matrix and cross-linked through a network of hemicelluloses polymers (Cosgrove *et al.*, 2005). Organized into a network with the cellulose microfibrils, the cross-linking glycans increase the tensile strength of the cellulose, whereas the coextensive network of pectins provides the cell wall with the ability to resist compression. This organisation provides the wall with nonlinear anisotropic mechanical properties and allows enzymatic regulation of cell growth expansion (Dyson *et al.*, 2012). Growth of the cell wall is accompanied by a continuous supply of new material to the inner wall to ensure wall integrity (Cosgrove, 2005)

Cellulose microfibrils are the primary load-bearing components of the cell wall. The way the microfibrils orientate and crosslink between them are key factors to determine to what extent and direction a cell expands (Darley *et al.*, 2001). In cells expanding

longitudinally, the cellulose microfibrils are mainly deposited in an orientation perpendicular to the axis of expansion, thus restricting radial expansion (Baskin, 2005).

The mechanical driven expansion of the wall is accompanied by the action of different cell wall remodelling enzymes (CWREs) acting on different components of the cell wall. Pectin methyl esterase (PME) can affect the consistency of the cell wall removing methyl groups by breaking ester bonds that can then interact with calcium ions forming a pectate gel, thus stiffening the cell wall and reducing cell expansion (Micheli, 2001; Siedlecka *et al.*, 2008). Expansins induce wall stress relaxation and extension in a pH-dependent manner by disturbing the hydrogen bonds that hold the microfibrils in place within the wall (McQueen-Mason and Cosgrove, 1995). Xyloglucans endotransglycolases/hydrolases (XTHs) are thought to act in the loosening of the cell-wall by their XEH activity (xyloglucan endohydrolase) by breaking the bond between two hemicellulose crosslinks (Fry *et al.*, 1992; Nishitani and Vissenberg, 2007). Other members with XET activity (xyloglucan endotransglycosylase) catalyze the endo-cleavage of xyloglucan polymers (donors) and transfer of the newly generated reducing ends to other polymeric or oligomeric xyloglucan acceptor molecules (Smith and Fry, 1991; Nishitani and Tominaga, 1992). The XET action of XTH is thought as a mechanism for cell expansion as transglycosylation between two potentially load-bearing xyloglucan molecules could increase slippage of adjacent microfibrils, resulting in reversible cell wall loosening (Figure 5.1.1). Additionally, XTHs catalyze molecular grafting reactions that are required to integrate newly synthesized xyloglucan into the existing cell wall (Figure 5.1.2; Thompson *et al.*, 1997). Expression analyses have shown that XTH gene expression correlates with growth, such as in the elongation zone of the *Arabidopsis* roots or root hair initiation zone (Vissenberg *et al.*, 2001, 2003).

Also, XTH enzymatic action in situ has been correlated to growth (Fry *et al.*, 1992; Catalá *et al.*, 1997; Vissenberg *et al.*, 2000; 2005; Van Sandt *et al.*, 2007). On the other hand, XET activity has been detected in non-expanding tissues where its cell wall-tightening role may contrast the wall-loosening effect of active XTHs (Palmer and Davies, 1996) and in some cases specific XTH genes appear to be down regulated during rapid growth (Catalá *et al.* 2001).

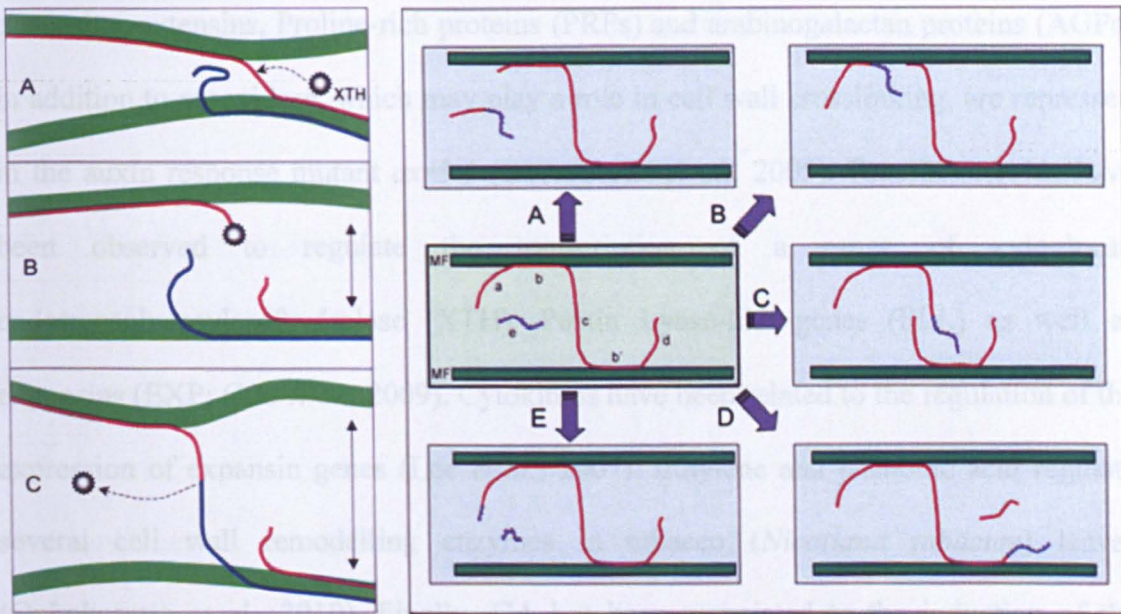


Figure 5.1 Graphical representation of the two main roles proposed for XTHs (XET action) in growing cells. 1) Cell wall restructuring. (Step 1; panels A to B) XTH cleaves a xyloglucan chain (red line), which acts as a tether between two cellulose microfibrils. This xyloglucan chain is broken and a xyloglucan–XTH complex is formed. When the cell is turgid, the microfibrils can slip apart, as shown by the unbroken arrows. (Step 2; panels B to C) The xyloglucan–XTH complex is now out of reach of the new non-reducing terminus but within reach of the non-reducing terminus of an adjacent xyloglucan chain (blue line). This adjacent chain can act as an acceptor substrate and to re-form a new tether between the two microfibrils. **2) Cell wall integrational restructuring.** The figure shows the five possible forms of integrational endotransglucosylation between a newly secreted xyloglucan (blue line) and a previously wall-bound xyloglucan chain (red line). The reducing terminus is the right-hand end of each chain. In the initial state (green shaded left center panel), four different segments of the wall-bound chain are differentiated: (a) a non-reducing loose end, (b, b') regions anchored to cellulose microfibrils by hydrogen bonds, (c) a tether between the microfibrils, (d) a reducing loose end. e) Arrows (A to D) indicate what happens when XTH cleaves the wall-bound chain at sites a to d, respectively, and the newly secreted chain acts as acceptor. Arrow E shows what happens if the XTH targets the newly secreted chain at site e and the previously wall-bound chain acts as acceptor (reproduced from Rose *et al.*, 2002).

In summary, many different families of CWREs affect the properties of the cell-wall and, as a consequence, impact the cell's growth rate. Hormonal regulation of these

CWREs is thought to play an important part in the regulation of cell expansion (Wu *et al.*, 1994; Catalá *et al.*, 1997). Therefore, understanding the relationship between specific hormone signalling pathways and specific CWREs is necessary in order to gain knowledge about the process of cell expansion in roots.

Different CWREs have been directly linked to specific plant hormones. In the case of auxins, xyloglucan endotransglucosylases (XTHs), pectinmethylesterases (PMEs), expansins, extensins, Proline-rich proteins (PRPs) and arabinogalactan proteins (AGPs) in addition to peroxidase, which may play a role in cell wall crosslinking, are repressed in the auxin response mutant *axr3-1* (Overvoorde *et al.*, 2005). Brassinosteroids have been observed to regulate the transcription of a range of xyloglucan endotransglycosylase/hydrolase (XTH), Pectin Lyase-like genes (PLL) as well as expansins (EXP; Guo *et al.*, 2009). Cytokinins have been related to the regulation of the expression of expansin genes (Lee *et al.*, 2007). Ethylene and jasmonic acid regulate several cell wall remodelling enzymes in tobacco (*Nicotiana tabacum*) leaves (Onkokesung *et al.*, 2010). Finally, GA has been associated to the induction of the expression of specific members of the XTH family. Liu *et al.*, (2007) observed that the expression of *AtXTH21* (At2g18800), which it is mainly expressed in root and flower, was induced by treatment with GA₃ but not other hormones. *AtXTH21* is involved in the maintenance of the thickness, integrity and strength of the cell wall during cell elongation. Study of loss-of-function mutants using T-DNA insertion lines for *AtXTH21* resulted in dwarf plants with short roots and thinner cell walls. On the other hand, studies with over expression lines (*35S::XTH21*) resulted in plants with thicker cell walls. Thus, *AtXTH21* gene seems to play a key role in the growth of the primary roots by changing the deposition of cellulose and the elongation of cell wall. In rice, Jan *et*

al., (2004) explained that *OsXTH8* (*Oryza sativa* XTH-related gene) expression in the leaf was up-regulated by GAs and there was very little effect of other hormones on its expression. Transgenic rice expressing an RNAi construct of *OsXTH8* exhibited reduced growth. These results indicate that *OsXTH8* is differentially expressed in rice leaf sheath in relation to gibberellins and potentially involved in cell elongation processes. These connections between XTHs and GA suggested that this hormone may directly regulate members of the XTH family as means to promote endodermal root cell expansion. Therefore an analysis of members of the XTH family regulated by GA has been carried out in this project to test this hypothesis.

5.1.2 GA-regulated root-expressed XTH genes

Expression analyses have shown that XTH gene expression is high in regions of active wall formation such as in elongation zones, and in regions where wall deposition continues after cell enlargement has ceased or where other forms of wall remodelling take place (Yokoyama *et al.*, 2004).

XTHs are encoded by large gene families, with *Arabidopsis thaliana* possessing 33 XTH genes. The 33 XTH genes are distributed across all five chromosomes of *Arabidopsis*, with one third of the genes occurring as clusters consisting of two to four members (Figure 5.2; Yokoyama and Nishitani 2001), most likely consequential from genome duplication and gene reshuffling (Blanc *et al.* 2000). It has been suggested that individual XTH genes have evolved to be expressed with distinct developmental, organ-, tissue- or cell-specific expression or may be upregulated to respond to distinct developmental, hormonal or environmental stimuli (Vissenberg, *et al.*, 2005; Becnel *et*

al., 2006). In vitro studies have shown that divergent XTHs exhibit one or both of the two distinct biochemical activities (xyloglucan endotransglucosylation (XET) and xyloglucan hydrolysis (XEH). Thus, it is thought that the different members of the XTH family are unlikely to be functional redundant and that they may have unique expression, regulation and physiological properties. In fact, loss of a single XTH can result in significant developmental defects, such as a reduction of root length as reported by Osato *et al.*, (2006).

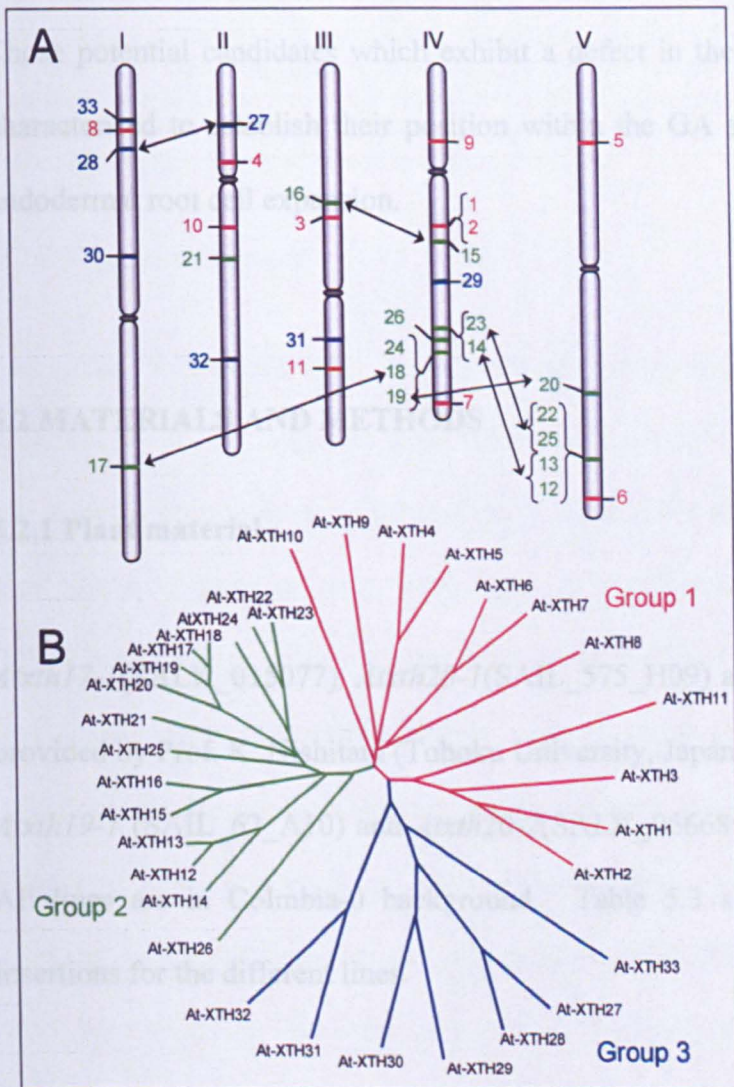


Figure 5.2 **Chromosome distribution and phylogenetic relationship between the members of the Arabidopsis XTH gene family.** (A) Physical map showing the distribution of the Arabidopsis XTH genes among the five chromosomes. Arrows indicate genes which are duplicated. (B) Dendrogram of all 33 Arabidopsis XTH genes based on the predicted amino acid sequences. The family of 33 Arabidopsis XTH genes is divided into three major groups in agreement with their phylogeny and also on the structure and organization of individual genes. For A and B of the figure, genes from groups 1, 2 and 3 are shown in red, green and blue, respectively. (Reproduced from Rose *et al.*, 2002)

With the aim to identify those XTHs that could potentially be components of the GA regulatory network regulating root endodermal cell expansion, I analysed available transcriptomics data to select XTH genes which were GA regulated, significantly expressed in the elongation zone of the root and in the endodermis.

From the XTH selected genes, mutant studies with available T-DNA lines and RNAi lines were carried out to identify mutants with a potential defect on root/cell expansion.

Screening of GA-related genes for defects on root growth will be the first step to try to identify genes which may be part/components of the GA signalling network that regulate endodermal root cell expansion.

Those potential candidates which exhibit a defect in their root growth will be further characterised to establish their position within the GA signalling network to regulate endodermal root cell expansion.

5.2 MATERIALS AND METHODS

5.2.1 Plant material

Atxth17-1(SALK_015077), *Atxth20-1*(SAIL_575_H09) and XTH18-RNAi were kindly provided by Prof. K. Nishitani (Tohoku University, Japan). *Atxth17-2* (SALK_008429), *Atxth19-1* (SAIL_62_A10) and *Atxth20-2*(SALK_066689) were obtained from NASC. All lines are in Columbia-0 background. Table 5.3 shows the site of the T-DNA insertions for the different lines.



Figure 5.3. **Insertion sites of the T-DNA lines within the genes of the selected *xth* mutants.** Graphical representation of the selected *Atxth*s where the relative location of the T-DNA insertion between the gene is shown. Each individual figure is accompanied by the name given to each mutant on this thesis together with the gene size. Green arrows correspond to the T-DNA insertions with the given name to the insertion line annotated by the side of it. The orange boxes correspond to exons and yellow lines to introns. Blue perpendicular lines designate sites of restriction enzymes.

5.2.2 Gene redundancy

Functional redundancy often occurs between genes which are closely related at the sequence level. Phylogenetic trees are useful tools to determine how closely related one gene is from another and therefore to think about alternative screenings different than single mutants to see a phenotype. A dendrogram has been drawn for XTH CWREs subfamily, using bioinformatics tools such as Clustal (<http://www.ebi.ac.uk>) and Dendroscope (available from: <http://www-ab.informatik.uni-tuebingen.de/software/dendroscope/welcome.html>) software. For each of the genes, I also integrated expression levels in (A) the different zones of the roots obtained from the 5-sectional root transcriptomics dataset produced on CPIB (introduced on chapter 4) (B) Also, the expression levels for each gene in the elongation zone of Arabidopsis roots treated with GA at different time points (30, 60 and 180 minutes) (data produced in

CPIB, unpublished data), plus (C)the levels of expression of the different XTHs in the root endodermis (Birnbaum *et al.*, 2003)

5.2.3 Functional analysis of root development for *xth* mutants

Root growth analyses for single and double *xth* mutants were carried out to look for defects on the primary root growth as described in section 2.2.1. Seedlings were surface sterilised and growth as described in section 2.1

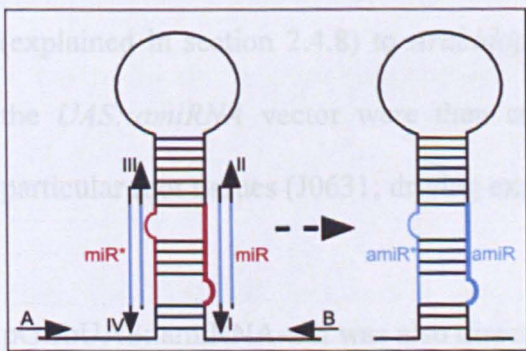
For those lines which presented a decrease on the root growth when compared to the wild type Colombia, confocal analysis were carried out to study the associated phenotype further. Meristem size, as well as meristem and elongation zone cell number and cell size were measured as described in section 2.2.3.

5.2.4 amiRNA approach to study an *xth* quadruple mutant

Phylogenetic studies revealed that XTH17, XTH18, XTH19 and XTH20 have a strong functional relationship and therefore they may be involved in similar developmental processes and site of actions. If this is the case, the effect of a single knock out may be covered for the action of any of the other three family members and therefore single knock outs would not be sufficient to see a phenotype. Hence, an amiRNA construct to knock down all four genes simultaneously was designed using the WMD3 – Web micro RNA designer (<http://wmd3.weigelworld.org>). The artificial microRNA designer WMD delivers 4 oligonucleotide sequences (Table 5.1), which are used to engineer the artificial microRNA into the *Arabidopsis* endogenous miR319a precursor by site-directed mutagenesis (Figure 5.4). A plasmid pRS300 which contains the miR319a precursor in pBSK was used as a template for the PCRs (Appendix IV).

Oligos for amiRNA "TATAAGTGTGAAAGTTAGCGA"
I-a miR-s gaTATAAGTGTGAAAGTTAGCGAtctctcttttgtattcc
II-a miR-a gaTCGCTAACTTTCACACTTATAtcaaagagaatcaatga
III-a miR*s gaTCACTAACTTTCAGACTTATTtcacaggtcgtgatatg
IV-a miR*a gaAATAAGTCTGAAAGTTAGTGAtctacatatattcct

Table 5.1 Oligos designed to create amiRNA vector to downregulate *XTH17*, *XTH18*, *XTH19* and *XTH20* simultaneously



	forward oligo	reverse oligo	template
(a)	A	IV	pRS300
(b)	III	II	pRS300
(c)	I	B	pRS300
(d)	A	B	(a)+(b)+(c)

I: microRNA forward II: microRNA reverse
 III: microRNA* forward IV: microRNA* reverse

Figure 5.4. **Cloning strategy.** The amiRNA containing precursor is generated by overlapping PCR. A first round amplifies fragments (a) to (c), which are listed in the table above. These are subsequently fused in PCR (d). Oligonucleotides A and B are based on the template plasmid sequence. They are located outside of the multiple cloning site of pBSK to generate bigger PCR products. (<http://wmd3.weigelworld.org>)

The final PCR product was then sequenced and after sequence confirmation was placed behind a promoter of interest and finally cloned into a binary plasmid.

For tissue specific expression of amiRNA, a GAL4 based transactivation approach was used. The final PCR product was placed downstream of GAL4 recognition motif (UAS) to regulate *UAS:amiRNA* transgene expression in a GAL4-dependent manner. This construct was then cloned into a binary vector (modified pGreen, pGIIbUAS, <http://www.pgreen.ac.uk/pGreenII/pGreenII.htm>).

Plasmid pRS300 and pGIIbUAS were kindly provided by Dr. Detlef Weigel. Protocol for the cloning of the amiRNA was followed as specified in Schwab *et al.*, (2006) and in section 2.4 of general materials and methods.

The pGIIbUAS vector containing the amiRNA sequence to downregulate the 4 *XTHs* (pGIIbUAS::amiRNA-xth) was transformed in *Agrobacterium tumefaciens* GV3101 strain containing the pSOUP vector and then transferred by flower dip transformation (explained in section 2.4.8) to *Arabidopsis* C24 ecotype. C24 plants transformed with the *UAS::amiRNA* vector were then crossed with driver lines expressing GAL4 in particular root tissues (J0631; driving expression in all tissues of the elongation zone).

pGIIbUAS::amiRNA-xth was also directly transferred to the selected driver lines J0631 for rapid assessment of its function. At least 10 independent F1 plants were selected for each line and at least 3 independent plants segregating $\frac{3}{4}$ for BASTA^R in the T2 generation were taken to the T3 generation to get homozygous. For the driver lines, 3 independent plants segregating for both BASTA R and Kan R (for selection of the GAL4 vector) were taken to the T3 to get homozygous lines.

5.2.5 Tissue-specific expression profiles of XTHs

Representation of the root tissue-specific expression pattern of the four XTHs on greater detail were obtained from the Bio-Array Resource web-based tools (<http://bar.utoronto.ca/welcome.htm>) based on the Schmid *et al.* (2005) Map of Arabidopsis Development, the AtGenExpress Consortium data.

5.3 RESULTS

5.3.1 Selection of GA regulated XTHs members

A phylogenetic tree of the 33 annotated XTH genes in *Arabidopsis thaliana* was performed to get information of the hierarchical relationship of the different members as a way to assess the possible redundancy between them for further screenings (Figure 5.5)

From the 33 XTHs members a total of 15 (*AtXTH4*, *AtXTH5*, *AtXTH8*, *AtXTH12*, *AtXTH13*, *AtXTH15*, *AtXTH16*, *AtXTH17*, *AtXTH18*, *AtXTH19*, *AtXTH21*, *AtXTH23*, *AtXTH27*, *AtXTH30*, *AtXTH33*) appear to be significantly expressed (>100) in the accelerating elongation zone of the root (zone 2). Of these 15 genes, only *AtXTH8* and *AtXTH19* are not significantly expressed in the decelerating elongation zone (zone 3). Additionally, there are 4 members that are expressed in zone 3 but not zone 2 (*AtXTH14*, *AtXTH24*, *AtXTH28*, *AtXTH31*).

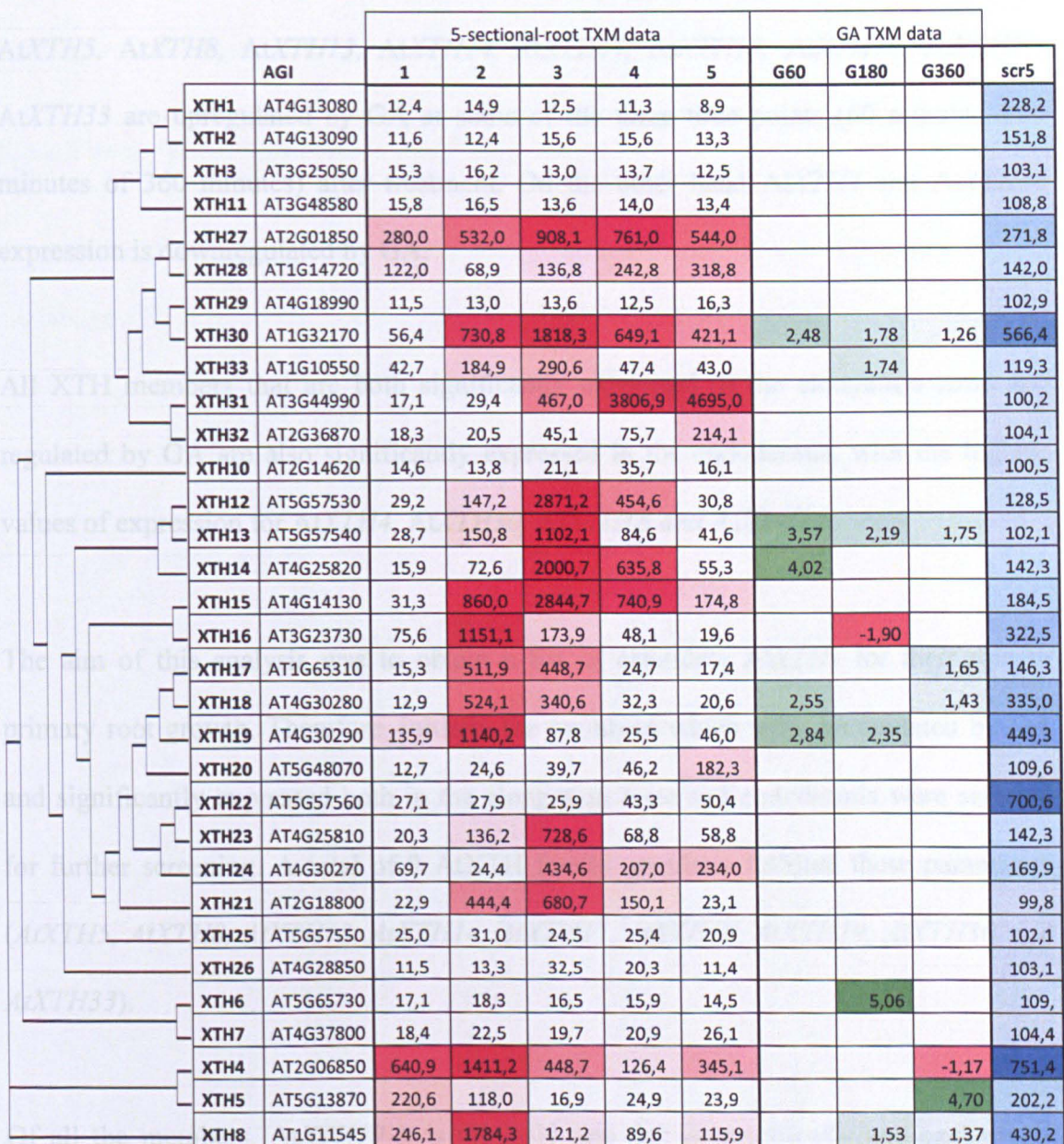


Figure 5.5 XTH family tree with associated expression values on different root developmental areas, endodermis and for whole roots treated with GA at different time points. The different branches represent the hierarchical relationship between the 33 different members of the XTH family. Next to each gene, there are their normalised expression values for the 5 different developmental zones of the root as established on the 5-sectional root transcriptomics data set (1:meristem; 2:accelerating elongation zone; 3: decelerating elongation zone; 4: mature zone; 5: rest of the root/lateral root emergence). Red-grade colour indicates significant expression of a gene for a given developmental zone, going from low to high expression for stronger colours. Next to it, there are indicated the significant fold change expression values for this genes on the whole roots when treated with external GA. Green indicate genes which are upregulated whilst red denote downregulation of a gene. Also, in the last column (SCR5) are shown the expression values of all the XTH genes on the endodermis. Genes are considered to be significantly expressed when normalised expression values are >100.

Of the XTH significantly expressed in the elongation zone of the root (zones 2 and 3), *AtXTH5*, *AtXTH8*, *AtXTH13*, *AtXTH14*, *AtXTH17*, *AtXTH18*, *AtXTH19*, *AtXTH30*, *AtXTH33* are upregulated by GA at some of the three time points (60 minutes, 180 minutes of 360 minutes) after treatment. On the other hand *AtXTH4* and *AtXTH16* expression is downregulated by GA.

All XTH members that are both significantly expressed in the elongation zone and regulated by GA are also significantly expressed in the endodermis, with the highest values of expression for *AtXTH4*, *AtXTH30*, *AtXTH18* and *AtXTH19*.

The aim of this analysis was to obtain a list of candidate *AtXTHs* for their role in primary root growth. Therefore, initially the members which were upregulated by GA and significantly expressed both in the elongation zone and endodermis were selected for further screening. A total of 9 *AtXTH* family members fulfilled these parameters (*AtXTH5*, *AtXTH8*, *AtXTH13*, *AtXTH14*, *AtXTH17*, *AtXTH18*, *AtXTH19*, *AtXTH30*, and *AtXTH33*).

Of all the members, *AtXTH19* it is the only one that is specifically and exclusively expressed in the accelerating elongation zone with a high fold change expression under GA treatment at two of the time points (60 minutes and 180 minutes) and with strong endodermal expression. Besides, *AtXTH17*, *AtXTH18*, which are closely related to *AtXTH19* and also fulfilled the initial selection parameters were selected. Additionally, based on the phylogenetic analysis, *AtXTH20* is strongly related to the other three members it was also selected for further analysis. A genetic and molecular approach

was used to identify components of the GA regulatory network regulating root endodermal cell expansion.

5.3.2 Tissue specific expression profiles of XTHs

To gain insight into the roles of these four phylogenetically closely related genes, the tissue-specific expression profiles for the four *Arabidopsis* XTH genes, *AtXTH17*, *AtXTH18*, *AtXTH19* and *AtXTH20* were examined based on the information on array gene expression profiles on BAR (Toronto Bio-Array Resource web; Figure 5.6)

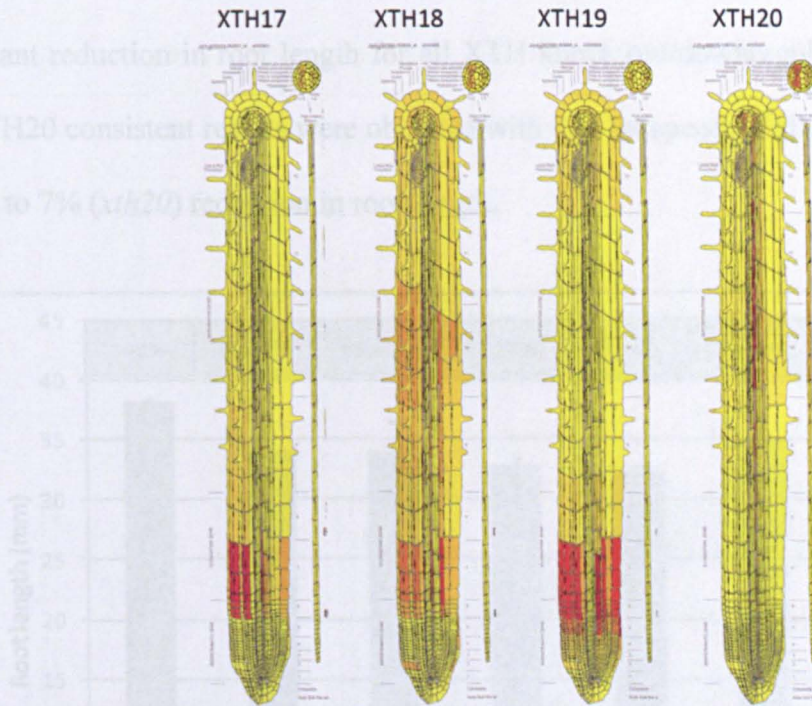


Figure 5.6. Tissue specific expression profiles of *AtXTH17*, *AtXTH18*, *AtXTH19* and *AtXTH20* in the *Arabidopsis* root

AtXTH17 and *AtXTH18* were expressed in all cell types in the elongating and differentiating region of the root (Figure 5.6 a,b). *AtXTH19* is expressed in the meristem, elongating regions and maturation zone (endodermis mainly, Figure 5.6 c). *AtXTH20* is expressed specifically in vascular tissues in the mature region of the root.

5.3.3 Selected *AtXTH* mutants present a decrease in the primary root length

Assessment of the growth of the primary root was carried out for mutants of the four related XTHs members selected. Two independent T-DNA lines knock outs for *AtXTH17* and *AtXTH20* were investigated whereas for *AtXTH18* a RNAi line was used. For *AtXTH19*, only one homozygous T-DNA line was investigated (details of their double mutants were created. As shown in Figure 5.5, the two insertion sites in section 5.2.1).

Figure 5.7 illustrates the root lengths of the different *AtXTH* mutants versus a wild type control (Colombia-0) at 7 days after germination (dag). The results revealed a significant reduction in root length for all XTH knock out/downregulated. For XTH17 and XTH20 consistent results were obtained with two independent alleles showing 11% (*xth17*) to 7% (*xth20*) reduction in root length.

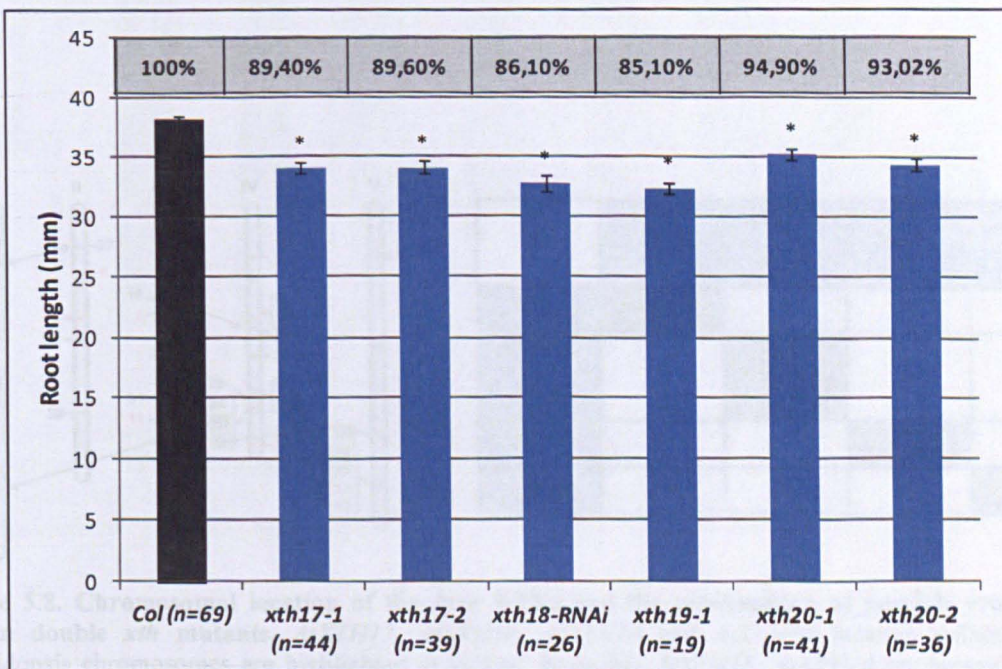


Figure 5.7 Growth of the primary root is reduced in the *xth* mutants. Measures of the primary root length of wild-type Col-0, *AtXTH17-1*, *AtXTH17-2*, *AtXTH18-RNAi*, *AtXTH19-1*, *AtXTH20-1* and *AtXTH20-2*. Error bars represent standard error. Asterisks indicate statistical significance between Col-0 and the mutants (Student's t test $P < 0,05$). On top of each column bar the value indicates percent root growth to Col-0 control.

5.3.4 Double *xth* mutants present an additive effect

Considering the close genetic relationship between these four members there exists the possibility that the lack of activity of one of the mutants would be compensated in part by one of the other three *AtXTHs*. Also, it is possible that they act cooperatively and so there may be an additive effect on the phenotype. To investigate this possibility further, their double mutants were created. As shown in Figure 5.8 *AtXTH18*, *AtXTH19* are located fairly close to each other on chromosome IV so it was not possible to create double mutants for this combination.

For the rest of the possible combinations crosses were done between the single mutants and the successful double homozygous mutants were isolated and confirmed in the F2 generation to analyse the primary root length (Figure 5.9).

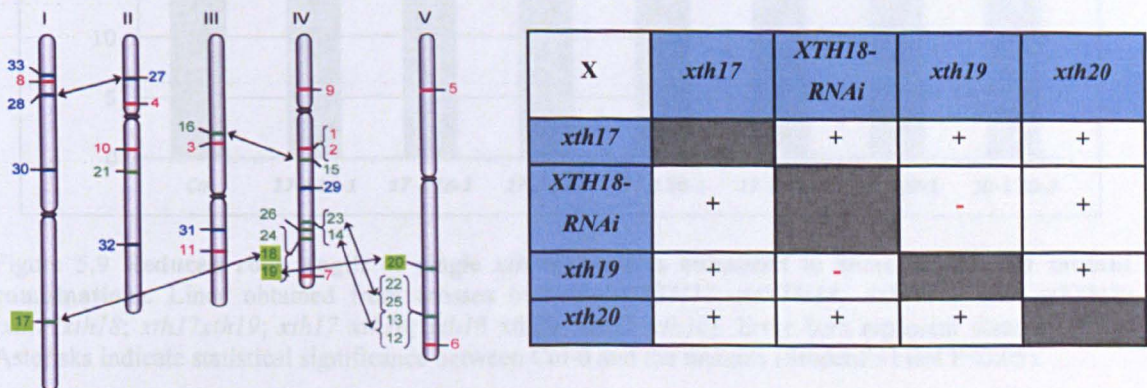


Figure 5.8. Chromosomal location of the four XTHs and the combination of possible crosses to obtain double *xth* mutants. *AtXTH17*, *AtXTH18*, *AtXTH19* and *AtXTH20* location within the 5 Arabidopsis chromosomes are highlighted in yellow. Note that *AtXTH18*, *AtXTH19* are located in the lower arm of chromosome 4 and therefore crosses between these two are not viable. On the right there is a table summarising the combination of crosses carried out to obtain double *xth* mutants.

A total of 8 different double mutant combinations were created from the crosses of the different alleles available (table 5.3)

<i>xth17 xth18</i>	<i>xth17-1 xth18RNAi</i> <i>xth17-2 xth18RNAi</i>
<i>xth17 xth19</i>	<i>xth17-1 xth19-1</i> <i>xth17-2 xth19-1</i>
<i>xth17 xth20</i>	<i>xth17-1 xth20-1</i> <i>xth17-2 xth20-2</i>
<i>xth18 xth20</i>	<i>xth18RNAi xth20-1</i>
<i>xth19 xth20</i>	<i>xth19-1 xth20-2</i>

Table 5.3 **XTH** double mutants available for genetic studies. For each of the possible double *xth* mutants are shown the different alleles combinations obtained for genetic studies.

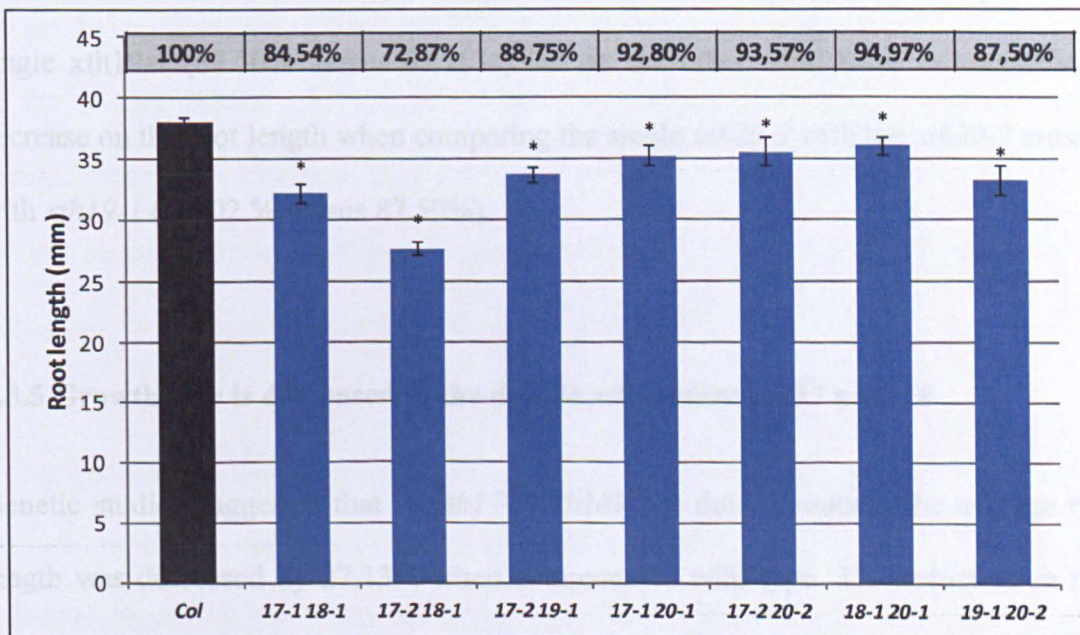


Figure 5.9 **Reduced root length of single *xth* mutants is enhanced in some double *xth* mutant combinations.** Lines obtained from crosses between *AtXTH17*, *AtXTH18*, *AtXTH19* and *AtXTH20* (*xth17xth18*; *xth17xth19*; *xth17 xth20*; *xth18 xth20*; *xth19 xth20*). Error bars represent standard error. Asterisks indicate statistical significance between Col-0 and the mutants (Student's t test $P < 0,05$).

As shown in the graph above (Figure 5.9), there is some additive effect between some of the double *xth* mutants. The double mutant combination with a stronger effect on the observed single phenotype is in the case of *xth17* crossed with *xth18*. There is a

different response between the two different alleles used. In the case of the *xth17-1*, when crossed with *xth18RNAi* the percentage of root growth respect to the control is 84.54%. But in the case of *xth17-2*, the reduction on the root length is much accentuated with a total growth of 72.87 % compared to the control. For *xth17 xth19* double mutant, with an 88.75% of growth, the total length of the root is smaller by just 1% when compared with single *xth17-2* mutant and it is actually 3% larger when compared with the single *xth19-1* mutant. For the two different lines for *xth17 xth20*, the overall percentage of root growth is similar with a 92.80% and 93.57% respectively. These two values are similar to the values observed for the single *xth20* alleles. In the last combination of double *xth*s, *xth19-1 x xth20-2*, there is an small increase respect to the single *xth19-1* (87.50% versus 85.10%) but on the other hand there is a significant decrease on the root length when comparing the single *xth20-2* with the *xth20-2* crossed with *xth19-1* (93.02 % versus 87.50%).

5.3.5 Growth rate is decreased in the double *xth* mutant *xth17 x xth18*

Genetic studies suggested that in *xth17-2 xth18RNAi* double mutant, the average root length was decreased by 27.13% when compared to wild type. The reduction in root length is clearly additive as both single mutants only show about 12% reduction in root length (Figure 5.10).

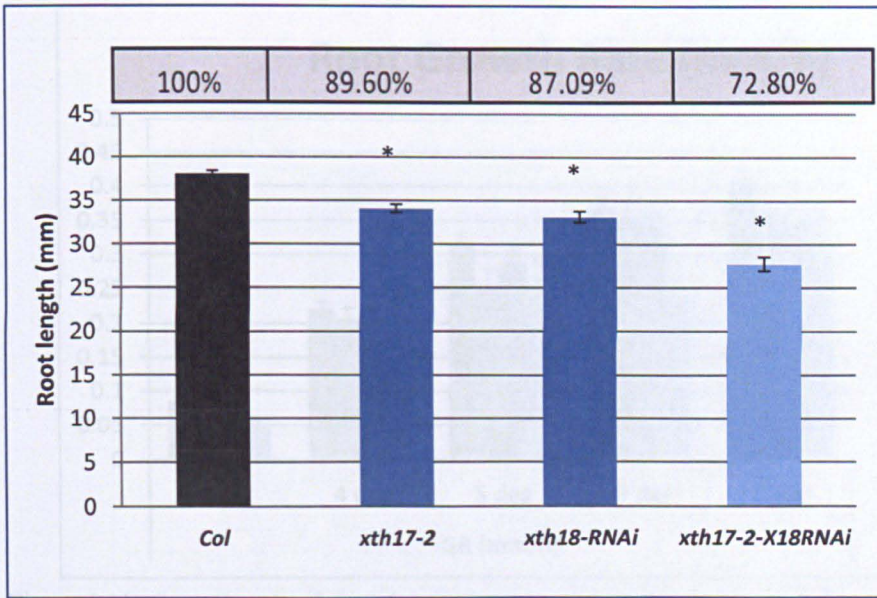


Figure 5.10 *xth17 xth18* showed a stronger root length reduction respect the single mutants. Error bars represent standard error. Asterisks indicate statistical significance between Col and the mutants (Student's t test $P < 0,05$).

To get a greater insight as how *AtXTHs* affect the primary root length, the growth rates of the double mutant *xth17-2 xth18-1* and the parental lines were measured over a period of time. As shown in figure 5.11 the growth rate (GR; mm/h) trend for all the lines in general is a rapid increase in growth rate from 3 days after germination (dag) to 4 dag and then the growth rate increases from 4 dag to 6 dag.

The growth rate is significantly reduced for the single and double mutants compared to the wild type at 3 (dag). The same trend follows at 4 dag, except for *xth17-2*. At 5 dag however, the *xth17-2* and the double mutant are the ones which have a significant lower GR. At 6 dag, only *xth17-2 x xth18-1* appears to have a lower significant GR when compared to the wild type. At 6 dag the growth rate stabilises and there is not a big increase in growth rate at 7 dag compared to 6 dag. For the double *xth* mutant, the trend is similar except that at 6 dag there is not an increase but rather a small decrease in the growth rate compared to 5 dag, and the growth rate is considerably smaller compared to the single mutants. Lastly, at 7 dag the double mutant together with the single *xth18-RNAi* mutant have a significant reduced growth rate compared to the single mutant.

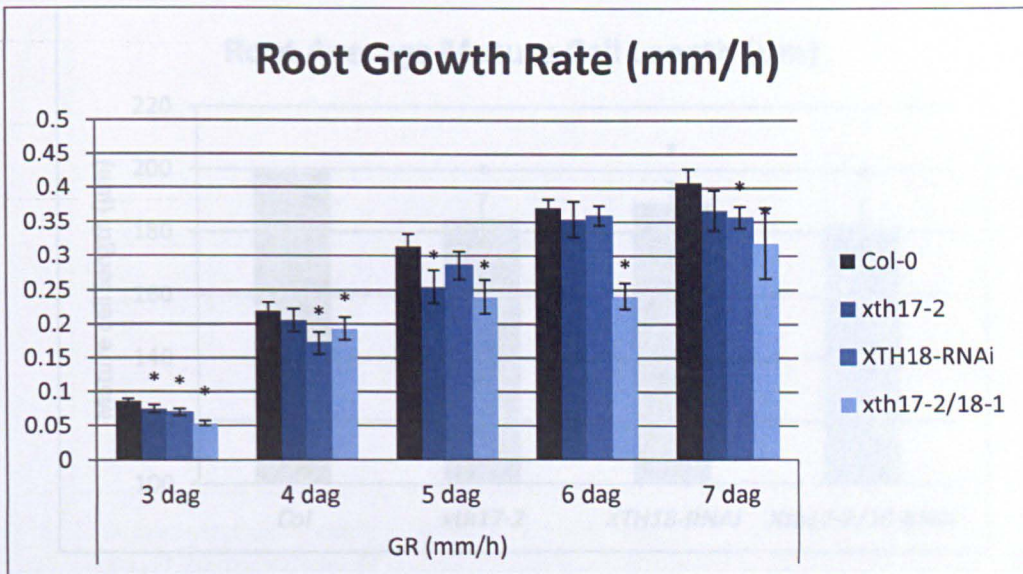


Figure 5.11. Growth rate of the of the *xth* mutants is reduced compared to the Col over a period of days. Time course analysis of the GR (mm/h) of the primary root of wild-type Col-0 *xth17-2*, *xth18-RNAi* and *xth17-2 xth18-RNAi*. Error bars represent standard error. Asterisks indicate statistical significance between Col-0 and the mutants (Student's t test $P < 0,05$).

5.3.6 Mature cell length is significantly decreased in the double mutant *xth17* x *xth18*

To further investigate the role of XTHs in regulatory root growth the root phenotype of both *xth17* and *xth18* single and double mutants was analysed at the cellular level.

In order to understand at what level the down-regulated or not-expressed *AtXTHs* are affecting the primary root length, the root phenotype of the single and double mutants were analysed at the cellular level.

Shown in figure 5.12, the mature cortical cell length of *xth17-2* and *XTH18-RNAi* and of *xth17-2 XTH18-RNAi* double mutant was reduced significantly compared to the wild type control, the double *xth* presenting the smaller average mature cell length.

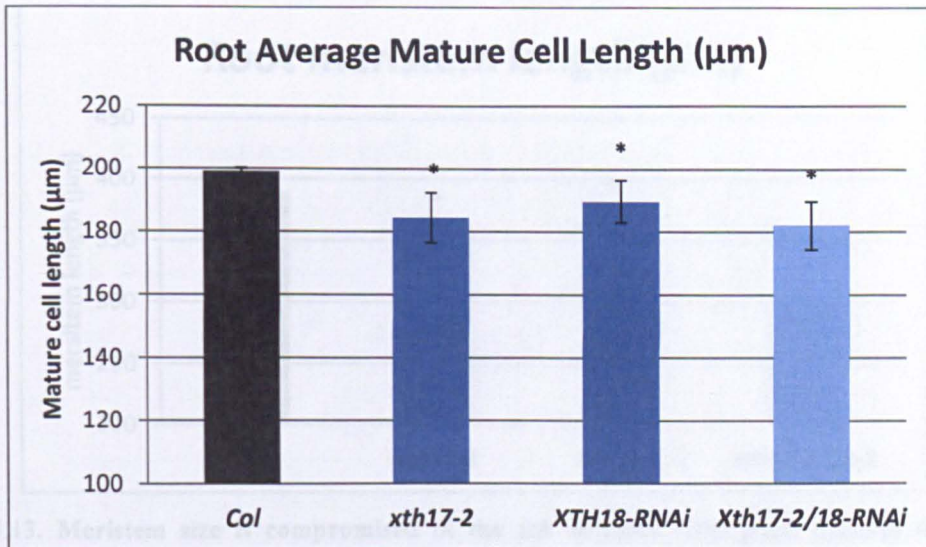


Figure 5.12. **The cell length of mature cortical cells is reduced in the *xth* mutants.** The average cell length for mature cortical cells of the primary root was measured for wild-type Col-0, *xth17-2*, *xth18-1* and *xth17-2 xth18-RNAi*. Error bars represent standard error. Asterisk indicates that the difference on mature cell length between Col-0 and the *AtXTHs* is statistically significant (Student's t test $P < 0.05$).

5.3.6 Meristem size is significantly decreased in the *xth17 xth18* double mutant

The difference on the mature cell length between the wild type and mutants indicates that a reduction on the overall primary root length is in part consequence of shorter mature cortical cell lengths of the *xth* mutants.

The primary root length in the double mutant *xth17-2 xth18-1* is reduced a 27.20% respect the wild type (Col-0) length and the difference on the mature cell length between the two is only of 10%. Therefore, it is likely that there are other factors contributing to the bigger difference on the primary root length rather than the mature cell length alone. Thus, the meristem length of the single and double mutants was next measured to see if a reduction in meristem length is also contributing to the reduction in the primary root length.

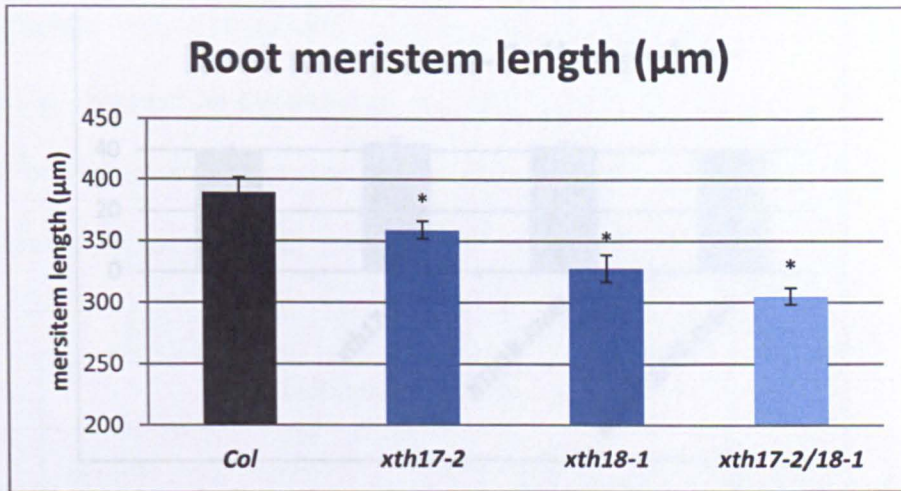


Figure 5.13. **Meristem size is compromised in the *xth* mutants.** This graph displays the average meristem length of wild-type Columbia, *xth17-2*, *xth18-1* and *xth17-2 xth18-1*. Error bars represent standard error Asterisks indicate statistical difference on meristem size between Col-0 and the *AtXTHs* (Student's t test $P < 0.05$).

The analysis showed that the meristem length was significantly reduced both in the single mutants (*xth17-2* and *xth18-1*) and *xth17-2 xth18-1* when compared to the wild type control (Figure 5.13). Therefore, the shorter meristem phenotype of the *AtXTH* mutants plays a role in their shorter primary roots.

5.3.7 Number of cells in the meristem is not affected in the double mutant *xth17 xth18*

Meristem analysis above suggests that the loss of *xth17-2* and/or *xth18-1* functions alters the meristem size. To test if the reduction in meristem size is due to fewer cells in *xth* mutants the number of cells in the meristem of the wild type and mutants were counted (Figure 5.14).

As shown in figure 5.14, no significant difference in the number of meristematic cells was found between the *Atxth* mutants and Col-0.

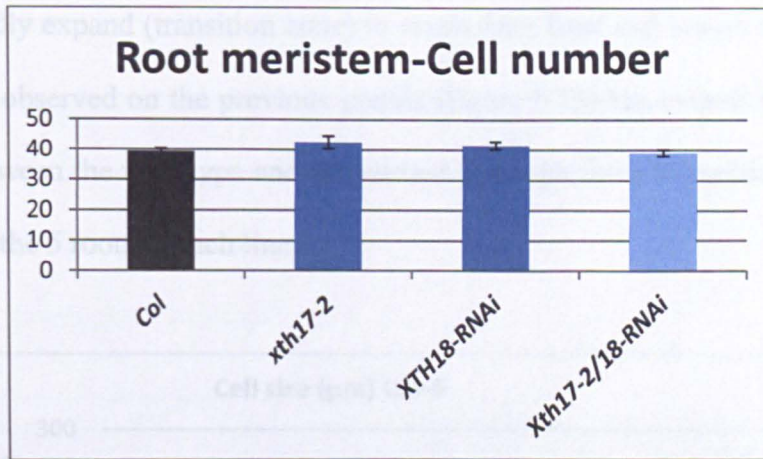


Figure 5.14. **The number of cells on the meristem does not differ between Colombia and *xth17xth18*.** Analysis of the average cell number for the meristems of wild-type Col-0 the single *xth* mutants *xth17-2* and *xth18-1* and *xth17-2 xth18-1*. Error bars represent standard error. Asterisks indicate statistical significance between Col-0 and the mutants (Student's t test $P < 0,05$).

5.3.8 The transition from meristem to elongation zone happens in a more abrupt fashion in the double mutant *xth17 xth18*

The previous analyses have shown that XTH affect the primary root length by modifying the mature cell length and the meristem size. The smaller meristem size of the *Atxth* mutants is not related to the number of cells produced as shown in figure 5.15. Therefore, it is conceivable that in *Atxth* mutants meristematic cells are smaller resulting in a smaller meristem size.

To corroborate this assumption, the morphology of the root tip was looked in greater detail. The cell number and cell size of all the cells from the root tip through the transition zone to the mature zone of the root were examined to spot any difference at any level between the wild type and the *Atxth* mutants (Figure 5.15).

As observed in figure 5.16 there is a similar cell growth trend between the control and the mutant. Initially, it is observed that the cell length for the first 37 to 55 cells from the root and the mature zone of the root was similar with lengths below 50 μm . Then at certain stage,

the cells rapidly expand (transition zone) to reach their final cell length (mature zone of the root). As observed on the previous graphs (figure 5.15) the overall final cell length is similar between the wild type and the mutant although there is variability on the cell size between the 5 roots in each line.

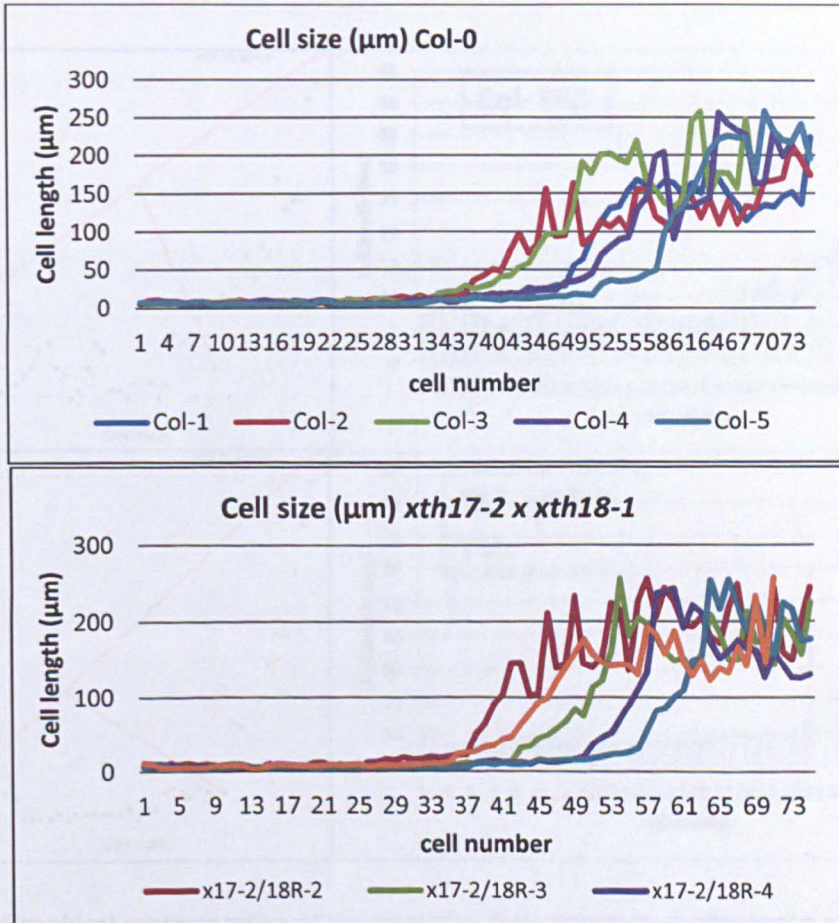


Figure 5.15. **Root tip development follows similar trends in Col-0 and *xth17 xth18*.** Cell size for cells from root tip to mature zone of the root were measured for Col-0 and *xth17 xth18*. Graphs for the wild type (top) and for *xth17 xth18* (bottom) show the cell number and its correspondent size from the cell from the root tip (cell number 1) to reach the mature zone of 5 individual roots for each line.

Graphic representation of the values observed for one representative root of each line (control vs double mutant) from the ones represented in the figure 5.15 is shown in Figure 5.16. In this analysis, attention is specially given to the transition zone area of the root and the mature zone of the root was excluded from this analysis. The plots on

the left are automatically obtained from the Cell-o-Tape software which is based on the sequential changes in cell sizes that determine the transition zone in each root. The cells included before the transition zone (meristematic cells) are separated from the cells above the transition zone (elongating cells) by a red line. The plots on the right in figure 5.17 are shown the images of the plotted roots from figure 5.16 and their correspondent plot. On red dots are marked the end of each single cell and a red line the transition zone for this root.

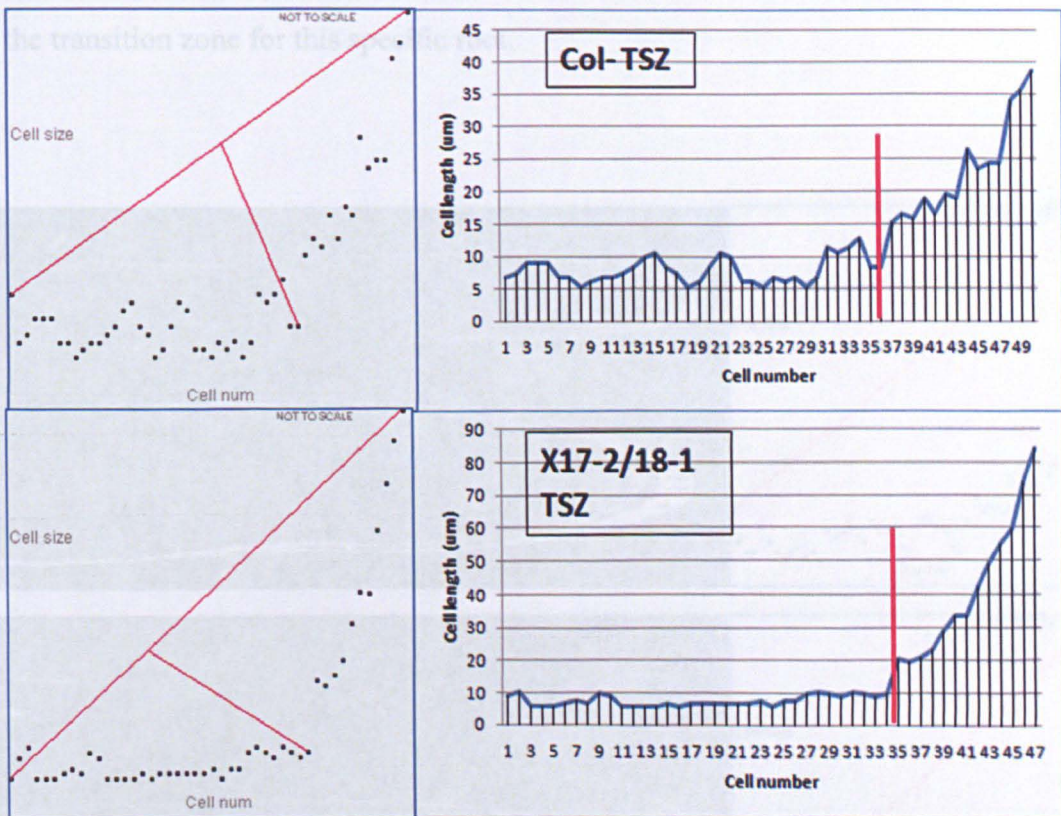


Figure 5.16 Graphical representation of the transition from meristem to elongation zone of the root on terms of cell number and cell size. Top panel graphs correspond to Colombia, bottom panel to *xth17 xth18*. The plots on the left were directly obtained from the Cell-o-Tape software and represent the cell number and cell size of the plotted root. The red line indicates the transition zone to separate cells included on the meristem from cells belonging to the elongation zone of the root. The images on the right correspond to the graphical representation of the values from the left plots to scale, indicating the number of cells before and after the transition zone (with the vertical red line) and their correspondent sizes. The image on top corresponds for one representative root of the wild type (Colombia-0). The image on the bottom corresponds to a representative root of the double *xth* mutant.

From this analysis it is clear that the cell expansion pattern differs between Col-0 and *xth17-2 xth18-1* roots with cells from Col-0 gradually expanding from the meristem to the elongation zone. In order to determine if there was a significant difference between the wild type and the mutant, the data from the cell expansion analysis was analysed to add a fitted line (Appendix 3).

the elongation zone, whereas in the double *xth* mutant, the expansion of the cells seems to take place past the transition zone and happens in a more abrupt manner.

concluding that the cells are growing quicker in the transition zone of the double mutant than in wild type (Figure 5.17).

In figure 5.17 are shown the images of the plotted roots from figure 5.16 with their correspondent plot. On red dots are marked the end of each single cell and with a green line the transition zone for this specific root.

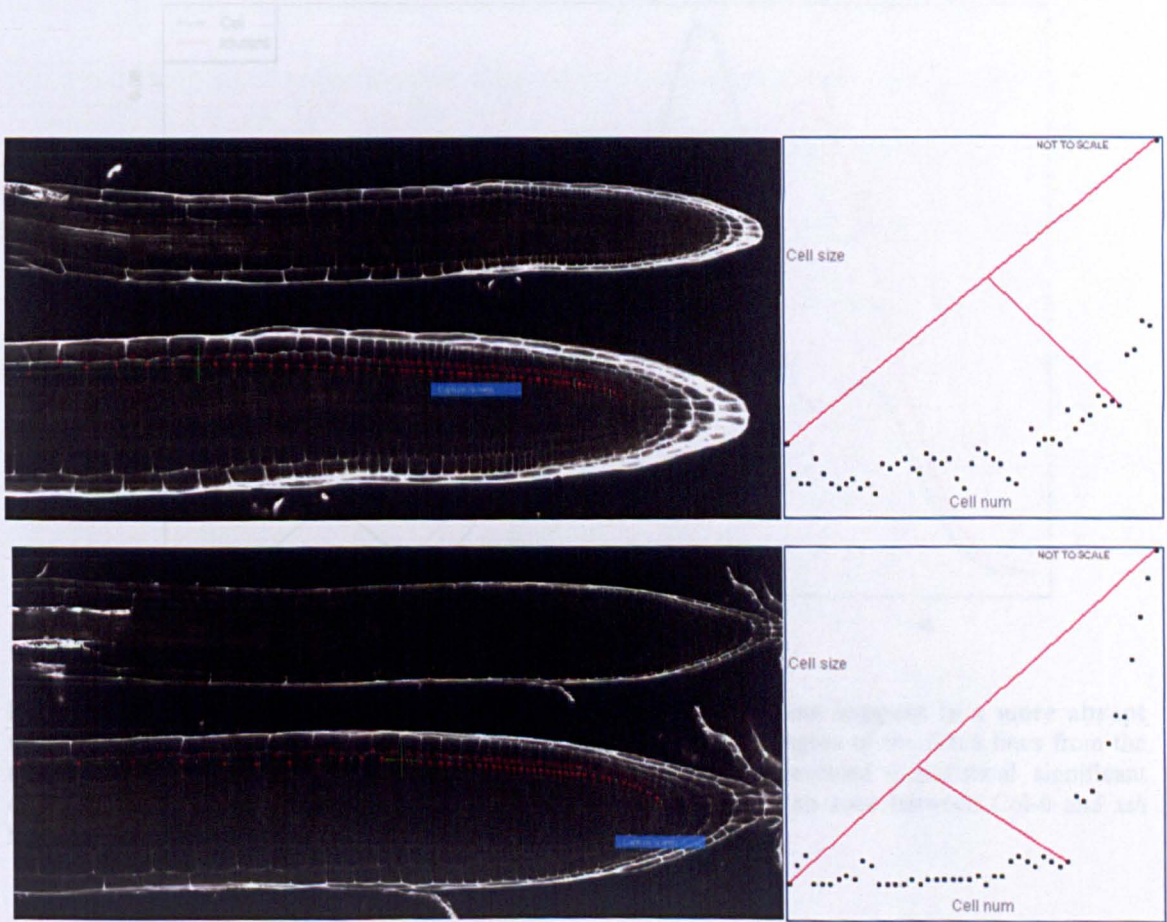


Figure 5.17 **Confocal image of the analysis of cell length and transition zone of the wild type and double mutant *xth17-2 xth8-1*.** On the left there are the confocal images of the analysed roots. On red dots are marked the end of each single cell and with a green line the transition zone for this specific root. On the right of the image are the plots for the cell lengths and transition zone obtained for these specific roots. The top root corresponds to Colombia and the bottom to *xth17-2 xth8-1*.

The presence of multiple genes encoding similar or related activities brings up the question whether individual members of a gene family have distinct functions. In order to determine if there was a statistical difference in the fashion of cell expansion between the wild type and the mutant, the data of cell expansion for each individual root was analysed to add a fitted line (Appendix V). A density plot of the angles between

Col-0 and *xth* mutants was created revealing that there is a statistically significant difference on the fashion of cell expansion between the wild type and the mutant, concluding that the cells are growing quicker in the transition of zone of the root in the mutant than in wild type (Figure 5.18).

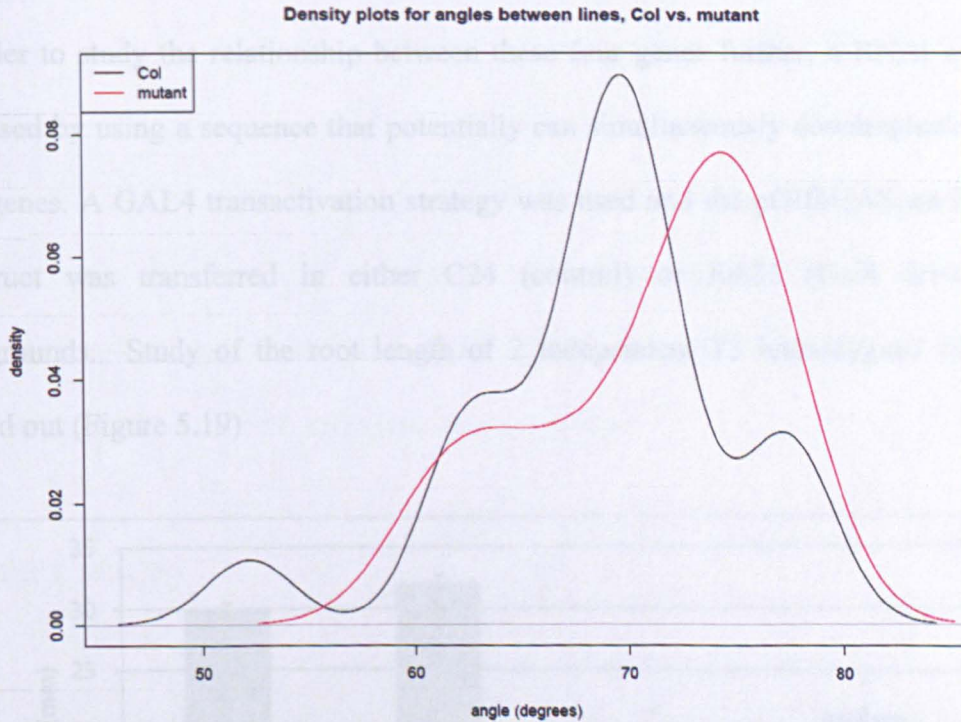


Figure 5.18. **The transition from the meristem to the elongation zone happens in a more abrupt fashion in the *xth* mutants than in Col-0.** Analysis of the different angles of the fitted lines from the analysis of the cell growth dynamics obtained from Cell-o-Tape revealed a statistical significant difference between the speed at which cells grow through the transition zone between Col-0 and *xth* mutants (Courtesy of Dr. Kim Kenobi).

5.3.9 Simultaneous downregulation of *AtXTH17*, *AtXTH18*, *AtXTH19* and *AtXTH20* leads to root with shorter lengths in a similar fashion as the double mutants

The presence of multiple genes encoding similar enzymatic activities brings up the question whether individual members, mainly those in each subfamily, are redundant in terms of its physiological role. In many gene families, mutation in an individual

member does not result in a mutant phenotype because of redundancy. In the case of single mutants *xth17*, *xth18*, *xth19* and *xth20* they all have a shorter root phenotype when compared to the wild type, thus indicating that each of the four genes play an important role in root growth. Moreover, combination of double *xth* mutants has a stronger root phenotype, indicating a potential cooperative role between these genes.

In order to study the relationship between these four genes further, a RNAi approach was used by using a sequence that potentially can simultaneously downregulate all the four genes. A GAL4 transactivation strategy was used and the pGIIbUAS:amiRNAXth construct was transferred in either C24 (control) or J0631 (Gal4 driver line) backgrounds. Study of the root length of 2 independent T3 homozygous lines was carried out (Figure 5.19)

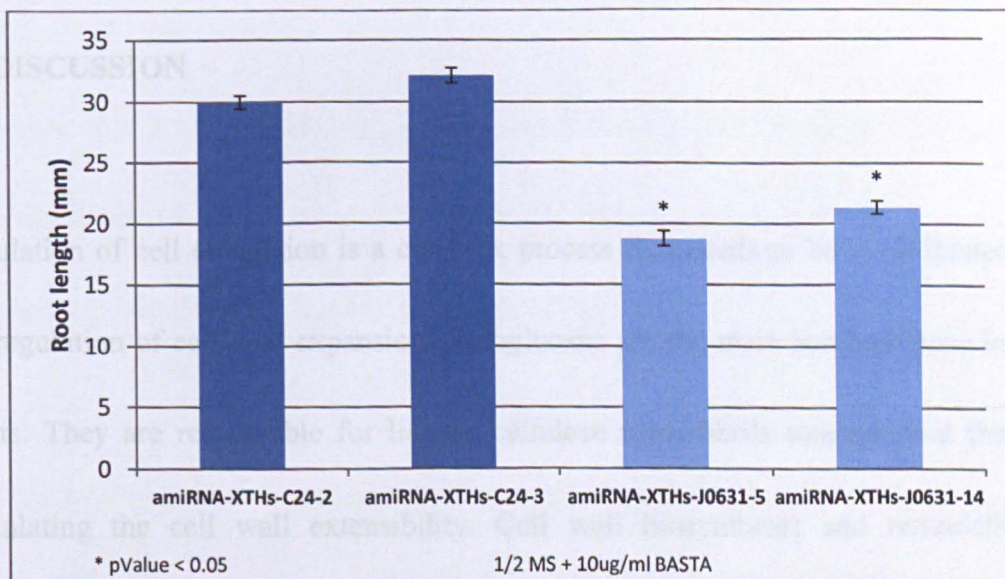


Figure 5.19. **The simultaneous downregulation of *XTH17*, *XTH18*, *XTH19* and *XTH20* appears to cause a strong reduction in the primary root length.** Measures of the primary root length of T3 homozygous lines for two independent transformed control lines (amiRNA-XTHs-C24-2 and amiRNA-XTHs-C24-3) and for two independent transformed J0631 lines (amiRNA-XTHs-J0631-5 and amiRNA-XTHs-J0631-14). Root length measured at 7 days after germination in media containing BASTA. Error bars represent standard error. Asterisk indicates statistical significance between amiRNA-XTHs-C24 and the amiRNA-XTHs-J0631 Student's t test $P < 0,05$).

The results suggest that there is a significant difference between the control lines (where the expression of the amiRNA sequence cannot be induced by lack of GAL4) and the transformed driver lines.

These results suggest that although all four *XTH* genes seem to play a role in the GA regulated cell wall expansion, they are may not essential for the modification of cell wall properties leading to cell expansion in the root. However, we cannot be certain about this until the expression of *xth17*, *xth18*, *xth19* and *xth20* for the different amiRNA lines have been assessed.

It is possible that by inducing the downregulation of *xth17*, *xth18*, *xth19* and *xth20* in specific tissues such as in the endodermis by transforming different driver lines, we could see some changes on the phenotypic response leading to clues as how they may act an interact between them in a tissue specific manner.

5.4 DISCUSSION

Regulation of cell elongation is a complex process that needs to be co-ordinated with the regulation of cell wall expansion. Xyloglucans are the main hemicellulose in dicot plants. They are responsible for linking cellulose microfibrils together and therefore modulating the cell wall extensibility. Cell wall biosynthesis and remodelling is regulated in a spatiotemporal and developmental manner by different hormones (reviewed by Sánchez-Rodríguez *et al.*, 2010). Hormones loosen up the cell wall architecture, preferentially through changes in the expression of EXP, PME and XTH genes (Cosgrove, 2005). XTHs act as cell wall loosening agents by catalysing cleavage

of xyloglucan chains, and subsequent re-ligation to different xyloglucan acceptor chains (Fry *et al.*, 1992). Expression analyses have shown that XTH gene expression correlates with growth, such as in the elongation zone of the *Arabidopsis* roots or root hair initiation zone (Vissenberg *et al.*, 2000, 2003). Also, XTHs have been found to play an important role in the root hair formation (Vissenberg *et al.*, 2001)

As described in previous chapters, GA regulates root cell expansion in the endodermis to promote root growth (Ubeda-Tomás *et al.*, 2008). GA has been directly associated with the regulation of *AtXTH21* which is thought to play an important role in root growth by altering cellulose deposition and extensibility of the cell wall (Liu *et al.*, 2007).

Therefore, in this chapter the interaction between GA and XTHs was analysed with the aim to establish a relationship between both components as part of the regulatory network regulating root endodermal cell expansion.

The primary aim of this chapter was to identify candidate XTHs which could be regulated by GA to promote root cell expansion through the analysis of available transcriptomics data sets. From this first analysis it was observed that a total of nine XTH family members (representing the quarter of the XTH family) are regulated by GA and significantly expressed in the elongation zone and endodermis. The high percentage

of identified XTH genes could be an indication of the strong involvement of GA in the regulation of cell expansion through the manipulation of CWREs expression. Also, bearing in mind that in the elongation zone of the root the cells go through rapid cell expansion to allow organ growth, it is not surprising to find so many XTH genes significantly expressed in this zone in order to cope with the fast pace turnover of new cell wall material and cell wall re-organization taking place.

All the 9 selected XTHs represent potential components of the GA regulatory network targeting endodermal cell expansion. To see how they act in regulating the primary root growth a genetic approach was used to study root phenotype in various *xth* mutant backgrounds. Bioinformatic studies suggest that *AtXTH19*, is a good candidate as it is strongly responsive to GA and shows high expression in the elongation zone. More importantly it shows very high expression in the endodermis.

Phylogenetic analysis, suggest that *AtXTH19* is closely related to *AtXTH17*, *AtXTH18* *AtXTH20*. *AtXTH17* and *AtXTH18* are also responsive to GA and are expressed in the elongation zone and endodermis and were part of the o shortlisted genes. Also, these four genes have been reported to be specifically expressed in roots (Yokoyama and Nishitani 2002, Vissenberg *et al.*, 2005). Therefore all these four genes were selected for further investigations.

From the 6 other identified *AtXTH* family members; *AtXTH8* had the strongest expression in the acceleration elongation zone. However, its regulation by GA is subtle (<2 fold) and may not play a key role in the GA regulated cell expansion in the endodermal cells of the elongation zone.

AtXTH30 stands out of the list for being highly expressed in the whole elongation zone (section 2 and 3) as well as the mature zone of the root (sections 4 and 5) and is also upregulated by GA for the 3 given time points. However, the fact that this XTH is expressed all along the root makes it more unlikely to be involved specifically in the GA promoted cell expansion in the endodermis. It is likely that *AtXTH30* may play a role in cell wall integrity processes. *AtXTH13* and *AtXTH14* appear to be highly expressed only in the deceleration elongation zone. Further investigation will clarify whether any of these genes have a role in GA regulated cell expansion.

Additionally two XTH members (*AtXTH4* and *AtXTH16*) were identified that are significantly expressed in the elongation zone and endodermis but are downregulated by GA. It would be interesting to create overexpression lines for these two genes to try to establish their role if any in the root cell expansion in relation to GA.

Surprisingly, *AtXTH21* which expression had been shown to be specifically enhanced by GA and is strongly expressed in flowers and roots tissues (Liu *et al.*, 2007), was not identified in our data. This disagreement may be due to the GA transcriptomics data used in the present analysis was obtained from mRNA isolated specially from roots and the expression analysis by Liu *et al.*, (2007) was from mRNA isolated from whole seedlings.

The tissue specific expression analysis correlates with the expression patterns observed from the transcriptomics five sectional data (figure 5.5). The overlap amongst the analysed XTHs may be an indication of their combinatorial actions to determine cell wall properties/expansion in specific tissues developmental sites of the root.

Analysis of primary root length of single T-DNA insertion lines and RNAi line for *AtXTH17*, *AtXTH18*, *AtXTH19* and *AtXTH20* resulted in roots with shorter length when compared to the wild type. Both T-DNA insertion lines for *xth20* showed a decrease on the root length which was quite unpredicted since they are not significantly expressed in the elongation zone of the root.

These results suggest that the four genes are necessary for a normal root growth and that they are not redundant in terms of their physiological roles. However, there exists the

possibility that they act cooperatively towards loosening of the cell wall and therefore the cell and root growth. Therefore, study of the multiple combinations between these four XTH mutants was needed to investigate this further. First, different combinations of double mutants were analysed before analysis of the quadruple knock out amiRNA lines. The analysis of double mutant resulted in some of the combinations of mutants showing an additive effect (eg. *xth17 x xth18*) and other combinations not showing any difference with the single mutant phenotype (eg. *xth17 x xth20*). Thus suggesting, that *AtXTH17*, *AtXTH18*, *AtXTH19* and *AtXTH20* may interact one with each other in a different fashion.

Further analysis of the double mutant *xth17 x xth18* revealed that there was a significant difference in the cell size of mature cells, which could explain the overall shorter root phenotype of the mutant. However, the reduction observed on the average mature cells was smaller than 10 % and the overall primary root length of the double mutant was 27% shorter than the wild type. Therefore, it is unlikely that the final cell length of the cell is the sole responsible of the root phenotype observed and that XTH may be affecting the development of the root at different level. Hence, it was then measured the meristem size of both the control and mutant lines to observed that *xth* mutants also have significant smaller meristems. Work by Ubeda-Tomas *et al.*, showed that GA regulates root growth by promoting cell proliferation. In absence of GA signalling

response (by targeting expression of *gai*) in the root meristem, the cell proliferation was disrupted and the root growth reduced. So, one possibility could be that based on the phenotype observed, that XTHs indirectly controls the rates of division regulated by GA through the promotion of the cell expansion that is needed to double the cell size in order for the cells to divide.

Meristem cell number and sizes were analysed in an attempt to establish the role of *AtXTHs* within the GA regulated root cell expansion. Contrary to what was expected, the number of meristematic cells in the control and the *xth* mutants was similar implicating that shorter meristems were caused by shorter meristematic cells. When this phenotype was looked in more detail it was observed that there was a different trend on cell size distribution through the meristem to the elongation zone between wild type and mutant. In the case of the mutant (*xth17-2 x xth18-1*) meristematic cell size remains fairly constant through the meristem and then after the transition zone cells start rapidly to expand. On the other hand, wild type meristematic cells have variable cells sizes that once they get through the transition zone start to gradually expand on the elongation zone.

These results on the analysis on cell expansion dynamics suggest that the transition from meristem to elongation zone of the root happens in a more abrupt fashion on the

XTHs mutants. One possible explanation for this behaviour in the XTH mutants, may be that given the associated properties as cell wall loosening agents, lack of the key XTHs regulated by GA to promote root cell expansion results in cells with more rigid cell walls on the meristem and elongation zone that prevent them from regular hormonal regulated expansion until they reach a point (towards the elongation zone of the root) where mechanical forces take over and prompt this quick expansion that is more difficult to associate to hormonal regulated cell expansion. It would be interesting to actually look at the extensibility of the mutants as well as the diameter of the roots to see if they present any difference in the properties and thickness of the cell wall that can be directly associated to the XTH function.

Most importantly, it still needs to be established whether the functionally characterised XTH mutants are actually directly regulated by GA and play a key role in the GA regulated root cell expansion. For, this it should be looked at how XTH expression is affected when endodermal cell elongation is disrupted by expression of *gai*. For this, XTH::GUS reporter lines could be crossed with *SCR::gai-GR-YFP*. Also, the expression of these genes should be compared with the *SCR::gai-GR-YFP* transcriptomics data produced during this PhD project to gain further understanding of their behaviour in relation to the GA signalling network.

6: SUMMARY AND CONCLUSION

6.1 SUMMARY

The *Arabidopsis* root has been extensively studied, generating a great deal of information about individual cell types, cell patterning, growth and differentiation, lateral root formation and responses to the environment (Benfey *et al.*, 2010). Root cell elongation is regulated by a complex network of hormone signals and their signalling pathways (Ubeda-Tomás *et al.*, 2012). GA has been shown to primarily target the root endodermis to promote root growth by regulating cell elongation (Ubeda-Tomás *et al.*, 2008). However, the downstream genes and mechanisms target by GA are still unclear. In this thesis, reverse and forward genetics approaches have been employed in order to identify novel components of the gene regulatory network target by GA in this tissue.

1) Identification of putative mutants harbouring novel downstream components of the GA signalling pathway by forward genetics:

- Screening of a fast neutron mutagenized population of *SCR:gai-GR* lines to screen for mutants that suppress *gai* inducible root growth defect has been carried out
- Genetic and expression analysis resulted in the identification of 9 non-allelic mutations presenting a weak or partial root growth recovery
- Kinematics analysis of the growth of each mutant and characterisation of the putative mutants at the cellular level have revealed that 8 of the recovered mutants are affected at the level of cell expansion and 1 appears to be involved in cell division

- From the cloning of each of the mutants by next-generation sequencing it is expected to result in the identification of 9 novel mutants involved the GA regulation of root cell expansion to try to help to build up the GA regulatory network

2) Identification of putative GA downstream signalling components by reverse genetics:

- An endodermal-specific transgenic line (*SCR:gai-GR*) that targets a non-degradable form of the GA signalling DELLA protein (*gai*) has been employed to perform a comprehensive transcriptomic time course dataset in order to pinpoint genes controlled by DELLA in this root cell type
- Bioinformatics analysis on the subsequent dataset, has resulted in the identification of a number of known GA signalling genes (including GA biosynthetic genes, XERICO and SCL3) as well as 60 putative downstream signalling components
- A list of 14 putative GA downstream targets including transcription factors, unknown genes and CWREs, have been selected for further functional characterisation to establish their potential role within the GA regulatory network targeting endodermal root cell expansion.
- Genetic studies employing knock outs has resulted in the identification of mutants with altered root lengths. Promoter studies have identified potential DELLA binding sites in these mutants and further reporter fusions studies will help to establish their spatial expression

- Comparison of the expression patterns of the candidate genes obtained on the present analysis with other GA-root available transcriptomics datasets, will be key to understand their role and behaviour as putative GA downstream targets and to establish their position within the GA regulatory network

3) Identification of GA regulated cell wall remodelling enzymes:

- Bioinformatics analyses has produced a list of 9 candidate XTHs cell wall remodelling enzymes, that appears to be regulated by GA and be significantly expressed in the endodermis of the elongation zone of the root.
- Functionally characterization of several members of the XTH family through the analysis of knock outs, have revealed elongation defects in multiple mutant combinations.
- Both a reduction in mature cell size and meristem length are responsible for the reduction in root length on the double mutant *xth17 xth18*
- Kinematic analysis of the root growth together with analysis at the cellular level suggest the transition from meristem to elongation zone of the root happens in a more abrupt fashion on the XTHs mutants
- Expression analysis of XTHs in GA mutant backgrounds will help to establish the basis of how GAs regulate XTHs to promote root cell expansion

6. 2 CONCLUSIONS

This research project has focused on the study of GA regulated endodermal cell expansion as a way to improve overall understanding of the molecular mechanisms regulating root development. Although a few DELLA targets have been identified, many of the downstream targets of the GA signalling pathway still remain unclear. The forward and genetic approaches followed to try to identify GA downstream targets have resulted in a large amount of data and a list of potential GA downstream targets that will contribute to shed light on this process. The transcriptomics data set produced can provide valuable information for the wider scientific community to build root gene regulatory networks controlling root development. In addition the candidate genes identified from the reverse genetic screen can unveil novel components specifically involved in the GA regulation of endodermal cell expansion and their functional characterisation will also help to understand how this highly regulated process takes place. The analysis of the fast neutron mutagenized *SCR::gai-GR* population has resulted in the identification of some exciting candidates that, once cloned, will be of major interest to try to build up a model of how the GA regulation of DELLA proteins leads to the stimulation of endodermal cell expansion. Also, the study of GA-regulated cell wall remodelling enzymes suggests a mechanism in which GA induced cell expansion take place at the level of cell wall expansion to contribute to the overall root growth. Although further studies are needed to establish the function and relationship between the DELLA proteins and all the identified genes, this project has been successful in producing a solid base from to which build up towards a complete understanding of the GA regulated endodermal cell expansion.

REFERENCES

- Abeles FB, Morgan PW, Saltveit Jr E** (1992) Ethylene in plant biology 2nd ed. (New York: Academic Press, San Diego, California, USA).
- Achard P, Cheng H, De Grauwe L, Decat J, Schoutteten H, Moritz T, Van Der Straeten D, Peng J and Harberd NP** (2006) Integration of plant responses to environmentally activated phytohormonal signals. *Science* **311**: 91–94.
- Achard P, Renou JP, Berthome R, Harberd NP and Genschik P** (2008) Plant DELLAs restrain growth and promote survival of adversity by reducing the levels of reactive oxygen species. *Current Biology* **18**: 656–660.
- Alabadí D, Blázquez MA** (2009) Molecular interactions between light and hormone signaling to control plant growth. *Plant Molecular Biology* **69**: 409–417.
- Alonso JM, Stepanova AN, Leisse TJ, Kim CJ, Chen H, Shinn P, Stevenson DK, Zimmerman J, Barajas P, Cheuk R, Gadriab C, Heller C, Jeske A, Koesema E, Meyers CC, Parker H, Prednis L, Ansari Y, Choy N, Deen H, Geralt M, Hazari N, Hom E, Karnes M, Mulholland C, Ndubaku R, Schmidt I, Guzman P, Aguilar-Henonin L, Schmid M, Weigel D, Carter DE, Marchand T, Risseeuw E, Brogden D, Zeko A, Crosby WL, Berry CC and Ecker JR** (2003) Genome-wide insertional mutagenesis of *Arabidopsis thaliana*. *Science* **301**: 653–657.
- Alonso JM, Ecker JR** (2006) Moving forward in reverse: genetic technologies to enable genome-wide phenomic screens in *Arabidopsis*. *Nature Reviews Genetics* **7**: 524–536.
- Alonso R, Oñate-Sánchez L, Weltmeier F, Ehlert A, Diaz I, Dietrich K, Vicente-Carbajosa J, Droge-Laser W** (2009) A pivotal role of the basic leucine zipper transcription factor bZIP53 in the regulation of *Arabidopsis* seed maturation gene expression based on heterodimerization and protein complex formation. *The Plant Cell* **21**: 1747–1761.
- Alvord WG, Roayaei JA, Quiñones OA and Schneider KT** (2007) Amicroarray analysis for differential gene expression in the soybean genome using Bioconductor and R. *Briefings in Bioinformatics* **6**: 415–431.
- Arabidopsis Genome Initiative** (2000). Analysis of the genome sequence of the flowering plant *Arabidopsis thaliana*. *Nature* **408**: 796–815.
- Ariizumi T, Murase K, Sun TP, Steber CM** (2008) Proteolysis-Independent downregulation of DELLA repression in *Arabidopsis* by the gibberellin receptor GIBBERELLIN INSENSITIVE DWARF1. *The Plant Cell* **20**: 2447–2459.
- Arnaud N, Girin T, Sorefan K, Fuentes S, Wood TA, Lawrenson T, Sablowski R and Ostergaard L** (2010). Gibberellins control fruit patterning in *Arabidopsis thaliana*. *Genes and Development* **24**: 2127–2132.

- Arteca RN and Bachman JM** (1987) Light inhibition of brassinosteroid-induced ethylene production. *Journal of Plant Physiology* **129**: 13–18.
- Barry CS and Giovannoni JJ** (2007) Ethylene and Fruit Ripening *Journal of Plant Growth Regulation* **26**: 143-159.
- Baskin TI** (2005) Anisotropic expansion of the plant cell wall. *Annual Review of Cell and Developmental Biology* **21**: 203-222.
- Becnel J, Natarajan M, Kipp A and Braam J** (2006) Developmental expression patterns of *Arabidopsis* XTH genes reported by transgenes and Genevestigator. *Plant Molecular Biology* **61**: 451–467.
- Beemster GTS and Baskin TI** (1998) Analysis of Cell Division and Elongation Underlying the Developmental Acceleration of Root Growth in *Arabidopsis thaliana* *Plant Physiology* **116**: 1515-1526.
- Belfield EJ, Gan X, Mithani A, Brown C, Jiang C, Franklin K, Alvey E, Wibowo A, Jung M, Bailey K, Kalwani S, Ragoussis J, Mott R and Harberd NP** (2012) Genome-wide analysis of mutations in mutant lineages selected following fast-neutron irradiation mutagenesis of *Arabidopsis thaliana* *Genome Research* **22**: 1306-1315.
- Benfey PN, Scheres B** (2000) Root development. *Current Biology* **16**: 813-815.
- Benfey PN, Bennett MJ and Schiefelbein J** (2010) Getting to the root of plant biology: impact of the *Arabidopsis* genome sequence on root research *The Plant Journal* **61**: 992-1000.
- Birnbaum K, Shasha DE, Wang JY, Jung JW, Lambert GM, Galbraith DW, Benfey PN** (2003) A gene expression map of the *Arabidopsis* root. *Science* **302**: 1956–1960.
- Blanc G, Barakat A, Guyot R, Cooke R and Delseny M** (2000) Extensive Duplication and Reshuffling in the *Arabidopsis* Genome *Plant Cell* **12**: 1093–1101.
- Blilou I, Xu J, Wildwater M, Willemsen V, Paponov I, Friml J, Heidstra R, Aida M, Palme K, and Scheres B** (2005) The PIN auxin efflux facilitator network controls growth and patterning in *Arabidopsis* roots. *Nature* **433**: 39–44.
- Bolstad BM, Irizarry RA, Gautier L and Wu Z** (2005) Preprocessing high-density oligonucleotide arrays. In: GentlemanR, CareyVJ, HuberW, IrizarryRA, DudoitS, editors. *Bioinformatics and Computational Biology Solutions Using R and Bioconductor*. New York: Springer
- Boyes DC, Zayed AM, Ascenzi R, McCaskill AJ, Hoffman NE, Davis KR and Görlach J** (2001) Growth Stage–Based Phenotypic Analysis of *Arabidopsis*: A Model for High Throughput Functional Genomics in Plants. *The Plant Cell* **13**: 1499–1510.
- Brady SM, Orlando DA, Lee JY, Wang JY, Koch J, Dinneny JR, Mace D, Ohler U, Benfey PN** (2007) A High-Resolution Root Spatiotemporal Map Reveals Dominant Expression Patterns *Sciences* **318**: 801-806.

- Brazma and Vilo** (2000) Gene expression data analysis. *Functional Genomics* **480**:17-21.
- Bruggemann E, Handwerger K, Essex C, Storz G** (1996) Analysis of fast neutron-generated mutants at the *Arabidopsis thaliana* HY4 locus. *The Plant Journal* **10**: 755–760.
- Buchanan BB, Gruissem W and Jones RL** (2000). *Biochemistry and Molecular Biology of Plants*. Rockville MD: American Society of Plant Physiologists.
- Cao D, Cheng H, Wu W, Soo HM, Peng J** (2006) Gibberellin mobilizes distinct DELLA-dependent transcriptomes to regulate seed germination and floral development in *Arabidopsis*. *Plant Physiology* **142**: 509-525.
- Carrera E, Holman T, Medhurst A, Dietrich D, Footitt S, Theodoulou FL, Holdsworth MJ** (2008) Seed after-ripening is a discrete developmental pathway associated with specific gene networks in *Arabidopsis*. *The Plant Journal* **53**:214-224.
- Carter NP** (2007) Methods and strategies for analyzing copy number variation using DNA microarrays *Nature Genetics* **39**: S16-21.
- Casimiro I, Marchant A, Bhalerao RP, Beeckman T, Dhooge S, Swarup R, Graham N, Inzé D, Sandberg G, Casero PJ, Bennett MJ** (2001) Auxin transport promotes *Arabidopsis* lateral root initiation. *Plant Cell* **13**: pp. 843–852.
- Catalá C, Rose JKC and Bennett AB** (1997) Auxin regulation and spatial localization of an endo- β -1-4-D-glucanase and a xyloglucan endotransglycosylase in expanding tomato hypocotyls *The Plant Journal* **12**:417-426.
- Catalá C, Rose JKC, York WS, Albersheim P, Darvill AG and Bennett AB** (2001) Characterization of a Tomato Xyloglucan Endotransglycosylase Gene That Is Down-Regulated by Auxin in Etiolated Hypocotyls *Plant Physiology* **127**: 1180–1192.
- Chang C, Kwok SF, Bleecker AB and Meyerowitz, EM** (1993) *Arabidopsis* ethylene-response gene ETR1: similarity of product to two-component regulators. *Science* **262**: 539-544.
- Chini A, Fonseca S, Fernández G, Adie B, Chico M, Lorenzo O, García-Casado G, López-Vidriero I, Lozano FM, Ponce MR, Micol JL, Solano R** (2007) The JAZ family of repressors is the missing link in jasmonate signalling. *Nature* **448**: 666-671.
- Choe S, Schmitz R J, Fujioka S, Takatsuto S, Lee M O, Yoshida S, Feldmann KA and Tax FE** (2002) *Arabidopsis* brassinosteroid-insensitive dwarf12 mutants are semidominant and defective in a glycogen synthase kinase 3 β -like kinase. *Plant Physiology* **130**: 1506-15.
- Chow B and McCourt P** (2006) Plant hormone receptors: perception is everything *Genes and Development* **20**: 1998-2008.

- Chudin E, Walker R, Kosaka A, Wu SX, Rabert D, Chang TK and Kreder DE** (2001) Assessment of the relationship between signal intensities and transcript concentration for affymetrix genechip(r) arrays. *Genome Biology* **3**: Research0005.
- Ciceri P, Locatelli F, Genga A, Viotti A, Schmidt RJ** (1999) The activity of the maize Opaque2 transcriptional activator is regulated diurnally. *Plant Physiology* **121**: 1321–1327.
- Clough SJ and Bent AF** (1998) Floral dip: a simplified method for *Agrobacterium*-mediated transformation of *Arabidopsis thaliana*. *The Plant Journal* **16**: 735-743
- Cosgrove DJ** (1993) How do plant walls extend? *Plant Physiology* **102**: 1-6.
- Cosgrove DJ** (2005) Growth of the plant cell wall. *Nature Reviews of Molecular Cell Biology* **6**: 850–861.
- Cui D, Neill SJ, Tang Z and Cai W** (2005) Gibberellin-regulated XET is differentially induced by auxin in rice leaf sheath bases during gravitropic bending. *Journal of Experimental Botany* **56**: 1327–1334.
- Cui HC, Levesque MP, Vernoux T, Jung JW, Paquette AJ, Gallagher KL, Wang JY, Blilou I, Scheres B and Benfey PN** (2007). An evolutionarily conserved mechanism delimiting SHR movement defines a single layer of endodermis in plants. *Science* **316**: 421–425.
- Darley CP, Forrester AM and McQueen-Mason SJ** (2001) The molecular basis of plant cell wall extension **47**: 179–195.
- de Lucas M, Daviere JM, Rodríguez-Falcón M, Pontín M, Iglesias-Pedraz JM, Lorrain S, Fankhauser C, Blázquez MA, Titarenko E and Prat S** (2008) A molecular framework for light and gibberellin control of cell elongation. *Nature* **451**: 480–484.
- De Rybel B, Audenaert D, Xuan W, Overvoorde P, Strader LC, Kepinski S, Hoyer R, Brisbois R, Parizot B, Vanneste S, Liu X, Gilday A, Graham IA, Nguyen L, Jansen L, Njo MF, Inzé D, Bartel B and Beeckman T** (2012) A role for the root cap in root branching revealed by the non-auxin probe naxillin *Nature Chemical Biology* **8**: 798–805.
- Dello Ioio R, Linhares FS, Scacchi E, Casamitjana-Martinez E, Heidstra R, Constantino P, Sabatina S** (2007) Cytokinins determine *Arabidopsis* root-meristem size by controlling cell differentiation. *Current Biology* **17**: 678-682.
- Derbyshire P, Findlay K, McCann MC and Roberts K** (2007) Cell elongation in *Arabidopsis* hypocotyls involves dynamic changes in cell wall thickness, *Journal of Experimental Botany* **58**: 2079-2089.
- Dolan L, Janmaat K, Willemsen V, Linstead P, Poethig S, Roberts K and Scheres B** (1993) Cellular organisation of the *Arabidopsis thaliana* root. *Development* **119**: 71-84.
- Du L, Poovaiah BW** (2004) A novel family of Ca²⁺/calmodulin-binding proteins involved in transcriptional regulation: Interaction with fsh/Ring3 class transcription activators. *Plant Molecular Biology* **54**: 549-569.

- Dyson R, Band L, Jensen O** (2012) A model of crosslink kinetics in the expanding plant cell wall: yield stress and enzyme action *Journal of Theoretical Biology* **307**: 125–136
- Eudes A, Mouille G, Thévenin J, Goyallon A, Minic Z and Jouanin L** (2008) Purification, Cloning and Functional Characterization of an Endogenous beta-Glucuronidase in *Arabidopsis thaliana* *Plant and Cell Physiology* **49**: 1331-1341.
- Feldmann KA, Malmberg RJ and Dean C** (1994) in *Arabidopsis* (eds Meyerowitz EM & Somerville CR) 137–172 (Cold Spring Harbor Laboratory Press, New York).
- Feng S, Martínez C, Gusmaroli G, Wang Y, Zhou J, Wang F, Chen L, Yu L, Iglesias-Pedraz JM, Kircher S, Schafer E, Fu X, Fan LM, Deng XW** (2008) Coordinated regulation of *Arabidopsis thaliana* development by light and gibberellins. *Nature* **451**: 475–479.
- French AP, Wilson MH, Kenobi K, Dietrich D, Voß U, Ubeda-Tomás S, Pridmore TP, Wells DM** (2012) Identifying biological landmarks using a novel cell measuring image analysis tool: Cell-o-Tape *Plant Methods* **8**: 7
- Filardo FF and Swain SM** (2003) SPYing on GA signaling and plant development. *Journal of Plant Growth and Regulation* **22**: 163–175.
- Finkelstein RR, Gampala SSL, Rock CD** (2002) Abscisic acid signalling in seeds and seedlings. *The Plant Cell* **14**: 515-545.
- Frigerio M, Alabadí D, Pérez-Gómez J, García-Cárcel L, Phillips AL, Hedden, P and Blázquez MA** (2006) Transcriptional regulation of gibberellin metabolism genes by auxin signalling in *Arabidopsis*. *Plant Physiology*. **142**: 553–563.
- Fry SC, Smith RC, Renwick KF, Martin DJ, Hodge SK and Matthews K.J** (1992) Xyloglucan endotransglycosylase, a new wall loosening enzyme activity from plants *Biochemistry Journal* **282**: 821-828.
- Fu X and Harberd NP** (2003). Auxin promotes *Arabidopsis* root growth by modulating gibberellin response. *Nature* **421**: 740–743.
- Furukawa M, He YJ, Borchers C, Xiong Y** (2003) Targeting of protein ubiquitination by BTB-cullin 3-Roc1 ubiquitin ligases. *Nature Cell Biology* **5**: 1001–1007.
- Gabriele S, Rizza A, Martone J, Circelli P, Costantino P, Vittorioso P** (2010) The Dof protein DAG1 mediates PIL5 activity on seed germination by negatively regulating GA biosynthetic gene *AtGA3ox1*. *The Plant Journal* **61**: 312-323.
- Gallego-Bartolomé J, Arana MV, Vandenbussche F, Žádníková P, Minguet EG, Guardiola V, van der Straeten D, Benkova E, Alabadi D, Blázquez M** (2011) Hierarchy of hormone action controlling apical hook development in *Arabidopsis*. *The Plant Journal* **67**: 622-634.
- Geyer R, Wee S, Anderson S, Yates J, Wolf DA** (2003) BTB/POZ domain proteins are putative substrate adaptors for cullin 3 ubiquitin ligases *Molecular Cell* **12**: 783–790.

- Gong JM, Waner DA, Horie T, Li SL, Horie R, Abid KB, Schroeder JI** (2009) Microarray-based rapid cloning of an ion accumulation deletion mutant in *Arabidopsis thaliana*. *Proceedings of the National Academy of Sciences* **43**: 15404-15409.
- Graebe JE** (1987) Gibberellin biosynthesis and control *Annuals Reviews of Plant Physiology* **38**: 419 – 465.
- Green PB** (1976) Growth and cell pattern formation on an axis: Critique of concepts, terminology and modes of study. *Botanical Gazette* **137**: 187-202.
- Griffiths J, Murase K, Rieu I, Zentella R, Zhang ZL, Powers SJ, Gong F, Phillips AL, Hedden P, Sun TP and Thomas SG** (2006) Genetic characterization and functional analysis of the *GID1* gibberellin receptors in *Arabidopsis*. *Plant Cell* **18**: 3399–3414.
- Guo H, Ye H, Li L and Yin Y** (2009) A family of receptor-like kinases are regulated by *BES1* and involved in plant growth in *Arabidopsis thaliana*. *Plant Signalling and Behaviour* **4**: 784–786.
- Hacham Y, Holland N, Butterfield C, Ubada-Tomas S, Bennett MJ, Chory J, Savaldi-Goldstein S** (2011) Brassinosteroids perception in the epidermis controls root meristem size. *Development* **138**: 839-848.
- Hauvermale AL, Ariizumi T and Steber CM** (2012) Gibberellin Signaling: A Theme and Variations on *DELLA* Repression *Plant Physiology* **160**: 83–92.
- Hedden P** (1997) The oxidases of gibberellin biosynthesis: Their function and mechanism *Physiologia Plantarum* **101**: 709-719.
- Hedden P and Phillips AL** (2000) Gibberellin metabolism: New insights revealed by the genes. *Trends in Plant Sciences* **5**: 523–530.
- Heo JO, Chang KS, Kim IA, Lee MH, Lee SA, Song SK, Lee MM and Lima J** (2011) Funneling of gibberellin signaling by the *GRAS* transcription regulator *SCARECROW-LIKE 3* in the *Arabidopsis* root *Proceedings of the National Academy of Sciences* **108**: 2166-2171.
- Hilhorst HWM** (1993) New aspects of seed dormancy. In: *Fourth International Workshop on Seeds. Basic and applied aspects of seed biology*. Côme D and Corbineau F (Eds.). Paris, ASFIS pp 571-579.
- Holdsworth MJ, Finch-Savage WE, Grappin P, Job D** (2008) Post-genomics dissection of seed dormancy and germination. *Trends in Plant Sciences* **13**: 7-13.
- Hou X, Hu WW, Shen L, Lee LYC, Tao Z, Han JH and Yu H** (2008) Global Identification of *DELLA* Target Genes during *Arabidopsis* Flower Development *Plant Physiology* **147**: 1126–1142

- Hou X, Lee LY, Xia K, Yan Y, Yu H** (2010) DELLAs modulate jasmonate signaling via competitive binding to JAZs. *Developmental Cell* **19**: 884–894.
- Hu J, Mitchum MG, Barnaby N, Ayele BT, Ogawa M, Nam E, Lai WC, Hanada A, Alonso JM, Ecker JR, Swain SM, Yamaguchi S, Kamiya Y and Sun TP** (2008) Potential Sites of Bioactive Gibberellin Production during Reproductive Growth in *Arabidopsis* *The Plant Cell* **20**:320-336
- Inoue T, Higuchi M, Hashimoto Y, Seki M, Kobayashi M, Kato T, Tabata S, Shinozaki K. and Kakimoto T** (2001) Identification of CRE1 as a cytokinin receptor from *Arabidopsis* *Nature* **409**: 10601–10603.
- Jan A, Yang G, Nakamura H, Ichikawa H, Kitano H, Matsuoka M, Matsumoto H, Komatsu S** (2004) Characterization of a xyloglucan endotransglucosylase gene that is up-regulated by gibberellin in rice. *Plant Physiology* **136**: 3670–3681.
- Jakoby M, Weisshaar B, Dröge-Laser W, Vicente-Carbajosa J, Tiedemann J, Krojce T, F Parcy** (2002) bZIP transcription factors in *Arabidopsis*, *Trends in Plant Science* **7**: 106-111.
- Jaillais Y and Chory J** (2010) Unraveling the paradoxes of plant hormone signaling integration. *Nature Structural and Molecular Biology* **17**: 642-5.
- Josse EM, Gan Y, Bou-Torrent J, Stewart KL, Gilday AD, Jeffree CE, Vaistij FE, Martinez-Garcia JF, Nagy F, Graham IA, Halliday KJ** (2011) A DELLA in Disguise: SPATULA Restrains the Growth of the Developing *Arabidopsis* Seedling. *The Plant Cell* **23**:1337-1351.
- Ko JH, Yang SH and Han KH** (2006) Upregulation of an *Arabidopsis* RING-H2 gene, XERICO, confers drought tolerance through increased abscisic acid biosynthesis *The Plant Journal* **47**: 343–355.
- Koornneef M and Van der Veen JH** (1980) Induction and analysis of gibberellin-sensitive mutants in *Arabidopsis thaliana* (L.) Heynl. *Theoretical and Applied Genetics* **58**: 257-263.
- Koornneef, M., Dellaert, L.W.M. and van der Veen, J.H.** (1982) EMS- and radiation-induced mutation frequencies at individual loci in *Arabidopsis thaliana* (L.) Heynh. *Mutat. Res.* **93**: 109-123.
- Koornneef M, Bentsink L, Hilhorst H** (2002) Seed dormancy and germination. *Current Opinion in Plant Biology* **5**: 33-36.
- Lara P, Onate-Sánchez L, Abraham Z, Ferrándiz C, Díaz I, Carbonero P, Vicente-Carbajosa J** (2003) Synergistic activation of seed storage protein gene expression in *Arabidopsis* by ABI3 and two bZIPs related to Opaque *Journal of Biology and Chemistry* **278**: 21003-21011.

- Lee BJ, Park CJ, Kim SK, Kim KJ, Paek KH** (2006) *In vivo* binding of hot pepper bZIP transcription factor CabZIP1 to the G-box region of *pathogenesis-related protein 1* promoter. *Biochemical and Biophysical Research Communications* **344**: 55-62.
- Lee DJ, Park JY, Ku SJ, Ha YM, Kim S, Kim MD, Oh MH and Kim J** (2007) Genome-wide expression profiling of *ARABIDOPSIS RESPONSE REGULATOR 7 (ARR7)* overexpression in cytokinin response *Molecular Genetics and Genomics* **277**: 115–137.
- Leung, J and Giraudat J** (1998) Abscisic acid signal transduction *Annual Review of Plant Physiology and Plant Molecular Biology* **49**: 199-222.
- Li X, Song Y, Century K, Straight S, Ronald P, Dong X, Lassner M and Zhang Y** (2001) A fast neutron deletion mutagenesis-based reverse genetics system for plants *The Plant Journal* **27**: 235-242.
- Li J, Li G, Gao S, Martinez C, He G, Zhou Z, Huang X, Lee JH, Zhang H, Shen Y, Wang H, Deng XW** (2010) *Arabidopsis* transcription factor ELONGATED HYPOCOTYL5 plays a role in the feedback regulation of phytochrome A signaling *The Plant Cell* **22**: 3634-3649.
- LiJ and Chory, J.** (1997). A putative leucine-rich repeat receptor kinase involved in brassinosteroid signal transduction. *Cell* **90**: 929–938.
- Liu YB, Lu SM, Zhang JF, Liu S, Lu YT** (2007) A xyloglucan endotransglucosylase/hydrolase involves in growth of primary root and alters the deposition of cellulose in *Arabidopsis*. *Planta* **226**: 1547–1560.
- Livak KJ and Schmittgen TD** (2001) Analysis of Relative Gene Expression Data Using Real-Time Quantitative PCR and the 2^{-ΔΔCT} Method *M&M -METHODS* **25**: 402–408.
- MacMillan J** (2002) Occurrence of gibberellins in vascular plants, fungi and bacteria. *Journal of Plant Growth and Regulation* **20**: 387–442
- Maere S, Heymans K and Kuiper M** (2005) BiNGO: a Cytoscape plugin to assess overrepresentation of Gene Ontology categories in biological networks. *Bioinformatics* **21**: 3448–3449.
- Marchant A, Swarup R and Bennett M J** (1999) Mutational studies of root architecture in *Arabidopsis thaliana*. In: Conference Proceedings of Phytosfere 99. European Plant Biotechnology Network. Gert E de Vries and Karin Metzlauff (eds). Elsevier Science B.V.
- McGinnis KM, Thomas SG, Soule JD, Strader LC, Zale JM, Sun TP and Steber CM** (2003) The *Arabidopsis* SLEEPY1 Gene Encodes a Putative F-Box Subunit of an SCF E3 Ubiquitin Ligase *The Plant Cell* **15**: 1120-1130.
- McQueen-Mason SJ, Cosgrove DJ** (1995) Expansin mode of action on cell walls. Analysis of wall hydrolysis, stress relaxation, and binding *Plant Physiology* **107**: 87-100
- Meyerowitz EM** (2001) Prehistory and history of *Arabidopsis* research *Plant Physiology* **125**:15-19.

- Meinke DW, Meinke LK, Showalter TC, Schissel AM, Mueller LA, Tzafrir I** (2003) A sequence-based map of Arabidopsis genes with mutant phenotypes. *Plant Physiology* **131**: 409–418.
- Medvedev P, Stanciu M, Brudno M** (2009) Computational methods for discovering structural variation with next-generation sequencing *Nature Methods* **6**: S13-20.
- Micheli F** (2001) Pectin methylesterases: cell wall enzymes with important roles in plant physiology *Trends in Plant Sciences* **6**: 414–419.
- Middleton AM, Úbeda-Tomás S, Griffiths J, Holman T, Hedden P, Thomas SG, Phillips AL, Holdsworth MJ, Bennett MJ, King JR, Owen MR** (2012) Mathematical modelling elucidates the role of transcriptional feedback in gibberellin signalling. *Proceedings of the National Academy of Sciences* **109**: 7571-7576.
- Miedes E, Lorences EP.** (2009) Xyloglucan endotransglucosylase/hydrolases (XTHs) during tomato fruit growth and ripening. *J Plant Physiol.* **166(5)**:489-98.
- Minic Z, Jamet E , San-Clemente H, Pelletier S, Renou JP , Rihouey C, PO Okinyo D, Proux C, Lerouge P and Jouanin L** (2009) Transcriptomic analysis of Arabidopsis developing stems: a close-up on cell wall genes. *BMC Plant Biology* **9**: 6.
- Moon J, Parry G, Estelle M** (2004) The ubiquitin-proteasome pathway and plant development. *The Plant Cell* **16**: 3181-3195.
- Moubayidin L, Perilli S, Dello Iolo R, Di Mambro R, Costantino P, Sabatini S** (2010) The rate of cell differentiation controls the *Arabidopsis* root meristem growth phase. *Current Biology* **20**: 1138-1143.
- Mustroph A, Zanetti ME, Jang CJ, Holtan HE, Repetti PP, Galbraith DW, Girke T, Bailey-Serres J** (2009) Profiling transcriptomes of discrete cell populations resolves altered cellular priorities during hypoxia in Arabidopsis *Proceedings of the National Academy of Sciences* **106**: 18843-8.
- Murase K, Hirano Y, Sun TP, Hakoshima T** (2008). Gibberellin induced DELLA recognition by the gibberellin receptor GID1. *Nature* **456**: 459–463.
- Murashige T and Skoog F** (1962) A revised medium for rapid growth and bioassays with tobacco tissue culture. *Physiologia Plantarum* **15**: 473.–497.
- Nakajima M, Shimada A, Takashi Y, Kim Y-C, Park SH, Ueguchi-Tanaka M, Suzuki H, Katoh E, Iuchi S, Kobayashi M, Maeda T, Matsuoka M and Yamaguchi I** (2006). Identification and characterization of *Arabidopsis* gibberellin receptors. *Plant Journal* **46**: 880–889.
- Nawya T, Lee JY, Colinas J, Wang JY, Thongrod SC, Malamy JE, Birnbaum K and Benfey PN** (2005) Transcriptional Profile of the Arabidopsis Root Quiescent Center *The Plant Cell* **17**: 1908-1925.

- Nemhauser JL, Hong F and Chory J** (2006) Different plant hormones regulate similar processes through largely nonoverlapping transcriptional responses. *Cell* **126**: 467-475.
- Nishitani K, Tominaga R** (1992) Endo-xyloglucan transferase, a novel class of glycosyltransferase that catalyzes transfer of a segment of xyloglucan molecule to another xyloglucan molecule *Journal of Biology and Chemistry* **267**: 21058-21064.
- Nishitani K and Vissenberg K** (2007) Roles of the XTH protein family in the expanding cell. In : Verbelen JP, Vissenber K (eds) The expanding cell. Plant Cell Monographs, vol 5, in Heidelberg New York (in press)
- Ogawa M, Hanada A, Yamauchi Y, Kuwahara A, Kamiya Y, Yamaguchi S** (2003) Gibberellin biosynthesis and response during *Arabidopsis* seed germination. *The Plant Cell* **15**: 1591-1604.
- Oh E, Zhu JY and Wang ZY** (2012) Interaction between BZR1 and PIF4 integrates brassinosteroid and environmental responses *Nature Cell Biology* **14**: 802–809.
- Olszewski N, Sun TP, Gubler F** (2002) Gibberellin signalling. *The Plant Cell* **14**: 561-580.
- Onkokesung N, Galis I, von Dahl CC, Matsuoka K, Saluz HP and Baldwin IT** (2010) Jasmonic acid and ethylene modulate local responses to wounding and simulated herbivory in *Nicotiana attenuata* leaves. *Plant Physiology* **153**: 785–798.
- Osato Y, Yokoyama R and Nishitani K** (2006) A principal role for AtXTH18 in *Arabidopsis thaliana* root growth: A functional analysis using RNAi plants. *Journal of Plant Research*. **119**: 153–162.
- Overvoorde PJ, Okushima Y, Alonso JM, Chan A, Chang C, Ecker JR, Hughes B, Liu A, Onodera C, Quach H, Smith A, Yua G and Theologis A** (2005) Functional Genomic Analysis of the *AUXIN/INDOLE-3-ACETIC ACID* Gene Family Members in *Arabidopsis thaliana* *The Plant Cell* **17**: 3282-3300.
- Overvoorde P, Fukaki H and Beeckman T** (2010) Auxin Control of Root Development. *Cold Spring Harb Perspect Biol*, 2(6):a001537-a001537
- Palmer SJ and Davies WJ** (1996) An analysis of relative elemental growth rate, epidermal cell size and xyloglucan endotransglycosylase activity through the growing zone of ageing maize leaves *Journal of Experimental Botany* **47**: 339–347.
- Penfield S, Li Y, Gilday AD, Graham S, Graham IA** (2006) *Arabidopsis* ABA INSENSITIVE4 regulates lipid mobilization in the embryo and reveals repression of seed germination by the endosperm. *Plant Cell* **18**: 1887–1899.
- Peng J, Carol P, Richards DE, King KE, Cowling RJ, Murphy GP and Harberd NP** (1997) The *Arabidopsis* GAI gene defines a signalling pathway that negatively regulates gibberellin responses. *Genes and Development* **11**: 3194–3205.

- Péret B, De Rybel B, Casimiro I, Benková E, Swarup R, Laplaze L, Beeckman T and Bennett MJ** (2009) *Arabidopsis* lateral root development: an emerging story *Trends in Plant Science* **14**: 399-408.
- Perrot-Rechenmann C** (2010) Cellular responses to auxin: Division versus expansion. *Cold Spring Harbour Perspectives in Biology*.
- Phillips AL, Ward DA, Uknes S, Appleford NEJ, Lange T, Huttly AK, Gaskin P, Graebe JE and Hedden P** (1995). Isolation and expression of three gibberellin 20-oxidase cDNA clones from *Arabidopsis*. *Plant Physiology* **108**:1049–57.
- Pintard L, Willems A, Matthias P** (2004) Cullin-based ubiquitin ligases: Cul3-BTB complexes join the family. *The EMBO Journal* **23**: 1681-1687.
- Plomion C, Leprovost G, Stokes A** (2001) Wood formation in trees. *Plant Physiology* **127**: 1513–1523
- Pysh LD, Wysocka-Diller JW, Camilleri C, Bouchez D and Benfey PN** (1999) The GRAS gene family in *Arabidopsis*: Sequence characterization and basic expression analysis of the SCARECROW-LIKE genes. *Plant Journal* **18**: 111–119.
- Quackenbush, J** (2002). Microarray data normalization and transformation *Nature Genetics* **32**: Suppl 496-501.
- Richards DE, King KE, Ait-ali T, Harberd NP** (2001) How gibberellin regulates plant growth and development: a molecular genetic analysis of gibberellin signaling. *Annual Review of Plant Physiology* **52**: 67-88.
- Robert HS, Quint A, Brand D, Vivian-Smith A, Offringa R** (2009) BTB and TAZ domain scaffold proteins perform a crucial function in *Arabidopsis* development. *The Plant Journal* **58**: 109-121.
- Robinson JT, Thorvaldsdóttir H, Winckler W, Guttman M, Lander ES, Gertz G, Mesirov JP** (2011) Integrative genomics viewer. *Nature Biotechnology* **29**: 24-26.
- Rose JKC, Braam J, Fry SC, Nishitani K** (2002) The XTH family of enzymes involved in xyloglucan endotransglucosylation and endohydrolysis: Current perspectives and a new unifying nomenclature. *Plant Cell Physiology* **43**: 1421.
- Ruzicka K, Simásková M, Duclercq J, Petrásek J, Zazimalová E, Simon S, Friml J, Van Montagu M, Benková E** (2009) Cytokinin regulates root meristem activity via modulation of the polar auxin transport. *Proceedings of the National Academy of Sciences* **106**: 4284-4289.
- Sakai H, Aoyama T, Oka A** (2000) *Arabidopsis* ARR1 and ARR2 response regulators operate as transcriptional activators. *The Plant Journal* **24**: 703-711.
- Salisbury FB and Ross CW** (1992) *Plant Physiology*, Eds. Belmont, CA

- Salmeron JM, Oldroyd GED, Rommens CMT, Scofield SR, Kim HS, Lavelle DT, Dahlbeck D, Staskawicz BJ** (1996) Tomato *prf* is a member of the leucine-rich repeat class of plant disease resistance genes and lies embedded within the *pto* kinase gene cluster. *Cell* **86**: 123-133.
- Santner A, Calderon-Villalobos LIA and Estelle M** (2009) Plant hormones are versatile chemical regulators of plant growth. *Nature Chemical Biology* **5**: 301 – 307.
- Sasaki A, Itoh H, Gomi K, Ueguchi-Tanaka M, Ishiyama K, Kobayashi M, Jeong DH, An G, Kitano H, Ashikari M and Matsuoka M** (2003) Accumulation of phosphorylated repressor for gibberellin signaling in an F-box mutant, *Science* **299**: 1896–1898.
- Savaldi-Goldstein S, Peto C, Chory J** (2007) The epidermis both drives and restricts plant shoot growth. *Nature* **446**: 199-202.
- Schiefebein JW and Benfey PN** (1991) The Development of Plant Roots: New Approaches to Underground Problems. *The Plant Cell* **3**., 1147-1 154.
- Schwab R, Ossowski S, Riester M, Warthmann N, Weigel D** (2006) Highly specific gene silencing by artificial microRNAs in Arabidopsis. *Plant Cell* **18** 1121–1133
- Schwechheimer D** (2008) Understanding gibberellic acid signalling – are we there yet? *Current Opinion in Plant Biology* **11**: 9–15.
- Siedlecka A, Wiklund S, Péronne M-A, Micheli F, Leśniewska J, Sethson I, Edlund U, Richard L, Sundberg B, Mellerowicz EJ** (2008). Pectin methyl esterase inhibits intrusive and symplastic cell growth in developing wood cells of *Populus*, *Plant Physiology* **146**: 554-565.
- Silveira AB, Gauer L, Pires JP, Cardoso PR, Carmello-Guerreiro S, Vincentz M** (2007) The Arabidopsis AtbZIP9 protein fused to the VP16 transcriptional activation domain alters leaf and vascular development *Plant Science* **172**: 1148-1156.
- Shannon P, Markiel A, Ozier O, Baliga NS, Wang JT, Ramage D, Amin N, Schiwikowski B and Ideker T** (2003) Cytoscape: a software environment for integrated models of biomolecular interaction networks *Genome Research* **13**: 2498–2504.
- Silverstone AL, Ciampaglio CN and Sun T** (1998) The *Arabidopsis* RGA gene encodes a transcriptional regulator repressing the gibberellin signal transduction pathway. *Plant Cell* **10**: 155–169.
- Silverstone AL, Jung H-S, Dill A, Kawaide H, Kamiya Y, Sun T-P** (2001) Repressing a repressor: gibberellin-induced rapid reduction of the RGA protein in *Arabidopsis*. *Plant Cell* **13**: 1555-1565.
- Slawson C and Hart GW** (2003) Dynamic interplay between O-GlcNAc and O-phosphate: the sweet side of protein regulation. *Current Opinion in Structural Biology* **13**: 631–636.

- Smalle J and Vierstra RD** (2004) The ubiquitin 26s proteasome proteolytic pathway. *Annual Review of Plant Biology* **55**: 555–590.
- Smith RC, Fry SC** (1991) Endotransglycosylation of xyloglucans in plant cell suspension cultures. *Biochemical Journal* **279**: 529–535.
- Somerville C, Bauer S, Brininstool G, Facette M, Hamann T, Milne J, Osborne E, Paredes A, Persson S, Raab T, Vorwerk S and Youngs H** (2004) Toward a systems approach to understanding plant cell walls. *Science* **306**: 2206–2211.
- Steber CM, Cooney SE and McCourt P** (1998) Isolation of the GA-response mutant *sly1* as a suppressor of ABI1-1 in *Arabidopsis thaliana*. *Genetics* **149**: 509–521.
- Stepanova AN, Yun J, Likhacheva AV and Alonso JM** (2007) Multilevel Interactions between Ethylene and Auxin in *Arabidopsis* Roots. *The Plant Cell* **19**:2169–2185.
- Steber CM., Cooney SE and McCourt P** (1998) Isolation of the GA-response mutant *sly1* as a suppressor of ABI1-1 in *Arabidopsis thaliana* *Genetics* **149**: 509–521.
- Stowe B and Yamaki T** (1957) The history and physiological action of the gibberellins. *Annual Review of Plant Physiology* **8**: 181–216.
- Sun TP, Goodman H M. and Ausubel FM** (1992) Cloning the *Arabidopsis gal* locus by genomic subtraction. *Plant Cell* **4**: 119–128.
- Sun TP and Gubler F** (2004) Molecular mechanism of gibberellin signaling in plants. *Annual Review of Plant Biology* **55**: 197–223.
- Sun TP** (2010) Gibberellin-GID1-DELLA: A pivotal regulatory module for plant growth and development. *Plant Physiology* **154**: 567–570.
- Sun TP** (2011) The molecular mechanism and evolution of the GA-GID1-DELLA signalling module in plants. *Current Biology* **21**: R338–R345.
- Swarup R, Kargul J, Marchant A, Zadik D, Rahman A, Mills R, Yemm A, May S, Williams L, Millner P, Tsurumi S, Moore I, Napier R, Kerr I and Bennett MJ** (2004) Structure-function analysis of the presumptive *Arabidopsis* auxin permease AUX1 *The Plant Cell* **16**: 3069–3083.
- Swarup R, Perry P, Hagenbeek D, van der Straeten D, Beemster GTS, Sandberg G, Bhalerao R, Ljung K, Bennett MJ** (2007) Ethylene upregulates auxin biosynthesis in *Arabidopsis* seedlings to enhance inhibition of root cell elongation. *The Plant Cell* **19**: 2186–2196.
- Taiz L** (1984) Plant Cell Expansion: Regulation of Cell Wall Mechanical Properties *Annual Review of Plant Physiology* **35**: 585–657.
- Tajima H, Iwata Y, Iwano M, Takayama S, Koizumi N** (2008) Identification of an *Arabidopsis* transmembrane bZIP transcription factor involved in the endoplasmic

reticulum stress response. *Biochemical and Biophysical Research Communications* **374**: 242-247.

Tanimoto, Roberts K, Dolan L (1995) Ethylene is a positive regulator of root hair development in *Arabidopsis thaliana*. *The Plant Journal* **8**: 943–948.

Thomas SG, Phillips AL, Hedden P. (1999). Molecular cloning and functional expression of gibberellin 2-oxidases, multifunctional enzymes involved in gibberellin deactivation. *PNAS* **96**:4698–703.

Thompson JE, Smith RC, Fry SC (1997) Xyloglucan undergoes interpolymeric transglycosylation during binding to the plant cell wall in vivo: evidence from ¹³C/³H dual labelling and isopycnic centrifugation in caesium trifluoroacetate. *Biochemical Journal* **327**: 699–708.

Tsukaya H, Beemster GT (2006) Genetics, cell cycle and cell expansion in organogenesis in plants. *Journal of Plant Research* **119**: 1–4.

Tyler L, Thomas SG, Hu J, Dill A, Alonso JM, Ecker JR and Sun T (2004) DELLA Proteins and Gibberellin-Regulated Seed Germination and Floral Development in *Arabidopsis*. *Plant Physiology* **135**:1008-1019.

Ubeda-Tomás S, Swarup R, Coates J, Swarup K, Laplaze L, Beemster GTS, Hedden P, Bhalerao R, Bennett MJ (2008) Root growth in *Arabidopsis* requires gibberellin/DELLA signalling in the endodermis. *Nature Cell Biology* **10**: 625 – 628.

Ubeda-Tomás S, Federici F, Casimiro I, Beemster GTS, Bhalerao R, Swarup R, Doerner P, Haseloff J, Bennett MJ (2009) Gibberellin signalling in the endodermis controls *Arabidopsis* root meristem size. *Current Biology* **19**: 1194-1199.

Ubeda-Tomás S, Beemster GTS, Bennett MJ (2012) Hormonal regulation of root growth: integrating local activities into global behaviour. *Trends in Plant Science* **17**: 326-331.

Ueguchi-Tanaka M, Ashikari M, Nakajima M, Itoh H, Katoh E, Kobayashi M, Chow TY, Hsing YI, Kitano H, Yamaguchi I and Matsuoka M (2005) GIBBERELLIN INSENSITIVE DWARF1 encodes a soluble receptor for gibberellin. *Nature* **437**: 693–698.

Ueguchi-Tanaka M, Nakajima M, Motoyuki A, Matsuoka M (2007) Gibberellin receptor and its role in gibberellin signaling in plants. *Annual Review of Plant Biology* **58**: 183–198.

Van Sandt VS, Stieperaere H, Guisez Y, Verbelen JP, Vissenberg K (2007) XET activity is found near sites of growth and cell elongation in bryophytes and some green algae: new insights into the evolution of primary cell wall elongation *Annals of Botany* **99**: 39-51.

Vanneste S, De Rybel B, Beemster GTS, Ljung K, De Smet I, Van Isterdael G, Naudts M, Iida R, Gruissem W, Tasaka M, Inze D, Fukaki H, Beeckman (2005). Cell cycle

progression in the pericycle is not sufficient for SOLITARY ROOT/IAA14-mediated lateral root initiation in *Arabidopsis thaliana*. *Plant Cell* **17**: 3035-3050.

Vincentz M, Bandeira-Kobarh C, Gauer L, Schlögl P, Leite A (2003) A evolutionary pattern of angiosperm bZIP factors homologous to the Maize Opaque2 regulatory protein. *Journal of Molecular Evolution* **56**: 105-116.

Vissenberg K, Martinez-Vilchez IM, Verbelen JP, Miller JG, Fry SC (2000) *In vivo* colocalization of xyloglucan endotransglycosylase activity and its donor substrate in the elongation zone of *Arabidopsis* roots. *The Plant Cell* **12**: 1229-1237.

Vissenberg K, Verbelen J-P and Fry SC (2001) Root Hair Initiation Is Coupled to a Highly Localized Increase of Xyloglucan Endotransglycosylase Action in *Arabidopsis* Roots *Plant Physiology* **127**: 1125–1135.

Vissenberg K, Van Sandt V, Fry S, Verbelen J (2003). Xyloglucan endotransglucosylase action is high in the root elongation zone and in the trichoblasts of all vascular plants from *Selaginella* to *Zea mays*, *Journal of Experimental Botany* **54**: 335-344.

Vissenberg K, Oyama M, Osato V, Yokoyama R, Verbelen JP, Nishitani K (2005) Differential expression of AtXTH17, AtXTH18, AtXTH19 and AtXTH20 genes in *Arabidopsis* roots. Physiological roles in specification in cell wall construction. *Plant Cell Physiology* **46**: 192–200.

Vogler H, Caderas D, Mandel T, Kuhlemeier C (2003) Domains of expansin gene expression define growth regions in the shoot apex of tomato. *Plant Molecular Biology* **53**: 267–272.

Wang Z, Gerstein M and Snyder M (2009) RNA-Seq: a revolutionary tool for transcriptomics. *Nature Reviews Genetics* **10**: 57-63.

Wasteneys GO (2004) Progress in understanding the role of microtubules in plant cells. *Current Opinion in Plant Biology* **7**: 651–660.

Weiss D and Ori N (2007) Mechanisms of Cross Talk between Gibberellin and Other Hormones. *Plant Physiology* **144**:1240-1246

Went FW (1928) Wuchsstoffe und Wachstum. Rec. Trav. Bot. Neerl., xxv. 1. 108. 1934: On the Pea-test Method for Auxin, The Plant Growth Hormone. *Proc. K*

Whitney SEC, Gidley MJ, McQueen-Mason SJ (2000) Probing expansin action using cellulose/hemicellulose composites. *The Plant Journal* **22**: 327-334.

Willige BC, Ghosh S, Nill C, Zourelidou M, Dohmann EM, Maier A and Schwechheimer C (2007) The DELLA domain of GA INSENSITIVE mediates the interaction with the GA INSENSITIVE DWARF1A gibberellin receptor of *Arabidopsis*, *Plant Cell* **19** 1209–1220.

- Wilson RN, Heckman JW and Somerville CR** (1992) Gibberellin is required for flowering in *Arabidopsis thaliana* under short days. *Plant Physiology* **100**: 403–408.
- Wu Y, Spollen WG, Sharp RE, Hetherington PR, Fry SC** (1994) Root growth maintenance at low water potentials. Increased activity of xyloglucan endotransglycosylase and its possible regulation by abscisic acid *Plant Physiology* **106**: 607-615.
- Yanagisawa S** (2004) Dof domain proteins: Plant-specific transcription factors associated with diverse phenomena unique to plants. *Plant and Cell Physiology* **45**: 386-391.
- Yamaguchi S** (2008) Gibberellin Metabolism and its Regulation *Annuals Review of Plant Biology* **59**: 225–51
- Yamamoto R, Demura T, Fukuda H** (1997) Brassinosteroids induce entry into the final stage of tracheary element differentiation in cultured *Zinnia* cells *Plant Cell Physiology* **38**: 980-3.
- Yang TF, Gonzalez-Carranza ZH, Maunders MJ and Roberts JA** (2008) Ethylene and the regulation of senescence processes in transgenic *Nicotiana sylvestris* plants *Annals of Botany* **101**: 301-310.
- Yang O, Popova OV, S uthoff U, Luking I, Dietz KJ, Golldack D** (2009) The *Arabidopsis* basic leucine zipper transcription factor AtbZIP24 regulates complex transcriptional networks involved in abiotic stress resistance *Gene* **436**: 45–55.
- Yokoyama R and Nishitani K** (2001) A comprehensive expression analysis of all members of a gene family encoding cell-wall enzymes allowed us to predict cis-regulatory regions involved in cell-wall construction in specific organs of *Arabidopsis*. *Plant Cell Physiology* **42**: 1025–1033.
- Yokoyama R, Rose JKC and Nishitani K** (2004) A surprising diversity and abundance of XTHs (xyloglucan endotransglucosylase/hydrolases) in rice, classification and expression analysis. *Plant Physiology* **134**: 1088–1099.
- Zhang H, Han W, De Smet I, Talboys P, Loya R, Hassan A, Rong H, Jürgens G, Paul Knox J, Wang MH** (2010) ABA promotes quiescence of the quiescent centre and suppresses stem cell differentiation in the *Arabidopsis* primary root meristem *The Plant Journal* **5**: 764-774.
- Zhang ZL, Ogawa M, Fleet CM, Zentella R, Hu J, Heo JO, Lim J, Kamiya y, Yamaguchi S and Sun TP** (2011) SCARECROW-LIKE 3 promotes gibberellin signaling by antagonizing master growth repressor DELLA in *Arabidopsis*. *Proceedings of the National Academy of Sciences* **108**: 2160-2165.
- Zentella R, Zhang ZL, Park M, Thomas SG, Endo A, Murase K, Fleet CM, Jikumaru Y, Nambara E, Kamiya Y, Sun TP** (2007) Global analysis of della direct targets in early gibberellin signaling in *Arabidopsis* *The Plant Cell* **10**: 3037-57.

Web links:

Affymetrix's : www.affymetrix.com

Anatomical and Fate virtual map: <http://www.bio.uu.nl/mg/pd/research/transcrframe.html>

Carbohydrate-Active EnZymes: <http://afmb.cnrs-mrs.fr/CAZY>)

Cell Wall Navigator Database: (<http://bioweb.ucr.edu/Cellwall/>)

Gene Ontology tool: (<http://www.geneontology.org/GO.tools.shtml>.)

ImageJ 1.4.1j (<http://rsb.info.nih.gov/ij/>)

NASC, the European Arabidopsis stock centre home page:
(<http://atensembl.arabidopsis.info/index.html>).

Primer 3 design tool: (<http://frodo.wi.mit.edu>)

The Arabidopsis Information Resource (TAIR) database: (<http://arabidopsis.org>).

The R Rroject for statistical computing: (www.r-project.org/)

Toronto Bio-Array Resource web (<http://bar.utoronto.ca/welcome.htm>)

Microsoft Corporation, Redmon, USA (<https://www.roche-applied-science.com>).

Cytoscape: <http://www.cytoscape.org/>

WMD3-Web MicroRNA Designer: (<http://wmd3.weigelworld.org>).

pGreen vector map: (<http://www.pgreen.ac.uk/pGreenII/pGreenII.htm>)

APPENDIX I. SCR:GAI-(gai)-GR-YFP transgene sequence

SCS1>>

GTCGACcctggaagtccgattgagaggagaggattgaccggagagagaccggagaaagatgggagtgaggagaagagattgggagacgaa
gagtaaccggacggcgagaagacgaggaaggtaatcggagtgatgcggtggagggaagagctgattgagagaagacatactccagactctgctca
cggaatctgtaggagtcgccattgccatggacattggaatcgccattagattgtgatcctctgcaacaaagcggatttggctggtgtaatggataagggat
agaggaagaggacttggatcagaaaacctttgatggcctaataatggcctataaactgtaactctgtagcgttggcaacaagagacttttaaggtttgt
tgccaaacagatattgcattggctatgtaatgtagaattttataatgtagtctattgctagatattgtaagtgacatttgattacaacatttcattttatt
tggtttaatgagcatttctattatagagacttggatgtaataaatggtgtctaaagataataaaaatatttataatacttctaaaattggataaatttgggaaat
cctaataatcagltaaatgaagataaagagtataaaaaaactatgtagtaaaatcattcacattttgtgataatagtagcattggtatcgttaagatcact
caaaaatcaaaaatgaagctaaaagggcagaaaagactattcaaatatggactggagaaagacattcagcttttacgctgagaaacttcatattgag
ccgtgtttgtgtgtaagagaagtaataaaaaataattgaaagtgaagaaaggagaagaaaaataagatcgtagaagcgtggatggttctcttggg
ttcactgccatgctgattataaattggccatggggctagtgttgcgtacaaaagtctaaaaatgtcagtcacaacagggtccaaaacttgaagaaaaata
ataataatagcaaaatttctaaaaattgtaaaaaagaacaaaagggaaaagatgaggatgcagatgaaagcaaaatgtcaaacactagttcagat
ttatcgggaactggggttgacagttggtgatgtagtaatggcctctcatcaaaacatgtgcatcttttctttttgtatttactgttttagctctacgtctgtcca
attcctctcaagtaaaatgcttaaatgataactaatacaaggggactaatgcttttcttttctatcctgtttgtctaaactttactgtgattcctttatttct
cctctcttagattagctggttaaggaataaccatcttctaattttagcacaaaattgcaagttggtccccatcttagtaagcacatcgtaccacactttg

SCS3>>

Atgtgtgagagacttctcatccatctctcataccaaacctaaatcaaatgactagtgggcaacctgctgactccatatgaccataactaataaatcggtt
atgaatccaactcatgtagctctatagaatagaaccattcattcacataatgaactgaatcgtacattttattacatcattactactcaatttgaatagca
agatcatcttttctattcaacaatttggatattcctaatttataactttgtcatacatcataatattctgaaatttggatataattgtaccggtccacgaaataga
gctctattattatagaccaacaaacaaaatattatcttctgtgttagttcagagagaggtaagaagaacgaaatggatcggcaaacggaagagct
caaacacacaacgacgaacatttccgatcaccacctaactcttcccattttatttttcaaaactcaaatlaaagaagaaaaaacagaacag
aGAGAGAAAGAGTTAAGATGAATAGAGATAGAGAGAAAGAGTTAAGATGAATAGAGATAGAAAGAGTCAT

PF1>>>

TAAATGTACGAAGCGACATTCACAATAA AAGGTGGAAGAGGAC TTAGATACGGGGATCC AAG
AGAGATCATCATCATCATCAAGATAAGAAGACTATGATGATGAATGAAGAAGACGACGGTAACG
GCATGGATGAGCTTCTAGCTGTTCTTGGTTACAAGGTTAGGTCATCCGAAATGGCTGATGTTGCTCAGAA
ACTCGAGCAGCTTGAAGTTATGATGTCTAATGTTCAAGAAGACGATCTTCTCAACTCGCTACTGAGACTG
TTCATAATAATCCGGCGGAGCTTTACACGTGGCTTATTCTATGCTCACCACCTTAATCCTCCGTCGTCT
AACGCCGAGTACGATCTTAAAGCTATCCCGGTGACGCGATTCTCAATCAGTTCGCTATCGATTCCGGCTT
CTTCGTCTAACCAAGCGCGGAGGAGATACGTATACTACAACAAGCGGTTGAAATGCTCAAACGGCG
TCGTGGAACCACTACAGCGACGGCTGAGTCAACTCGGCATGTTGTCTGTTGACTCGCAGGAGAACG

PF2 >>>

GTGTGCGTCTCGTTCACGCGCTTTTGGCTTGCCTGTTCAGAAAGAGAATCT GACTGTAGCGGAAGCTCT

<<< PR1

CGTGAAGCAAATCGGATTCTTAGCCGTTTCTC AATGCGAGGATGAGAAA GTCGCTACTTACTTCGCC
GAAGCTCTCGCGCGGCGGATTTACCGTCTCTCCGTCGCAGAGTCCAATCGACCACTCTCTCTCCGAT
ACTCTTCAGATGCACTTCTACGAGACTTGTCTTATCTCAAGTTCGCTCACTTACGGCGAATCAAGCGAT
TCTCGAAGCTTTTCAAGGGAAGAAAAGAGTTCATGTCATTGATTTCTCTATGAGTCAAGGTCTTCAATGGC
CGGCGCTTATGCAGGCTCTTGCCTTCGACCTGGTGGTCTCTCTGTTTTCCGGTTAACCGGAATTGGTC
CACCGGCACCGGATAATTTGATTATCTTCATGAAGTTGGGTGTAAGCTGGCTCATTTAGCTGAGGCGAT

PF3>>>

TCAGTTGAGTTTGAAGTACAGAGGATTTGTGGCTAACACTTTAGCTGATCTTGATGC TCGATGCTTGAGC
TTAGACC AAGTGAAGATTGAATCTGTTGCGGTTAACTCTGTTTTGAGCTTACAAGCTCTTGGGACGACC

<<< PR2

TGGTGCATCGATAAGGTTCTTGGTGTGGTGAATCAGATTAACCGGAGAT TTCACTGTGGTTGAGCAC
AATCGAACCAATAGTCCGATTTTCTTAGATCGGTTTACTGAGTCGTTGCATTATTACTCGACGTTGTT
GACTCGTTGGAAGGTGTACCGAGTGGTCAAGACAAGGTCATGTCGGAGGTTTACTTGGGTAACAGATC
TGCAACGTTGTGGCTTGTGATGGACCTGACCGAGTTGAGCGTCATGAAACGTTGAGTCAGTGGAGGAAC
CGGTTCCGGTCTGCTGGGTTTGGCGCTGCACATATTGTTTCAATGCGTTTAAAGCAAGCGAGTATGCTTT

GAIS2>>>

TGGCTCTGTTCAA CGGCGGTGAGGTTATCGGG TGGAGGAGAGTGACGGCTGTCTCATGTTGGGTTGG
CACACACGACCGCTCATAGCCACCTCGCTTGGAACTCTCCACCAATGAATTGGGTGGTGAAGCTCGA

<<< PR3

AAAACAAAGAAAAAATCAAAGGGATTACGCAAGC CACTGCAGGAGTCTCACAAGACACTTCGGAAAAATC
CTAACAAAACAATAGTTCTGTCAGCATTACCACAGCTCACCCCTACCTTGGTGTCACTGCTGGAGGTGAT
TGAACCCGAGGTGTTGTATGCAGGATATGATAGCTCTGTTCCAGATTACGCATGGAGAATTATGACCACA
CTCAACATGTTAGGTGGGCGTCAAGTATTGCAGCAGTGAATGGGCAAAGGCGATACCAGGCTTCAGA

AACTTACACCTGGATGACCAAATGACCCTGCTACAGTACTCATGGATGTTTCTCATGGCATTGCCCTGG
 GTTGGAGATCATAACAGACAATCAAGTGGAAACCTGCTCTGCTTTGCTCCTGATCTGATTATTAATGAGCAG
 AGAATGTCTCTACCCTGCATGTATGACCAATGTAAACACATGCTGTTTGTCTCCTCTGAATTACAAAGATT
 GCAGGTATCCTATGAAGAGTATCTCTGTATGAAAACCTTACTGCTTCTCTC**CTCAGTTCCTAAGGAAGGTC**
 TGAAGAGCCAAGAGTTATTTGATGAGATTGGAATGACTTATATCAAAGAGCTAGGAAAAGCCATCGTCAA
 AGGGAAGGGAAGTCCAGTCAAGACTGGCAACGGTTTTACCAACTGACAAAGCTTCTGGACTCCATGCAT
 GAGGTGGTTGAGAATCTCCTTACCTACTGCTTCCAGACATTTTTGGATAAGACCATGAGTATTGAATTCCC
 AGAGATGTTAGCTGAAATCATCACTAATCAGATACCAAATATTCAAATGGAATATCAAAAAGCTTCTGTT

YS1-F>>>

TCATCAAAAA**CAATTC**agcaagggcgaggagctgtcaccgggggtggtgccatcctggtcgagctggacggcgacgtaaacggccacaag
 ttcagcgtgtccggcgagggcgagggcgatgccacctacggcaagctgacctgaagttcatctgcaccaccggcaagctgcccggtccctggcccac
 cctcgtgaccacctcggctacggcctgcagtgtcctcggcctaccggaccacatgaagcagcagacttctcaagtccgcatgcccgaaggctac
 gtccaggagcgcaccatcttctcaaggacgacggcaactacaagaccggcggcggaggtgaagttcgagggcgacaccctggtgaaccgcatcgagc
 tgaagggcatcgacttcaaggaggacggcaacatcctggggcacaagctggagtacaactacaacagccacaacgtctatatcatgcccgacaagca
 gaagaacggcatcaaggtgaacttcaagatccgccacaacatcgaggacggcagcgtgcagctcggcaccactaccagcagaacacccccatcg
 gcgacggccccgtgctgctgcccgacaaccactacctgagctaccagtcggcctgagcaaaagaccccaacgagaagcgcgcatcacatggtcctgct

<<<YS1-R

ggagttcgtgaccgcccgggatcactc**tcggcatggacgagctgtacaag****CTCGAG**

Legend:

DELLA gai negative dominant mutant: Deleted in gai resulting in loss of 17 aa.

SCR promoter

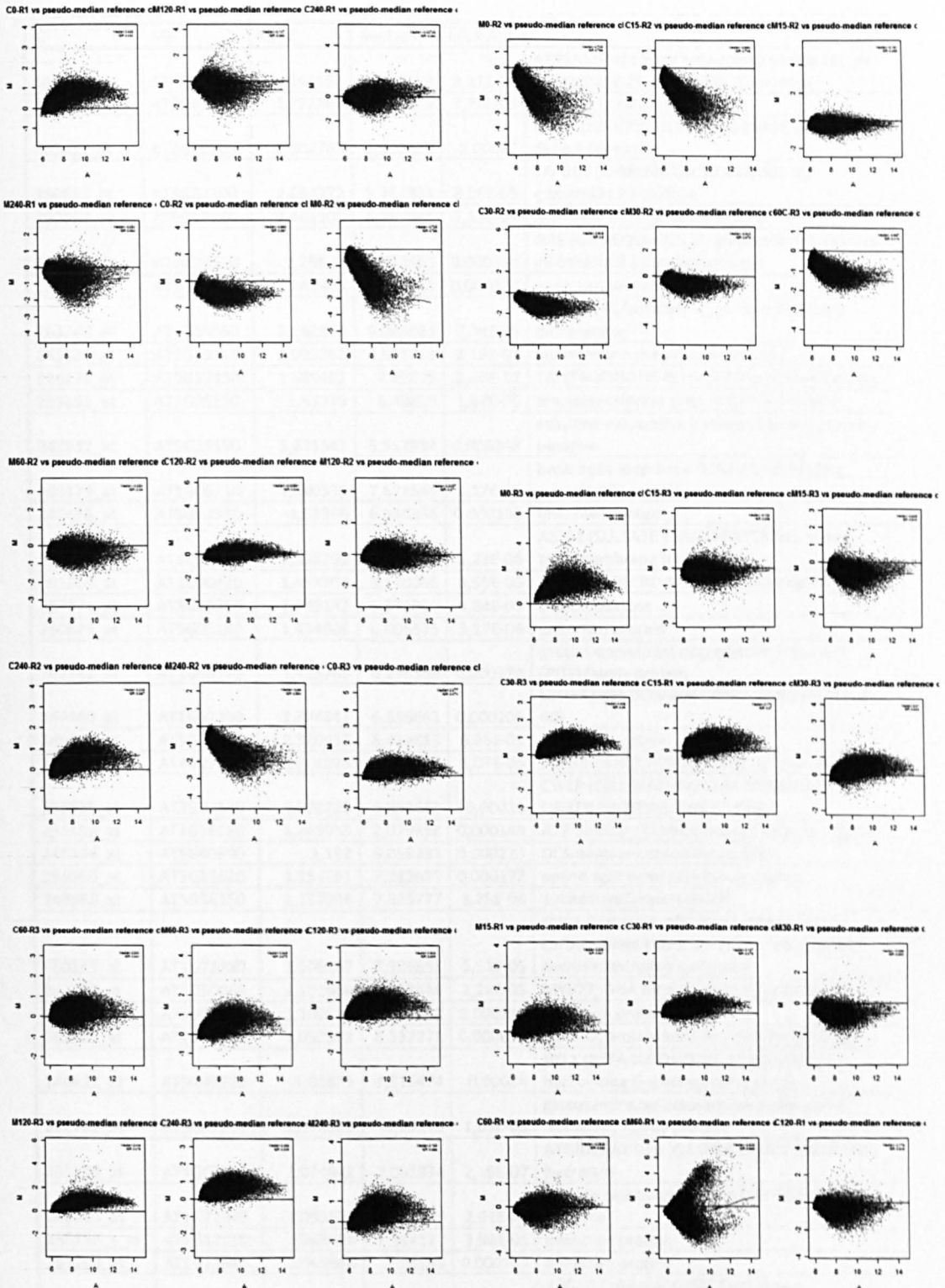
gai

GR

YFP

APPENDIX II. MA plots for *SCR::gai-GR* arrays probe intensities

Variability between the overall expression it is observed for the differnt arrays prior normalization.

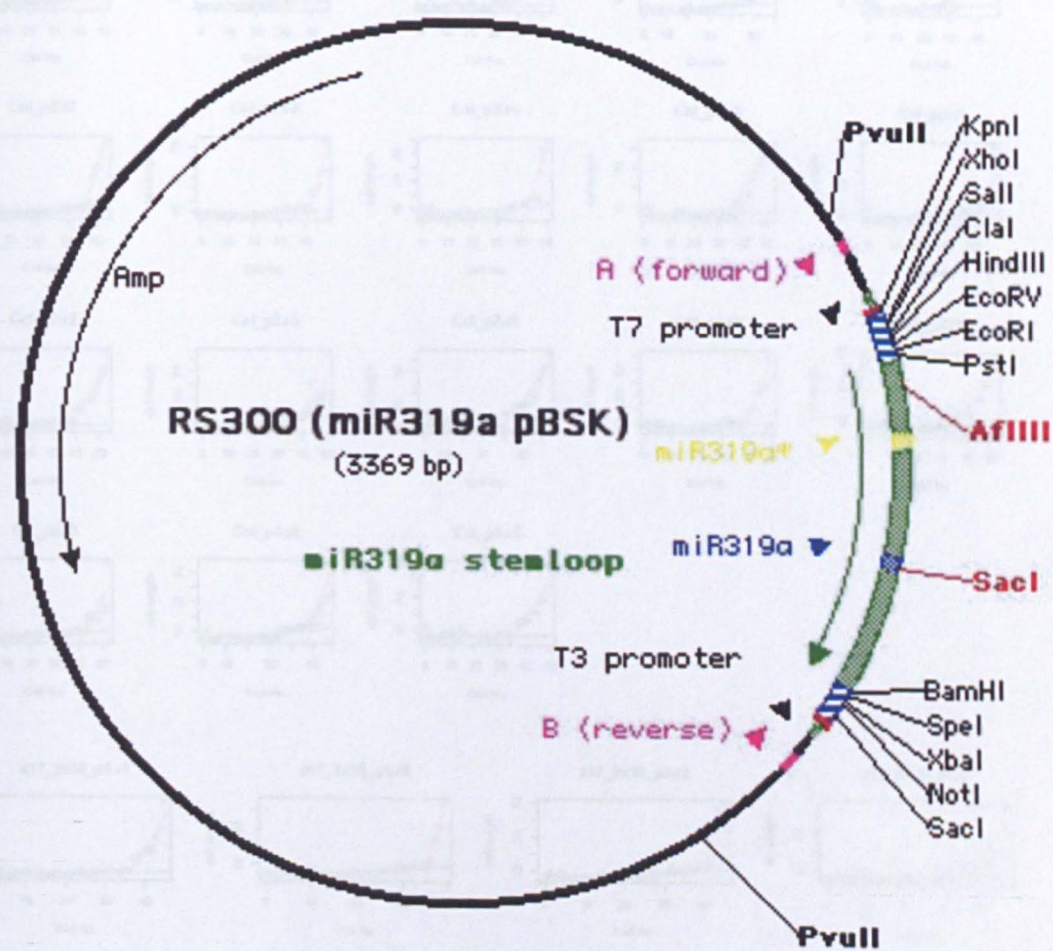


APPENDIX III. List of 41 intersecting genes.

Genes identified from the comparison between the wild type and transgenic population for overall the *SCRgai-GR* array.

ID	AGI	logFC	AveExpr	adj.P.Val	
248371_at	AT5G51810	4,344597	7,084623	8,81E-06	AT2353/ATGA200X2/GA200X2 (GIBBERELLIN 20 OXIDASE 2); gibberellin 20-oxidase
250515_at	AT5G09570	3,772364	8,981939	7,78E-05	unknown protein
265422_at	AT2G20800	2,802767	6,920439	0,00018	NDB4 (NAD(P)H DEHYDROGENASE B4); NADH dehydrogenase
250611_at	AT5G07200	2,654772	5,267831	8,28E-05	YAP169 (GIBBERELLIN 20 OXIDASE 3); gibberellin 20-oxidase
250062_at	AT5G17760	2,462105	6,787545	2,19E-07	AAA-type ATPase family protein
254065_at	AT4G25420	2,29827	5,368465	0,000214	GA5 (GA REQUIRING 5); gibberellin 20-oxidase/gibberellin 3-beta-dioxygenase
264832_at	AT1G03660	2,241445	6,6261	0,000307	unknown protein
261768_at	AT1G15550	2,163623	9,083021	7,78E-05	GA4 (GA REQUIRING 4); gibberellin 3-beta-dioxygenase
245136_at	AT2G45210	2,093362	6,691751	2,19E-07	auxin-responsive protein-related
266276_at	AT2G29330	1,689482	7,69079	2,86E-11	TRI (TROPINONE REDUCTASE); oxidoreductase
259353_at	AT3G05190	1,63979	6,40829	1,67E-05	aminotransferase class IV family protein
246932_at	AT5G25190	1,621542	5,557994	0,000248	ethylene-responsive element-binding protein, putative
263179_at	AT1G05710	1,580535	7,671545	3,17E-06	basic helix-loop-helix (bHLH) DNA-binding superfamily protein
247476_at	AT5G62330	-1,53866	6,950336	0,000168	unknown protein
264901_at	AT1G23090	1,538209	6,244268	1,23E-06	AST91 (SULFATE TRANSPORTER 91); sulfate transmembrane transporter
261866_at	AT1G50420	1,453708	8,140056	3,95E-06	SCL3 (SCARECROW-LIKE 3); transcription factor
257774_at	AT3G29250	1,439182	9,371096	4,84E-05	oxidoreductase
250823_at	AT5G05180	1,434906	6,005575	3,17E-06	unknown protein
262281_at	AT1G68570	1,423765	6,296369	0,000274	proton-dependent oligopeptide transport (POT) family protein
264469_at	AT1G67100	1,374941	6,335663	0,000205	LBD40 (LOB DOMAIN-CONTAINING PROTEIN 40)
249894_at	AT5G22580	1,320937	8,439813	6,26E-05	unknown protein
253828_at	AT4G27970	1,301075	5,843342	1,07E-05	SLAH2 (SLAC1 HOMOLOGUE 2); transporter
256825_at	AT3G22120	1,278725	6,938683	0,00018	CWLP (CELL WALL-PLASMA MEMBRANE LINKER PROTEIN); lipid binding
256459_at	AT1G36180	1,249033	7,079398	0,000148	ATP binding / biotin binding / catalytic / ligase
249364_at	AT5G40590	1,182	9,056233	0,000223	DC1 domain-containing protein
256650_at	AT3G13620	1,154361	7,282673	0,000172	amino acid permease family protein
249688_at	AT5G36160	1,137394	7,843777	8,25E-06	aminotransferase-related
260143_at	AT1G71880	1,106167	7,326553	2,61E-05	SUC1 (SUCROSE-PROTON SYMPORTER 1); carbohydrate transmembrane transporter/sucrose:hydrogen symporter
252193_at	AT3G50060	1,101069	7,518448	2,28E-05	MYB77; DNA binding / transcription factor
251751_at	AT3G55720	1,100532	7,272433	0,000287	unknown protein
263325_at	AT2G04240	1,092988	8,337271	0,000339	XERICO; protein binding / zinc ion binding
248622_at	AT5G49360	-1,08871	7,319474	0,00038	BXL1 (BETA-XYLOSIDASE 1); hydrolase, hydrolyzing O-glycosyl compounds
252282_at	AT3G49360	1,078329	6,25249	1,69E-05	glucosamine/galactosamine-6-phosphate isomerase family protein
251200_at	AT3G63010	1,074942	7,051374	2,19E-07	ATGID1B/GID1B (GA INSENSITIVE DWARF1B); hydrolase
262383_at	AT1G72940	1,055507	6,112147	2,61E-05	disease resistance protein (TIR-NBS class), putative
266150_s_at	AT2G12290	1,048428	7,314127	3,96E-05	unknown protein
261203_at	AT1G12845	1,045656	7,91999	0,000259	unknown protein
250604_at	AT5G07830	1,041561	8,420423	0,000229	ATGUS2 (ARABIDOPSIS THALIANA GLUCURONIDASE 2); beta-glucuronidase
245865_at	At1g58025	1,038518	4,707965	2,12E-06	DNA binding
254193_at	AT4G23870	-1,00247	5,046089	0,000341	unknown protein
245488_at	AT4G16270	-0,99658	4,375549	6,04E-06	peroxidase 40 (PER40) (P40)

APPENDIX IV. Map of the pRS300 vector



APPENDIX V. Root growth plots with fitted line for cell expansion dynamics studies

